UNIVERSITY OF SOUTHAMPTON

FACULTY OF ENGINEERING, SCIENCES and MATHEMATICS

School of Engineering Sciences

THE PYROLYTIC MECHANISM OF THE MAIN COMPONENTS IN WOODY BIOMASS AND THEIR INTERACTIONS

by

Dekui Shen

Thesis for the degree of Doctor of Philosophy

July 2011

UNIVERSITY OF SOUTHAMPTON

ABSTRACT

FACULTY OF ENGINEERING, SCIENCE & MATHEMATICS

School of Engineering Sciences

Doctor of Philosophy

THE PYROLYTIC MECHANISM OF THE MAIN COMPOENNTS IN WOODY BIOMASS AND THEIR INTERACTIONS

by Dekui Shen

The global demand of the volume of woody biomass (such as wood, logging residue, sawdust and so on) is huge and increased annually, due to its new application for the energy/fuel production during recent years. Pyrolysis is termed as a promising thermo-chemical technology to convert woody biomass to liquid, gas and solid fuels/chemicals. The better understanding of the pyrolysis mechanism of woody biomass is demanding considering the thermal performance of individual components (hemicellulose, cellulose and lignin) and their interactions .

In order to develop the current understanding of the pyrolysis of the individual components (hemicellulose, cellulose and lignin) in woody biomass and fill the knowledge gap on their interactions under pyrolytic conditions, the on-line pyrolysis and off-line pyrolysis study of the model compounds of the components and their "synthesized biomass" samples has been extensively investigated employing TGA-FTIR and fast pyrolysis unit, in terms of the mass loss variation against temperature together with the on-line identification of the evolved volatiles by FTIR, yield of pyrolyzed products (gas, bio-oil and char) from the fast pyrolysis unit, variation of the compositions in bio-oil and gas products against the fluidized-bed-reactor temperature, the chemical pathways for the chemical structure change of the macromolecules and the cracking of the primary fragments, and the interactions among the chemical components. The

proposed chemical pathways, indicating the possible competitive and/or consecutive relationship among the prominent compounds in bio-oil and gaseous product, give hints to improve the current kinetic scheme of the individual components.

Notably, the vapor-phase interaction among the components in the fluidized-bed reactor is investigated in terms of the product yield and variation of the prominent compounds in bio-oil and gaseous product, but their interactions in solid/liquid phase are not involved.

Keywords: woody biomass; pyrolysis; component; “synthesized biomass” sample;

Table of contents

List of tables

List of figures

DECLARATION OF AUTHORSHIP

I, …Dekui shen declare that the thesis entitled **"The pyrolytic mechanism of the main components in woody biomass and their interactions"** and the work presented in the thesis are both my own, and have been generated by me as the result of my own original research. I confirm that:

- this work was done wholly or mainly while in candidature for a research degree at this University;
- where any part of this thesis has previously been submitted for a degree or any other qualification at this University or any other institution, this has been clearly stated;
- where I have consulted the published work of others, this is always clearly attributed;
- where I have quoted from the work of others, the source is always given. With the exception of such quotations, this thesis is entirely my own work;
- I have acknowledged all main sources of help;
- where the thesis is based on work done by myself jointly with others, I have made clear exactly what was done by others and what I have contributed myself;
- parts of this work have been published as:

1) D.K. Shen, S. Gu, The mechanism for thermal decomposition of cellulose and its main products, Bioresource Technology, 100(24) (2009) 6496-6504.
2) D.K. Shen, S. Gu, A.V. Bridgwater, Study on the pyrolytic behavior of xylan-based hemicellulose using TG-FTIR and Py-GC-FTIR, Journal of Analytic and Applied Pyrolysis, 87(2) (2010) 199-206.
3) D.K. Shen, S. Gu, K.H. Luo, S.R. Wang, The pyrolytic degradation of wood-derived lignin from pulping process, Bioresource Technology, 101(15) (2010) 6136-6146.

Signed: ……..

Date:…….

Acknowledgement

First of all, I greatly appreciate my supervisor Dr. Sai Gu and co-supervisor Prof. Kaihong Luo for their prudent supervision and kind help on my PhD study. I am very happy that I could work with these two professional academics in Energy Technology Research Group in University of Southampton, since they helped me a lot not only on the research work, but also on my oversea life. Here, I sincerely send my all best wishes to them. Secondly, I would send my appreciation to my colleages working in Room 1051 in Building 25 (John Bruchmuller, Hani Tabbara, Lindsay-Marie Armstrong, Jun Xia……) for their help on my study and life. We, as brothers, had a lot of enjoyable time together (table games, table tennis, bowling, snooker, swimming and carting). This made me rapidly settle down and gradually enjoyed living here. My best friend Jiazhong Liu also gave me a lot of help on my study. There are lots of happy memories between us in my PhD life, which is the invaluable treasure in my life.

I greatly acknowledge the financial support for my PhD research work from Innovation China UK (ICUK) Proof of Concept Award and UK Engineering and Physical Sciences Research Council (EPSRC Grant No. EP/G034281/1). Importantly, I also thank the Institute for the Thermal Power Engineering of Zhejiang University, where the TG-FTIR experimental studies were carried out. Some of academics from that institute, Prof. S.R. Wang, Prof. M.X. Fang, Mr. Y. Zheng, Qi Wang and so on, should be appreciated for their technical support, data sharing and knowledge exchange during the collaborations on ICUK and MoST International Collaboration project.

Finally, I greatly appreciate the internal examiner (Prof. Charles Bank) and external examiner (Prof. James Clark from University of York) for their valuable comments and contributions on the PhD thesis. All the people who gave me help during my PhD study in Southampton are sincerely acknowledged.

Chapter 1: Introduction

1.1 Biomass energy

Biomass is the plant material derived from the photosynthesis reaction among CO_2 in the air, water and sunlight, to produce organic macromolecules (such as the polysaccharides and lignin) that form the building structure of biomass (McKendry 2002). The solar energy is stored in the chemical bonds of the structural components of biomass, while the carbon in the macromolecules is from CO_2. If the biomass is processed efficiently, either chemically or biologically, by extracting energy product and the carbon even all ends up with the evolution of CO_2, the whole process is carbon-cyclical and CO_2 neutral, as the evolved CO_2 is then available for producing new biomass. However, these two issues, renewable/inexhaustible and clean, are not the only stimulus for the world-wide interest in biomass as a potential energy source. Biomass is also an indigenous energy source, which is abundantly distributed in most countries in different forms as woody, herbaceous, aqueous plants. Its application may diversify the global energy-supply in many situations, which would lead to a more secure and sustainable energy supply over the fossil fuels in the future (Demirbas 2008).

Researchers characterise the various types of biomass in different ways but one simple method is to define five main types, namely (McKendry 2002):

- Woody plants, such as wood, logging residues and sawdust;
- Agricultural wastes, such as rice husks and corn straws;
- Herbaceous plants/grasses, and grasses;
- Aquatic plants, such as algae and floating grass;
- Animal wastes (manure) and municipal wastes.

Wood is an inexhaustible and natural raw material in origin, serving to strengthen stems, branches and roots of trees and other plants. The global demand of the volume of wood is huge and increased annually, due to its comprehensive application not only for the building/furniture materials, pulp and paper production and many other products, but also

for the energy/fuel production during recent decades. The woody biomass is mainly composed of cellulose, hemicellulose and lignin. Cellulose is the outstanding component in the biomass, accounting for more than 50% weight of dry biomass. It consists solely of units of anhydroglucose held together in a giant straight-chain molecule, building the framework of the plant cell-wall through cellulosic microfibrils. Hemicellulose, another important polysaccharide in biomass, is derived mainly from chains of pentose sugars and acts as the cement materials holding together the cellulose micelles and fibre (Theander 1985). Lignin, consisting of polymers of aromatic compounds, accounts for about 10%~35% of the weight of dry biomass with regard to the species of the biomass. The attention of this work would be confined to the woody biomass and its main chemical components.

1.2 The biomass conversion technologies

The established conversion methods for biomass energy to produce electricity, liquid, gas and solid fuels could be categorized into two groups as shown in Fig. 1-1: **thermo-chemical** (such as combustion, gasification, liquefaction and carbonization) and **bio-chemical** (such as fermentation and anaerobic digestion).

Fermentation and anaerobic digestion are two main established bio-chemical processes for biomass, together with a lesser-used process based on mechanical extraction/chemical conversion (McKendry 2002). Fermentation is used commercially on a large scale in various countries to produce ethanol from sugar crops (e.g. sugar cane, sugar beet) and starch crops (e.g. maize wheat). The fermentative conversion of lignocellulosic biomass (such as wood and grasses) is more complex, and the relevant techniques are currently at the pre-pilot stage. Anaerobic digestion is the conversion of organic material directly to a gas, termed biogas, a mixture of mainly methane and carbon dioxide with small quantities of other gases such as hydrogen sulphide (EU 1999). The biomass is converted by bacteria in an anaerobic environment, producing a gas with an energy content of about 20-40% of the lower heating value of the feedstock.

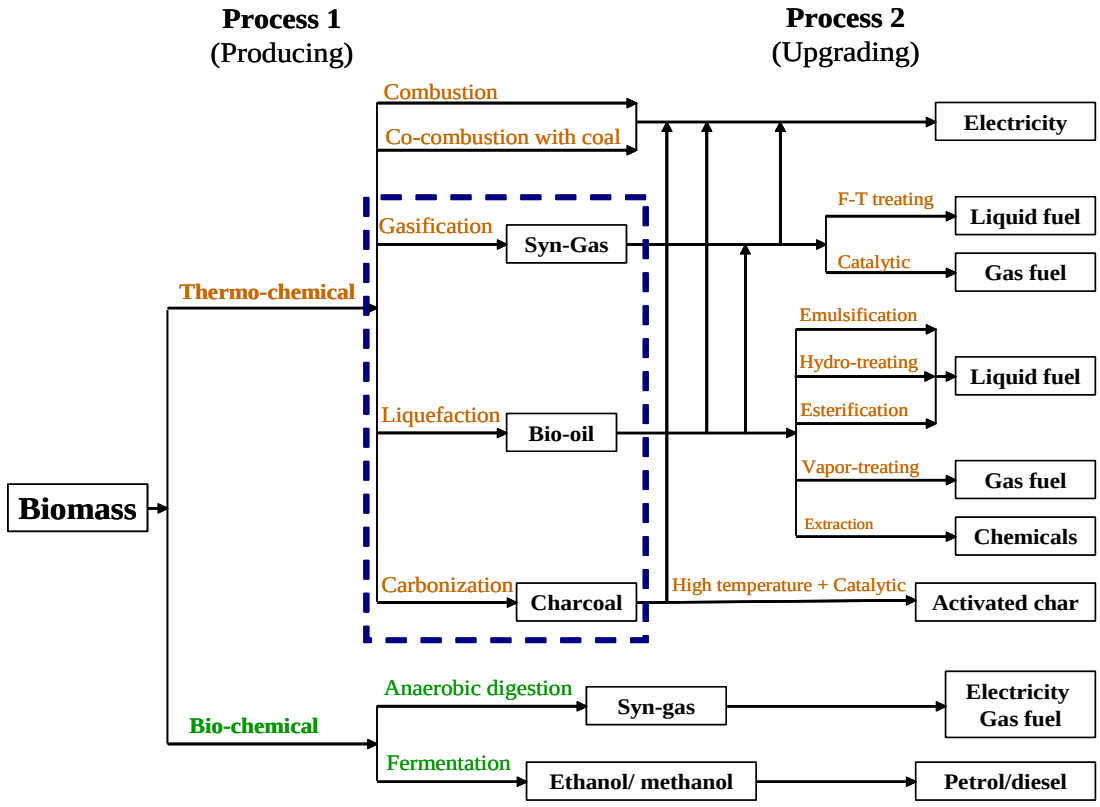

Fig. 1-1: The established conversion methods of biomass energy

Direct combustion and cofiring with coal for electricity production from biomass has been found to be a promising method for application in the nearest future. The ash deposition due to the content of the alkyl salts and the corrosive of the particles limits the application of this technology (Sondreal, et al. 2001). The pyrolysis of biomass is a thermal treatment that results in the production of gaseous products, liquid fuels/chemicals and charcoal, corresponding to the specified process of gasification (Beenackers 1999), liquefaction (Bridgwater 1999; Czenik and Bridgwater 2004). and carbonization (Prins, et al. 2006; Prins, et al. 2006) in Fig. 1-1, which differes from the main products, the operation conditions and the primary products separation and collection system. The pyrolysis is estimated to be one of the promising thermo-chemical conversion technologies for lignocellulosic biomass, due to the diversity of products, high mass conversion efficiency and energy efficiency. The industrialization and commercialization of this technology would be beneficial to

alleviate the fossil energy crisis, environmental deterioration and improve the global energy consumption structure.

1.3 The aim of this work

With the above brief discussion, pyrolysis is termed as a promising thermal technology to convert biomass to liquid, gas and solid fuels/chemicals. The better understanding of the pyrolysis mechanism of woody biomass is demanding considering the thermal performance of individual components (Stamm 1956; Shafizadeh, et al. 1972; Gardner, et al. 1985; Evans, et al. 1986; Ponder and Richards 1991; Antal and Varhegyi 1995; Blasi and Lanzetta 1997; Li, et al. 2001; Ferdous, et al. 2002; Hosoya, et al. 2007; Hosoya, et al. 2008; Liu, et al. 2008; Shen and Gu 2009), which would be beneficial for optimizing the conversion process, increasing the energy efficiency and reducing the by-product yield (Target 2 in Fig. 1-2).

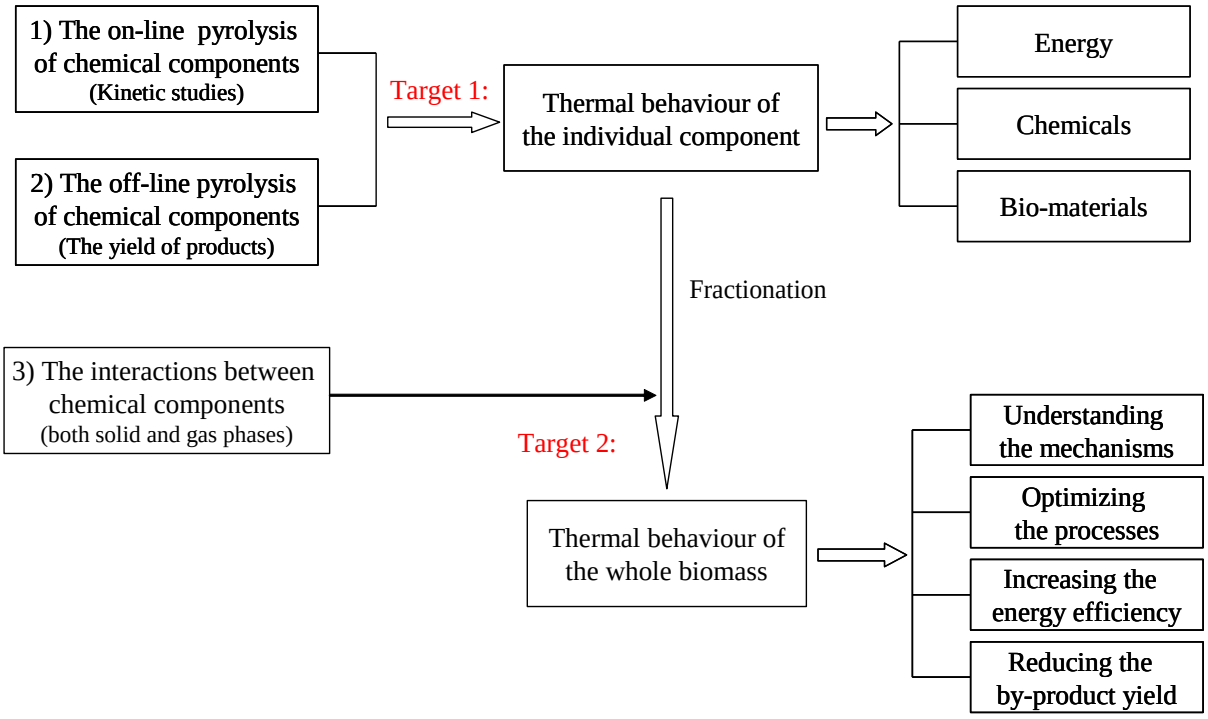

Fig. 1-2: the aims and objectives of this work

Moreover, the research on the pyrolysis of the chemical components in biomass could promote the direct application of the components in terms of energy, chemicals and bio-materials (Target 1 in Fig. 1-2), since the chemical components of biomass, sometimes largely existed as the residue from the industries (such as kraft lignin), is regarded as the potential feedstock for the conversion processes.

Therefore, this work would be focused on the pyrolytic mechanism of the individual components and their interactions, concerning the following issues (Fig. 1-2): 1) the on-line pyrolysis studies of the main chemical components (cellulose, hemicellulose and lignin), sometimes called kinetic study, is concentrated on the solid mass loss against temperature along with the evolution of the volatiles; 2) the off-line pyrolysis study of the main chemical components is to examine the yield of the main products (solid, gas and liquid), variation of the compositions in gaseous or liquid product influenced by the biomass species and experimental conditions, and the speculation of the chemical pathways for the pyrolytic reactions; 3) the interactions between the chemical components in woody biomass under the pyrolytic condition is to introduce the possible interacting mechanism regarding the mass loss process, the evolution of the volatiles and the yield of the specific products.

With regard to the main aims and objectives of this work, the thesis would be developed in the following parts:

Chapter 1 is the brief overview of the renewable energy sources and present situation, biomass energy and its conversion technologies, and the aim and objectives of this work.

Chapter 2 is the literature review concerning the on-line pyrolysis and off-line pyrolysis studies of the individual components in woody biomass (cellulose, hemicellulose and lignin), and their interactions during the pyrolysis process. Both the achievement and challenges in this field would be thoroughly discussed in this chapter.

Chapter 3 would present the methodology of this work, including the selection of the materials representing the main chemical components in woody biomass, the preparation of the samples of the individual components and "synthesized biomass", the TG-FTIR analysis (on-line pyrolysis) for recording the mass loss of solid and evolution of volatile against temperature, and fast pyrolysis experiments (off-line pyrolysis) involving the determination of the product yield from a fluidized-bed reactor system and the characterization of the compositions in liquid and gas products by means of GC-MS/FTIR.

Chapter 4 is the thorough discussion of the experimental results from the on-line pyrolysis and off-line pyrolysis of the individual components and the "synthesized biomass" sample, concerning the mass loss process together with the evolution of typical volatiles, yield of the products with the varied experimental conditions, variation of the compositions in the gas and liquid products, the speculative chemical pathways for the primary pyrolytic reactions of the supramolecules and secondary crackings of the fragments, the modified kinetic mechanism, and the mutual interactions among the components under pyrolytic conditions. This chapter would be discussed in four separate sections: cellulose, hemicellulose, lignin and interactions.

Chapter 5 is the conclusion of this research work, including the notable results of the pyrolytic mechanism of individual components and their interactions during the pyrolysis.

Chapter 6 is the discussion on future work.

Chapter 2: The literature review

2.1 Introduction

The research works on the pyrolytic behavior of the main chemical components of woody biomass are extensively reported in the literature, in terms of the following specific fundamental issues: 1) the on-line pyrolysis studies of the main chemical components (cellulose, hemicellulose and lignin) is focused on the solid mass loss and the evolution of the volatiles versus temperature, and the development of the kinetic model/mechanism for the component pyrolysis; 2) the off-line pyrolysis study of the main chemical components is to examine the yield of the main products (solid, gas and liquid) from the pyrolytic reactor, variation of the compositions in gaseous or liquid product influenced by the biomass species and experimental conditions, and the development of the possible chemical pathways for the pyrolytic reactions; 3) the interactions between the chemical components under the pyrolytic condition is to introduce the possible interacting mechanism of the components in the whole biomass, in terms of the mass loss process, the evolution of the volatiles and the yield of the specific products. The studies on the chemical components of woody biomass as mentioned above would be extensively overviewed, presenting both the development and challenges of the relevant issues.

2.2 The on-line pyrolysis of the main components of woody biomass

The thermogravimetric analysis (TGA) method is well-established for on-line pyrolysis of biomass and its components, where the mass loss of the solid sample could be exactly recorded versus temperature/time (Lee and Beck 1984; Avni and Coughlin 1985; Evans, et al. 1986; Simmons and Gentry 1986; Koufopanos, et al. 1989; Blasi 1993; Varhegyi, et al. 1994; Caballero, et al. 1995; Conesa, et al. 1995; Jakab, et al. 1995; Simkovic, et al. 1995; Bilbao, et al. 1997; Jakab, et al. 1997; Varhegyi, et al. 1997; Liu 2002; Branca and Blasi 2003; Safi, et al. 2004; Fang, et al. 2006; Grioui, et al. 2007; Shen, et al. 2009). The chemical kinetics of the pyrolysis of biomass and its components are mainly extrapolated from the analysis of the different mass loss stages. The kinetic models are validated through the correlation between the predicted data and the mass loss curve from

TGA, while the specific chemical phenomena and the prediction of the volatile yields are rarely referred in these models. Recently, TGA coupled with FTIR, GC, MS or other advanced analytical equipments is extensively employed to investigate the evolution of the volatile along with the pyrolysis of biomass and its components, in order to improve the kinetic models by involving the possible chemical reactions of the depolymerization of the macromolecules and the secondary cracking of the primary products.

Compared to hemicellulose and lignin, cellulose is the most intensely studied substance in the field of wood and biomass pyrolysis due to its predominant content (Arseneau 1971; Bradbury, et al. 1979; Antal, et al. 1980; Mohammed, et al. 1982; Piskorz, et al. 1986; Radlein, et al. 1991; Antal and Varhegyi 1995). The discussion will be mainly confined to the pyrolysis of celluloses and to a lesser extent hemicellulose (mainly xylan) and lignin. No attempt would be made to deal with other important carbohydrates or extractives.

2.3.1 Cellulose

Thermal decomposition of the cellulose (composed of the repeating glucopyranose units through theβ-(1-4) glycosidic linkage) has been vigorously studied for many years (Stamm 1956; Fengel 1969; Arseneau 1971; Broido and Nelson 1975; Shafizadeh and Bradbury 1979; Piskorz, et al. 1986; Agrawal 1988; Varhegyi, et al. 1994; Milosavljevic and Suuberg 1995; Bilbao, et al. 1997; Piskorz, et al. 2000; Li, et al. 2001; Dobele, et al. 2005; Mamleev, et al. 2007; Shen and Gu 2009). When heated either isothermally (where the heating temperature is constant) or dynamically (where the heating temperature is mostly linearly varied) under the inert atmosphere, cellulose initially undergoes the depolymerization and dehydration of the macromolecules, and then various fragmentation, elimination and condensation reactions to produce non-condensible volatiles, condensable vapor (liquid tar after cooling) and a carbonaceous char as the solid residue. A large number of studies have been published describing the investigations of the kinetics of pyrolysis of cellulose, and proposing the chemical reaction schemes for both primary and subsequent decomposition steps. The

outstanding contributions in the kinetics study of cellulose pyrolysis given by the groups led by Broido and Shafizadeh about 30-40 years ago are carefully reviewed by Antal and Varhegyi, and compared with their work in (Varhegyi, et al. 1993; Varhegyi, et al. 1994; Antal and Varhegyi 1995; Varhegyi, et al. 1997). Here, the development of the kinetics of cellulose pyrolysis would be systematically overviewed, involving most of recent studies implemented by other groups led by Piskorz, Di Blasi, Banyaz, Agrawal, Wooten, Hosoya and so on. Several controversial points addressed in previous studies would be intensively discussed, concerning the existence of the intermediate anhydrosugars, secondary cracking of the volatiles and the formation of char residue.

Historically, it was perhaps that Broido' s group firstly called attention to the intriguing phenomena of cellulose pyrolysis and proposed the established kinetic scheme in 1960s (Broido and Kilzer 1963; Kilzer and Broido 1965). As described in **Scheme 1** (Fig. 2-1) (Kilzer and Broido 1965; Broido and Weinstein 1971), the decomposition of cellulose can be represented through two competing reactions: the first step is estimated to be important at low temperatures and slow heating rates, accounting for the slight endothermic formation of anhydrocellulose below 553 K detected by DTA. At about 553 K a competitive, more endothermic unzipping reaction is initiated for the remained cellulose, leading to the tar formation. The third step presents the exothermic decomposition of anhydrocellulose to char and gas. This Broido' s kinetic scheme is re-examined by Argawal (Agrawal 1988), revealing that the rates of anhydrocellulose formation are comparable to those of the depolymerization process only in one case for temperatures of ~ 543 K in the isothermal, fixed-bed conditions. Then, the mechanism is approved through the isothermal, fluid-bed experiments in the temperature range 523-573 K, providing a complete set of kinetic data for the Broido model (Agrawal 1988). It is worthy noting that the formation of the anhydrocellulose as an intermediate product is undetectable in the experiments, and no kinetic data for the char forming reaction are reported in the above publications. These ambiguities stimulated the global researchers' interests in the kinetic studies of cellulose pyrolysis, resulting in a vigorous debate in the following years.

Scheme 1:

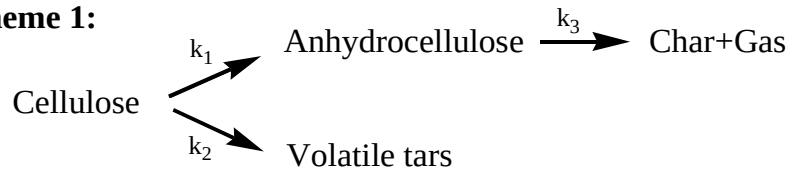

Fig. 2-1: the kinetic model for cellulose pyrolysis proposed by Broido and Weinstein (1971) (Broido and Weinstein 1971)

In 1975, Broido and Nelson examined the effect of thermal pretreatments at 230-275 ^{o}C on the cellulose char yields varying from 13% (no thermal pretreatment) to over 27% (Broido and Nelson 1975). They employed the large samples of cellulose (100 mg of shredded cellulose, and 7 cm × 3 cm sheets, individually wrapped several layers deep around a glass rod), which might incur the char formation from solid-vapor interactions during the prolonged thermal pretreatment. The previous kinetic model (**Scheme 1**) is correspondingly improved as described in **Scheme 2** (Fig. 2-2), eliminating the formation of the anhydrocellulose as an intermediate product.

Scheme 2:

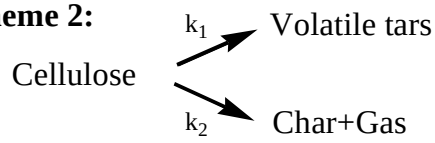

Fig. 2-2: the kinetic model for cellulose pyrolysis proposed by Broido and Nelson (1975) (Broido and Nelson 1975)

One year later, Broido (Broido 1976) reported a kinetic analysis of a 1000 h (about 6 weeks) study of cellulose pyrolysis under vacuum by thermogravimetry (TG) at 226 ^{o}C. The analog computer was employed to simulate mass loss according to the model given in **Scheme 3** (Fig. 2-3). The product "A" (later called "active cellulose") formed through step 1 performs as an important intermediate for the subsequent formation of both volatiles and char. Some data at high temperatures were also analyzed and activation energies for the steps were correspondingly reported. Later with regard to

Scheme 3, Varhegyi et al. found a better fit to the thermo-analytical curve when the active cellulose ("A") was eliminated from the reaction model as described in **Scheme 4** (Fig. 2-4). Nevertheless, the kinetic Scheme 3 for cellulose pyrolysis proposed by Broido (Broido 1976) has become the foundation for almost all subsequent research in this field (Antal and Varhegyi 1995).

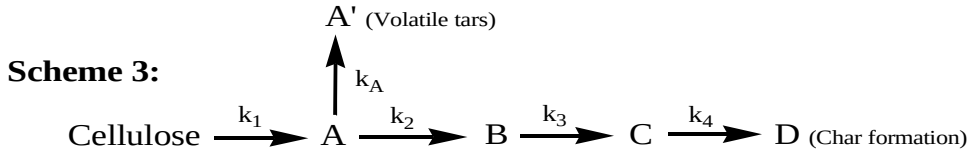

Fig. 2-3: the kinetic model for cellulose pyrolysis proposed by Broido (1976) (Broido 1976)

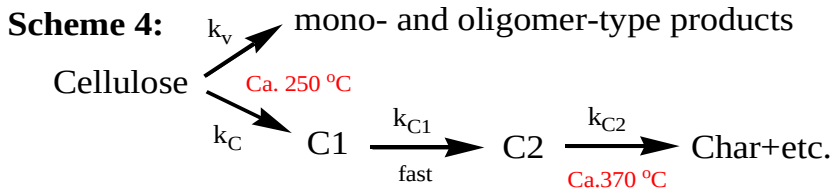

Fig. 2-4: the kinetic model for cellulose pyrolysis proposed by Varhegyi et al. (1994) [20]

In 1979, the Shafizadeh's group undertook a kinetic study of cellulose pyrolysis through the pyrolysis apparatus consisted of a horizontal, cylindrical and electrically heated furnace containing a Pyrex tube where another Pyrex tube was placed (Bradbury, et al. 1979). 250 mg sample of cellulose was tested in the pyrolysis apparatus at the temperature ranging from 259 to 341 ^{o}C, and a chemical reaction model for cellulose displayed in **Scheme 5** (Fig. 2-5) was proposed to give a good fit to the weight loss data through the numerical integration.

The **Scheme 5** is slightly different from those proposed by Broido and the co-workers but largely confirms the previous findings, which is even titled as "Broido-Shafizadeh

model" in somewhere (Antal and Varhegyi 1995; Colomba 1998; Liao 2003; Wooten, et al. 2004). At the low temperatures (259-295 ^{o}C), the initiation period (characterized by an accelerating rate of weight loss (Shafizadeh, et al. 1979)) has been explained as a formation of "active cellulose" through the depolymerization process (reduction of the DP) with the activation energy of 242.8 kJ/mol. Then, the "active cellulose" undergoes the two competitive reactions to produce either char and gas (activation energy 153.1 kJ/mol) or primary volatiles (197.9 kJ/mol). At high temperatures (above 295 ^{o}C), no initial period of accelerating rate of weight loss was observed in Shafizadeh's study (Bradbury, et al. 1979). Thus cellulose degradation mechanism was described simply via two competitive first-order reactions, where the formation of "active cellulose" is eliminated from **Scheme 5**. This mechanism is then confirmed by Antal and Varhegyi' TGA study of cellulose pyrolysis with the heating rate of 40 K/min, attaining the activation energy for the formation of volatiles as 238 kJ/mol and 148 kJ/mol for the formation of char and gas (Varhegyi, et al. 1994).

Scheme 5:

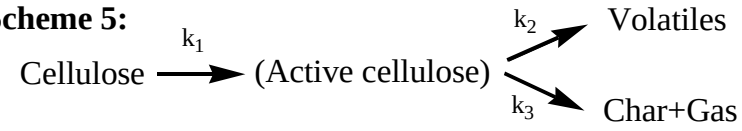

Fig. 2-5: the kinetic model for cellulose pyrolysis proposed by Bradbury et al. (1979) (Bradbury, et al. 1979)

The primary volatiles from cellulose pyrolysis are postulated to be anhydrosugars of which Levoglucosan appears to be the predominant product from cellulose (Piskorz, et al. 1986). In 1982, Shafizadeh improved the mechanism **Scheme 5** since the volatiles (anhydrosugars) displayed in Scheme 5 act not only the main primary product from cellulose, but also the intermediates for the formation of the small fragments through the secondary cracking reactions (Shafizadeh 1982). Although the role of vapor-solid interactions in the char formation was referred in Schafizadeh et al's study (1979): "… pyrolysis of levoglucosan is approved to give some residual char, and it has been suggested that char formation is not a primary step but is a result of repolymerization of

volatile material (Shafizadeh, et al. 1979), this relationship between the char formation and volatiles is not involved in the mechanisms proposed by him. Actually, the char formation through the vapor-solid interactions is also observed and presented in some other publications (Piskorz, et al. 1986; Mok, et al. 1992; Varhegyi, et al. 1993; Antal and Varhegyi 1995; Wooten, et al. 2004; Hosoya, et al. 2007; Hosoya, et al. 2008).

Scheme 6:

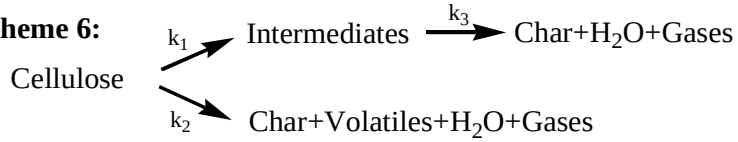

Fig. 2-6: the kinetic model for cellulose pyrolysis proposed by Varhegyi et al. (1993) (Varhegyi, et al. 1993)

Varhegyi proposed a mechanism for cellulose pyrolysis in a sealed crucible, displayed in **Scheme 6** (Fig. 2-6) (Varhegyi, et al. 1993). The kinetic **Scheme 6** confirms the secondary char formation from the repolymerization of intermediate (volatiles) catalyzed by the water from the dehydration reaction, giving a good fit to nine different DSC experiments completed by Mok et al. (Mok, et al. 1992). However, the structure and composition of the char residue from cellulose pyrolysis is ambiguous and the variation of its characteristics is difficult to detect, restraining the improvement of the kinetic mechanism for cellulose pyrolysis.

The argument between Antal-Varhegyi and Broido-Shafezadeh is remarkable, concerning the existence of "active cellulose" during the pyrolysis of cellulose. Antal and Varhegyi presented that no evidence was found to support the inclusion of the initiation step displayed in the **Scheme 5** (titled as "Broido-Schafezadeh model"), whatever this step proceeded at an immeasurably high rate at conditions of interests, or it does not exist (Antal and Varhegyi 1995). The kinetic **Scheme 7** (Fig. 2-7) proposed by Banyasz et al. (Banyasz, et al. 2001) fully excluded the notion of "active cellulose" and explained the experimental facts solely by cellulose depolymerization through two reaction channels, confirming the results by Antal and Varhegyi. Moreover, the weight-loss data of

cellulose pyrolysis at primarily higher temperatures and heating rates has been more successfully predicted by omitting the active cellulose intermediate (Wooten, et al. 2004). In 1995, Antal et al. concluded that the pyrolysis behavior of cellulose samples is well represented by a simple, single-step, irreversible, first-order rate law with a single high activation energy (Antal and Varhegyi 1995). Most of the kinetic models discussed above (mainly derived from TGA studies) are possibly outstanding for simulating the mass loss curve of cellulose, but not involving the information about the formation of specific products. Besides, the uncertainty on the existence of "active cellulose" (intermediate) and the ambiguity of the char formation is still persisting, which needs to be specified demanding the employment of the advanced analytical equipments (such as FTIR, GC-MS, HPLC, NMR and so on).

Scheme 7:

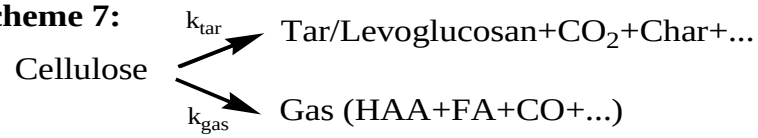

Fig. 2- 7: the kinetic model for cellulose pyrolysis proposed by Banyasz et al. (2001) (Banyasz, et al. 2001)

With the development of the advanced analytical equipments, the depolymerization of cellulose and the formation of cellulose with a lower DP (active cellulose) at the low temperatures has been evidenced in several reports (Wooten, et al. 2004), even under flash pyrolysis conditions (Diebold 1994; Boutin, et al. 1998; Piskorz, et al. 2000; Lede, et al. 2002). In 2002, Lede et al. directly observed a transient "intermediate liquid compound" in small pellets of cellulose that had been heated by radiant flash pyrolysis in an imaging furnace, which is characterized by HPLC/MS and found to be composed predominantly of anhydro-oligosaccharides (such as levoglucosan, cellobiosan and cellotriosan) (Lede, et al. 2002). In the slow heating experiments of cellulose, Wooten (Wooten, et al. 2004) revealed that intermediate cellulose (IC) is an ephemeral component that appears and then disappears over the course of 60 min of heating at 300 ^{o}C, while the rapid disappearance of IC in samples that have been heated at only a slightly higher temperature (i.e., 325 ^{o}C) further demonstrates the transient nature of IC.

This behavior clearly identifies the compound(s) as a reaction intermediate, and the authors correspondingly associated this intermediate compound with the "active cellulose" in the Broido and Shafezadeh kinetic models (**Scheme 3** and **Scheme 5**) (Broido 1976; Bradbury, et al. 1979). Thus, some recent researchers have attained the formation of "active cellulose" as an intermediate during cellulose pyrolysis, as presented in **Scheme 8** (Fig. 2-8) (Piskorz, et al. 1986; Piskorz, et al. 1989) and **Scheme 9** (Fig. 2-9) (Diebold 1994).

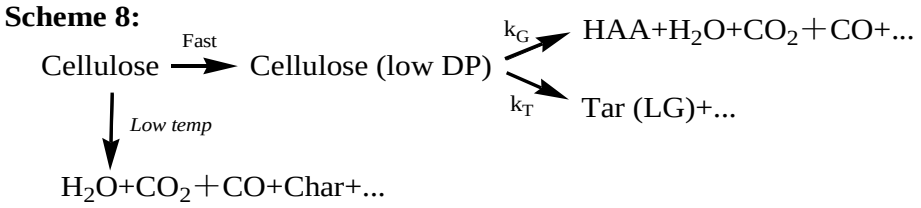

Fig. 2- 8: the kinetic model for cellulose pyrolysis proposed by Piskorz et al. (1986) (Piskorz, et al. 1986)

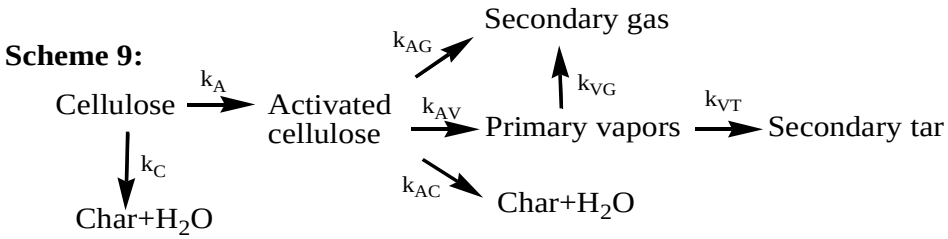

Fig. 2-9: the kinetic model for cellulose pyrolysis proposed by Diebold (1994) (Diebold 1994) and similarly proposed by Wooten et al. (2004) (Wooten, et al. 2004)

Both **Scheme 8** and **Scheme 9** establish the formation of water, primary char and "active cellulose" during the low temperature step of cellulose pyrolysis, but the char formed by the repolymerization of the cellulose with low DP ("activated cellulose") is not considered in **Scheme 8**.

Previously, Bradbury et al. (Bradbury, et al. 1979) and Antal (Antal and Varhegyi 1995) suggested that char formation might result from the repolymerization of volatile materials such as levoglucosan. This phenomenon is approved by Hosoya (Hosoya, et al. 2007), presenting that the secondary char from cellulose is formed from the repolymerization of anhydrosugars (levoglucosan). The experimental data from the Wooten et al.'s study (Wooten, et al. 2004) shows that a precursor-product relationship does exist between intermediate cellulose ("active cellulose") and the aliphatic and aromatic components of the char. The kinetic **Scheme 10** (Figure 2-10) proposed by Mamleev (Mamleev, et al. 2007) also confirms this finding, elucidating that whatever intermediate or levoglucosan (LG) and cellobisan are all performed as the precursor for the formation of char.

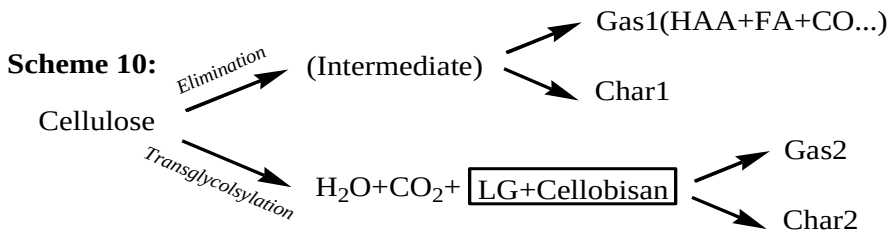

Fig. 2-10: the kinetic model for cellulose pyrolysis proposed by Mamleev et al. (2007) (Mamleev, et al. 2007)

Nowadays, it might be not difficult to evidence the existence of "active cellulose" or other important products with the help of the advanced analytical equipments, but the chemical reaction mechanism for cellulose pyrolysis is still ambiguous and controversial. One of the possible routes to improve the understanding of the structure changes of cellulose molecules and formation of the specific products is to employ the study of thermal decomposition of the relevant derivatives. Furthermore, the molecular dynamic simulation, well-established for estimating the dynamic mechanism from the microscopic point of view, would be another innovative method to specify the chemical pathways. The intermolecular hydrogen bonding and that between the different molecular chains would be another uncertainty for understanding the pryolytic behavior of cellulose, especially for the initial stage of the cellulose pyrolysis.

2.2.2 Hemicellulose

Hemicellulose constitutes approximately 10-35% of the weight of most woods (Fengel and Wegener 1984; Hosoya, et al. 2007). The structure of hemicellulose extracted from biomass is more complicated than that of cellulose, due to the abundant side-chains linked through different glycosidic bonds (Dumitriu 2005). It may include several components such as xylose and mannose, which are the prevalent monomers for hardwood and softwoods, respectively, glucose, galactose, arabinose and other polysaccharides as the monomer for side-chains (Fengel and Wegener 1984). Due to its lower content in biomass, few studies have been carried out on the pyrolysis of hemicellulose, which is thermally less-stable than other components in biomass and plays an important role in the initiation of the pyrolytic reactions of wood (Shafizadeh, et al. 1972).

A summary of the on-line pyrolysis studies of hemicellulose (essentially xylan) both static (isothermal) and dynamic (variable temperature) is presented by Di Blasi and Lanzetta (Blasi and Lanzetta 1997), in terms of one-step and multi-step reaction mechanisms (Table 2-1). The isothermal experiments have been carried out by TGA technique (Ramiah 1970; Bilbao, et al. 1989; Blasi and Lanzetta 1997), an open oven (Stamm 1956) and a tube furnace (Koufopanos, et al. 1989). Dynamic studies have also been conducted through TGA techniques and tube reactors (Ramiah 1970; Min 1977; Simkovic, et al. 1988; Bilbao, et al. 1989; Williams and Besler 1993) with the heating rate from 1.5 to 80 K/min and temperature in the range 468 - 993 K. The simplest model of xylan pyrolysis is a one-step global reaction (Stamm 1956; Ramiah 1970; Min 1977; Bilbao, et al. 1989; Williams and Besler 1993) (Fig. 2-11 (1)). Evaluation of the kinetic parameters (activation energy and pre-exponential factor) through one-step reaction (isothermal) kinetics shows comparable values for the data reported in (Ramiah 1970; Koufopanos, et al. 1989) (E=10.2~30 kcal/mol and A=590~4.6×10^{7} min^{-1}), whereas those obtained through data in (Stamm 1956) are much higher (E=26.7 kcal/mol and A=2.16×10^{12}). It is plausible that this behavior is due to the different experimental conditions and, more precisely, to possible oxidation processes in (Stamm 1956). .

Table 2-1: the summary of the on-line pyrolysis studies of hemicellulose (especially xylan)

Reactor	Sample	Heating Rate	Temperature	Kinetic mechanism	Author(s)
Glass bulb in an oil bath or an electric oven	Hemicellulose isolated from Douglas fir sawdust (40-60 μm)	Isothermal	383-493 K	One-step reaction	(Stamm 1956)
TGA/DTA	50 mg xylan (from beech wood holocellulose)	Isothermal	477-494 K	Two-step reactions	(Shimizu and Teratani 1969)
TGA/DTA under vacuum	200 mg potassium xylan (30-50 μm	Isothermal 4 K/min	488-523 K 468-538 K	One-step reaction Two-step reactions	(Ramiah 1970)
Ceramic tube + gas detector	Kinetics as difference from wood (0.7 g fir and 0.79 g beech)	30 k/min	~ 833 K	One-step reaction	(Min 1977)
DuPont 990 modelar thermal analysis system	Xlyan from larchwood	Isothermal	473-563 K	Multi-step reactions	(Bar-Gadda 1980)
TGA	Kinetics as difference from wood (100 mg of wild cherry wood)	1.7-9.4 K/min	~ 673 K	Multi-step reactions	(Ward and Braslaw 1985)

TGA	2-4 mg of commercial xylan	1.5-80 K/min	473-673 K	One-step reaction	(Bilbao, et al. 1989)
TGA	Sawdust 50 mg (0.3-0.85 mm)	5-80 K/min	~ 973 K	Multi-step	(Koufopanos, et al.
Tube furnace	Sawdust 150 mg (0.3-0.85 mm)	Isothermal	573-973	reactions	1989)
TGA/DTA	1-2 mg xylan from beech sawdust	10, 80 K/min	~ 623 K	Two-step reactions	(Varhegyi, et al. 1989)
Tube furnace with high heating rate (~ 100 K/s)	Commercial xylan	Isothermal	473-613 K	Two-step reactions	(Di Blasi and Lanzetta 1997)
Thermobalance (Dupont 951)	Kinetics as difference from walnut, hornbeam and pine (25-27 mg)	10 K/min	~ 723 K	Two-step reactions	(Muller-Hagedorn, et al. 2003)

Comparable reaction rates are also observed under dynamic condition (Koufopanos, et al. 1989; Williams and Besler 1993), for comparable heating rates. However, the activation energies decrease and the pre-exponential factors increases with the heating rate in one case (Williams and Besler 1993), whereas the opposite trend is seen in the other study (Koufopanos, et al. 1989). Though one-step mechanism is useful to describe the global solid degradation rate, they cannot be applied to predict product distribution from chemical reactor simulation, as a constant ratio of char to volatile yields is assumed, which might be substantially influenced by the variation of experimental conditions.

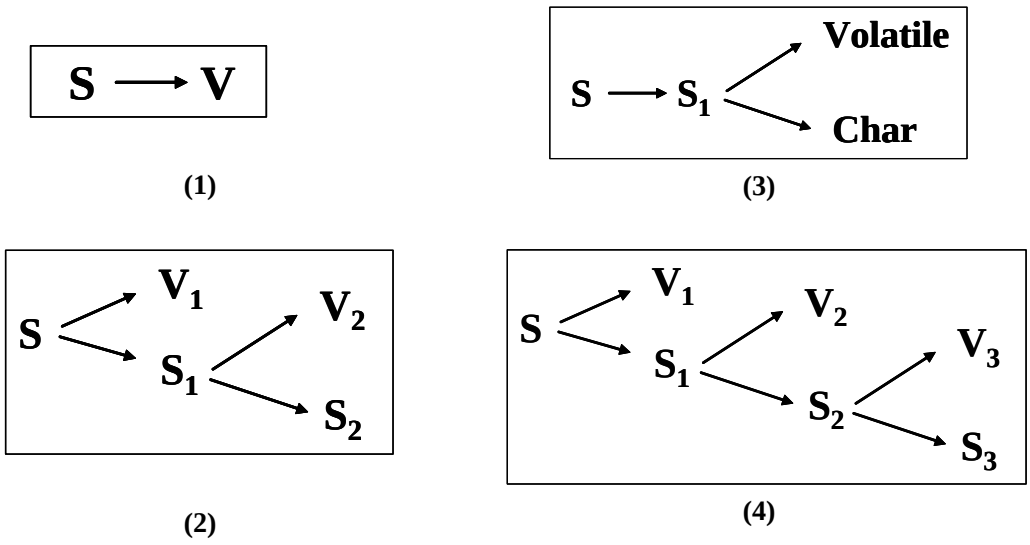

Fig. 2-11: the kinetic mechanisms of hemicellulose degradation

Some studies on the thermal degradation of xylan and the related model compounds have shown the existence of a two-step decomposition mechanism (Shimizu and Teratani 1969; Ramiah 1970; Shafizadeh, et al. 1972; Simkovic, et al. 1988; Varhegyi, et al. 1989; Blasi and Lanzetta 1997) (Fig. 2-11 (2)). "Cleavage of the glycosidic group, polymerization of the glycosyl units, decomposition of the sugar moiety within a narrow range of temperature was postulated in (Shafizadeh, et al. 1972). Mass spectrometric (Simkovic, et al. 1988), DTA (Varhegyi, et al. 1989) and calculated DTG (Muller-Hagedorn, et al. 2003) curves also appear to confirm the existence of consecutive steps. The estimation of kinetic data for mechanisms based on the two consecutive reactions of xylan pyrolysis

has also been proposed in (Shimizu and Teratani 1969; Varhegyi, et al. 1989; Blasi and Lanzetta 1997).

The multi-step reaction mechanism has been presented in (Bar-Gadda 1980; Ward and Braslaw 1985; Koufopanos, et al. 1989). The kinetic scheme proposed in (Koufopanos, et al. 1989) for xylan pyrolysis includes a zero-order stage, presumably describing a sort of depolymerization process, followed by two reactions for the formation of volatiles and a solid charred residual, through 1.5 order Arrhenius reactions which is similar as that of cellulose (Fig. 2-11 (3)). These two reactions are not truly competitive because the two activation energies are equal. Thus, this model again predicts a solid char yield not dependent on temperature. Three consecutive steps are considered in (Ward and Braslaw 1985) for the kinetics of hemicellulose pyrolysis, derived as the different between those of wood and the other two components (lignin and cellulose) (Fig. 2-11 (4)). Again, a constant ratio between total volatile and char yield is assumed. Compared to the kinetic scheme proposed by Ward and Braslaw, Bar-Gadda chose a model composed from nucleation, growth of nuclei and a diffusion-controlled decay for the pyrolysis of hemicellulose in the temperature range of 200-290 ^{o}C.

In all above cases, kinetic data have been estimated assuming that the temperature of the samples is the same as that of heating system and no temperature gradients are established through the sample. Apart from (Bilbao, et al. 1989; Varhegyi, et al. 1989), rather large amounts of powdered sample have been degraded and it is unlikely that the above assumptions are valid. Antal (Antal and Varhegyi 1995) pointed out that these conditions are difficult to achieve, and that heat transfer limitations may cause large errors in the evaluation of the intrinsic kinetics of solid degradation. Other limitations are usually encountered in both the dynamic and the isothermal investigations on hemcielluloses degradation currently available. The main draw back of the dynamic analysis is that the heating rate, which highly affects the reaction process, is much slower than those usually achieved in chemical reactors (gasification and pyrolysis). Therefore, the degradation kinetics may not be valid for conditions different from those under which they have been derived. In the static analysis two different methodologies are followed

to attain the isothermal stage, that is very slow heating rate (1.5-2.5 K/min) to avoid intra-particle temperature gradients (Shimizu and Teratani 1969; Bilbao, et al. 1989), or the sample holder is introduced in a pre-heated or high-heating-rate reactor in order to keep short the first dynamic stage (Koufopanos, et al. 1989; Blasi and Lanzetta 1997). However, in the first case, the weight loss is not negligible in the heating stage and the subsequent interpretation of the data may be lacking of an important part of the whole process. In the second case, the results may be seriously affected by heat transfer limitation.

Finally, a question may arise as to how the degradation process of the same material, under similar conditions, can be described either by a one-step global reaction or by a multi-step mechanism. An answer to this question is given in (Varhegyi, et al. 1989). It is shown that the time derivate of the solid weight fraction as a function of the temperature exhibits a double peak, which is well fitted by a two-step, consecutive reaction scheme with the deviations 1.3-1.7%. Furthermore, it is noted that the DTG curves can also be fitted by a one-step reaction, but the deviation becomes rather greater (10%). Small deviations (1.2%) are, on the contrary, observed when the slope is much less evident. This may explain why in several cases one-step reaction scheme appear to describe the kinetics of xylan degradation quite well. These models, whatever one-step reaction or multi-step reactions, can predict the global solid degradation rates or mass losses, but no information can be obtained on the dependence of product yields/distributions on reaction temperature. Therefore, the detection and characterization of the volatiles with the elevated temperature should be carried out, together with solid degradation. This may help figure out the possible chemical pathways of the product formation, in order to improve the current kinetic models of hemicellulose degradation.

2.2.3 Lignin

Thermal decomposition of lignin, which is estimated as the most thermally stable component in wood, occurs in a broad temperature range from 200 to 500 ^{o}C (even higher than 500 ^{o}C) resulting in 30-50% char and a significant amount of low molecular

mass volatiles, in addition to the monomeric and oligomeric products (Koufopanos, et al. 1989; Caballero, et al. 1995; Varhegyi, et al. 1997; Colomba 1998). Among the major components of biomass, lignin presents the greatest difficulty in understanding the relationship between structure and the devolatilization mechanisms that occur during typical thermochemical conversion processes (Evans, et al. 1986). This is due to the complexity of its 3-D polymerized structure which is varied for different wood species, and the difficulty in isolating lignin without significantly altering the structure. There are a great number of studies on specifying the relationship between lignin structure and its pyrolytic mechanisms (Antal 1985; Evans, et al. 1986; Amen-Chen 2001).

Thermogravimetric methods have been largely applied for lignin on-line pyrolysis studies. Results from these types of experiments can be used to interpret the kinetics of lignin and wood pyrolysis (Nguyen, et al. 1981; Koufopanos, et al. 1989). These studies have shown that lignin is the most heat-resistant component in wood. The weight loss profile depends on the lignin isolation methods (Gardner, et al. 1985; Evans, et al. 1986) and the nature of wood species (Faix, et al. 1988). Shafizadeh and McGinnis (Shafizadeh and McGinnis 1971) studied the components of cottonwood by TGA and concluded that the pyrolysis of wood was the sum of the pyrolysis of the separated components. The showed that milled wood lignin started devolatilizing in low yields at low temperature and continued to devolatilize with the increased temperature, but only experienced a 50% weight loss at 500 ^{o}C. The pyrolysis of an acid lignin was even more refractory starting at higher temperature and giving higher char yields. This work has been expanded by Gardner et al. (Gardner, et al. 1985) to include a variety of lignins prepared from hardwood and softwood species. They found that thermal behavior during pyrolysis depends upon the degree of condensation present in the initial lignin. TGA was a simple and accurate method to determine the extent of lignin condensation. Domburg et al. (Domburg, et al. 1974) applied thermal analysis to lignin preparations isolated from aspen and spruce. They found that the thermal stability of alky-aryl ether bonds in coniferous lignin was higher than in deciduous lignins, but also depend on the method of lignin isolation, increasing with the severity of the procedure. Antal (Antal 1985) used TGA and differential thermal gravimetry to provide evidence for the role of competitive

mechanisms: a low activation energy pathway that involved condensation reactions and a high activation energy step that produced lignin monomers. Antal also cites other work that supports a low-temperature condensation mechanism.

The kinetics of isothermal pyrolysis of lignins occurring in hard wood was studied by Pasquali and Herrera (Pasquali and herrera 1997) using thermogravimetric technique (TG/TGA). The thermograms in all the studied species were determined the kinetic parameters for the isothermal pyrolysis in the temperature range between 226 and 435 ^{o}C using Avrami-Erofeev equation for solid state reactions and the Ahhenrius equation, involving the first-order global kinetic model. The similar single-reaction, first-order decomposition model for lignin was also derived by Nunn et al. (Nunn, et al. 1985) employing a heated grid to study lignin pyrolysis. The thermal behavior of a hardwood lignin was investigated by thermogravimetric analysis (TGA) and differential scanning calorimetry (DAC). Kinetic parameters were determined for pyrolysis of lignin from room temperature to 300 at 15 K/min. The maximum rate of thermal destruction of lignin occurred between 246-259 ^{o}C. The DSC thermogram of lignin showed an endothermic peak at approximately 113 ^{o}C. The kinetic model was applied, since the weight loss data showed the first-order decomposition with Ahhrenius behavior. The activation energy value obtained for lignin was in the range of 8-68 kcal/mol corresponding to the mass loss from 0.4-1.0, but not involving the information of chemical reactions. Comparatively, maximum rate of weight loss has been observed between 360 and 470 ^{o}C for spruce, beech and bamboo milled-wood lignin (MWL) by Faix et al. (Faix, et al. 1988).

Dominguez et al. (Dominguez, et al. 2008) determined thermal stability of 17 organosolv lignin samples pyrolysis through thermogravimetric analysis. The kinetic parameters of lignin pyrolysis were calculated by Borchardt-Daniels' method assuming *n*th-order reaction, giving the average value of 28.1 kJ/mol. Avni (Avni and Coughlin 1985) investigated the kinetics of lignin pyrolysis using TGA in the range 20-800 ^{o}C at atmospheric pressure. A conversion-dependent activation energy model is proposed for representing the kinetics of lignin pyrolysis, giving a special case of a Gaussian

distribution of an activation energy model. This continuous distribution type model is improved and then applied for the lignin decomposition by the later workers (Caballero et al. (Caballero, et al. 1995; Caballero, et al. 1996) and Fedrous et al. (Ferdous, et al. 2002)), but it appears to be too complex for the kinetic calculations (Varhegyi, et al. 1997). Thermogravimetric analysis provides valuable information on pyrolysis kinetics, but it does not provide further information concerning the nature of the evolved volatile compounds.

Thermogravimetry-mass spectrometry (TG-MS) (Evans, et al. 1986; Faix, et al. 1988; Jakab, et al. 1995; Jakab, et al. 1997) and thermogravimetry-Fourier transform infrared spectroscopy (TG-FTIR) (Fenner and Lephardt 1981; Pasquali and herrera 1997; Liu, et al. 2008) have been applied to analyse the volatile compounds formed during pyrolysis. These techniques allow a rapid characterization of vapors produced by pyrolysis before condensation so as to avoid any possible rearrangement of oil that may occur during storage.

Fenner and Lephardt (Fenner and Lephardt 1981) applied TG-FTIR to Kraft pine lignin from ambient temperature to 850 ^{o}C. Two steps of decomposition were distinguished by these authors, the first between 120 ^{o}C and 300 ^{o}C and the second in the range 300-480 ^{o}C. The highest rate of weight loss was initiated at 300 ^{o}C and extended to 480 ^{o}C. At this temperature, the weight loss corresponded to nearly 50% of the kraft lignin. Formic acid, formaldehyde, sulphur dioxide, carbon dioxide and water were identified among the volatile compounds released during the first decomposition step. The formation of formaldehyde was attributed to the C_{β}-C_{γ} cleavage in the alkyl side chains having HO-groups in the γ-position. Following the same reasoning, acetaldehyde can be expected from a C_{β}-C_{γ} cleavage. But this compound has not been reported among the volatile compounds. Water was detected throughout the degradation temperature range. Carbon monoxide and carbon dioxide were detected at temperatures approximately 50 ^{o}C higher that the initial appearance of water. The low temperature at which oxygenated compounds evolved indicated that aliphatic HO-groups were easily removed by alkyl C-C cleavage of phenylpropane side chains, particularly at the terminal

positions yielding formaldehyde and carbon monoxide or dioxide. Moreover, the dehydration reactions yielded compounds with alkyl or vinyl bonds. Light compounds such as methanol and methane initially evolved together at approximately 300 ^{o}C. However methanol evolution was detected in a narrower temperature range at 300-500 ^{o}C than methane at 300-650 ^{o}C.

Faix et al. (Faix, et al. 1988) identified the volatiles released during the course of a milled-wood lignin thermal degradation of beech and spruce species by TG-MS. They reported a wide temperature range of water evolution which was in agreement with the findings of Fenner and Lephardt (Fenner and Lephardt 1981) using TG-FTIR for a Kraft lignin sample study. Both the original moisture in the feedstock and the pyrolytic water contributed to the water release. Water release was found in a temperature range 100-290 ^{o}C, 475-480 ^{o}C and 590-610 ^{o}C during drying and dehydration reactions. Dehydration reactions produced new C-C bonds, which increased the lignin heat resistance. Dehydration of aliphatic HO-groups was most likely the source of pyrolytic water as already proposed by Fenner and Lephardt (Fenner and Lephardt 1981). Faix et al. (Faix, et al. 1988) concluded that the softwood lignins were easier to dehydrate than the hardwood lignins. Methyl radicals were detected at a pyrolysis temperature range 300-600 ^{o}C. They believed that the demethylation of methoxy groups in guaiacyl and syringyl occurs at about 450 ^{o}C while the alkyl chains decompose at about 600 ^{o}C. Evolution of methoxy radicals was also detected at almost the same temperatures as the methyl radicals observed by Fenner and Lephardt (Fenner and Lephardt 1981). These radicals were mainly attributed to the decomposition of terminal aliphatic HO-groups. Formaldehyde and acetaldehyde were also detected among the volatile compounds from lignin pyrolysis. Formaldehyde was mostly produced between 320 ^{o}C and 350 ^{o}C. In contrast, acetaldehyde evolution was not uniform.

Liu et al. (Liu, et al. 2008) studied the pyrolysis of lignin extracted from birch (hardwood) and fir (softwood) using TG-FTIR in the range of 20-800 ^{o}C with the heating rates of 10, 20 and 40 K/min. The spectra of gas release exhibited the three main pyrolytic regimes for both two lignins: 1) the initial pyrolysis stage at 100 ^{o}C and 85 ^{o}C for fir and birch

lignin mainly caused by the release of water; 2) first major stage for fir and birch lignin at 223 ^{o}C and 227 ^{o}C attributed to the vigorous evolution of diverse volatiles including monomeric phenols, CO, CO_2, acetic acid, formaldehyde, methanol and water; 3) the second major stage for birch and fir lignin at 425 ^{o}C and 375 ^{o}C corresponding to the formation of CO, CO_2, hydrocarbons and methanol. Although the evolution of volatile compounds located in which temperature range is not well specified, the pyrolytic regime(s) for lignin, except the initial stage as drying of lignin sample, is in accordance with the findings by Fenner and Lephardt (Fenner and Lephardt 1981). A separated-stage kinetic model, involving the three pyrolytic regimes, is proposed by Liu (Liu, et al. 2008), also giving the calculated kinetic parameters for the two lignin species at different heating rates. The pyrolytic regime(s) of lignin extracted from different raw materials between room temperature and 600 ^{o}C is also determined through DTA analysis by El-Kalyoubi and El-Shinnawy (El-kalyoubi and El-shinnawy 1985): endothermic tendency around 100 ^{o}C because of the free water evaporation, and two exothermic process at about 320 ^{o}C and 480 ^{o}C in the active pyrolysis temperature range while the first exothermic peak represents the main oxidation and decomposition reaction and the final exothermic peak represents charring. However, the DTA analysis of lignin pyrolytic regimes is not incorporated in his global reaction model. Squire and Solomon (Squire and Solomon 1983) and King and Solomon (King and Solomon 1983), in collaboration with Avni et al., have extensively studied the pyrolysis of steam explosion lignin extracted by a variety of solvents. Mechanisms are discussed that cover three reaction regimes with the help of ionization mass spectrometric analysis of the volatiles/tars: 1) low-temperature processes below 350 ^{o}C where aliphatic hydroxyl groups are eliminated to give water, formaldehyde and residual olefins; 2) medium-temperature processes from 350 ^{o}C to 600 ^{o}C where lignin depolymerizes and light gases derived from functional groups are evolved; and 3) high-temperature processes from 600 ^{o}C to 1000 ^{o}C where the tar undergoes secondary cracking.

Gardner et al. (Gardner, et al. 1985) studied the effect of the lignin isolation methods on their thermal degradation behavior. Lignin from different wood species was isolated separated by the hydrochloric acid, Klason, enzymatic and steam exploded methods.

The fractions were compared by differential thermogravimetric analysis (DTA). The Klason lignin was more heat-resistant than the other lignin fractions and exhibited a broad DTA peak, while the steam exploded and the enzymatic lignins exhibited sharper peaks. The authors related these observations to the more condensed structure of the Klason lignin due to the drastic conditions used for its isolation. Klason lignin pyrolysis yielded considerably less guaiacol, methylguaiacol, syringol and syringaldehyde than HCl-lignin from the same wood species. However, a detailed analysis of the phenolic compounds was not provided. Avni et al. (Avni and Coughlin 1983; Avni, et al. 1985) studied the pyrolysis of lignin separated by steam-explosion and solvolysis methods. Flash pyrolysis, as well as slow heating rate pyrolysis, was carried out in a heated grid in which on-line, in-situ gas and tar pyrolysis was performed by Fourier transform infrared spectroscopy. Evans et al. (Evans, et al. 1986) also investigated the pyrolysis of lignin isolated from different methods by using TG-MS, estimating that only ball-milled lignin gives a close approximation of the peak distribution observed in the whole biomass sample, while steam explosion and kraft lignin may be important pyrolysis feedstocks themselves but the results of pyrolysis studies of there feedstocks should be applied to whole lignocellulosics with caution. The results of the comparisons indicate that problems may occur if a separated lignin is to be used to determine the pryolysis characteristics of lignin in native biomass samples.

Jakab's laboratory (Jakab, et al. 1993; Jakab, et al. 1995; Jakab, et al. 1997) have contributed a great deal of studies on pyrolysis of lignins from different species and isolation methods (steam-explosion, Alcell, Indulin and Sucrolin) by thermogravimetry/mass spectrometry (TG-MS). The intensity and the evolution profile of the products reflect the severity of the isolation procedure and the origin of the lignin. They also estimated that the methane yielded from the methoxyl group content provided evidence that the scission of methoxyl groups results in the formation of methane as well as methanol (Jakab, et al. 1995). At high temperatures, complex char forming reactions occur involving the complete rearrangement of the carbon skeleton and the release of gas products. The presence of cations (Na^+, NH_4^+, Ca^{2+}) has a significant effect on the course of decomposition, finding that sodium enhances the formation of char and gaseous

products. Jakab et al. (Jakab, et al. 1991; Jakab, et al. 1993; Jakab, et al. 1997) carried out TG-MS studies to clarify the details of the reactions, but the corresponding mechanisms were too complex for mathematical modeling. To date, the kinetic model for lignin pyrolysis is only related to (mass-loss) separated pyrolytic stage(s), but not involving the specific chemical reactions and the information of volatiles evolution.

2.3 The off-line pyrolysis of the main components of woody biomass

The off-line pyrolysis study of biomass and its components, employing the pyrolysis reactor, condensing system and gas collecting system, is utilized to investigate the yield of the products. The compounds in the liquid and gaseous products are identified by GC-MS, HPLC, NMR and so on, which sometimes are equipped with the pyrolysis reactor (Evans, et al. 1986; Piskorz, et al. 1986; R.J. Evans and Milne 1987; Piskorz, et al. 1988; Padkel and Roy 1991; Pakdel, et al. 1992; Banyasz, et al. 2001; Liao 2003; Arias, et al. 2006; Hosoya, et al. 2007; Hosoya, et al. 2007; Nakamura, et al. 2007; Bridgwater 2008; Hosoya, et al. 2008; Hosoya, et al. 2008; Hosoya, et al. 2008; Kawamoto, et al. 2008; Nowakowski and Jones 2008; Kumar, et al. 2009). The main purpose of the off-line pyrolysis study could be summarized as: 1) obtaining the yield of the main products (gas, liquid and char) and the distribution of the specific compounds in the products under different operating conditions (such as reactor, temperature and residence time); 2) proposing the possible chemical pathways for the decomposition of the macromolecules and secondary cracking of volatiles, in order to understand the formation of the specific compounds in the gaseous, liquid or solid phase; 3) optimizing the design and operating conditions for the thermal conversion process, to promote the yield of high-quality fuel and/or high-valued chemicals from biomass or its components.

2.3.1 Cellulose

Compared to the on-line pyrolysis study of cellulose, the off-line pyrolysis of cellulose is mostly carried out under the relatively high temperature (higher than 400 ^{o}C) or high heating rate (more than or around 1000 ^{o}C/s) (Hajaligol, et al. 1982; Piskorz, et al. 1986; Richards 1987; Radlein, et al. 1991; Boutin, et al. 1998; Wooten, et al. 2004; Hosoya, et

al. 2007; Aho, et al. 2008), concerning the following issues: 1) the distributions of the gas, liquid and solid products; 2) the formation of the specific compounds and the pyrolytic chemical pathways. How these two issues may be influenced by the pyrolytic reactors and the variables like temperature, residence time, heating rate, pressure, particle size, catalytic salts and crystallinity is extensively examined in the literature, in order to promote the product specificity, maximize the yield and improve the understanding of the pyrolytic mechanism.

In this work, the emphasis is on the effects of the predominant factors such as the reactor type, temperature or heating rate, residence time on the distributions of the products (gas, liquid and solid) from cellulose pyrolysis. Considering the complexity of chemical constituents in gas and liquid products, the attention would be confined to those few compounds which have been established to be producible in good yield (such as levoglucosan, hydroxyacetaldehyde, furfural, CO, CO_2 and so on), in order to meet the interests in potential industrial applications.

The distributions of gas, liquid and solid products

Regarding the commercialization of the pyrolytic technology for bio-energy conversion, the designed pyrolytic reactor involving the variation of the operating parameters (temperature, residence time, pressure and so on) has remarkable effects on the threshold of the specific product yield and the operating cost of the process (Beenackers 1999; Bridgwater 1999; Garcia-bacaicoa, et al. 2008; Kumar, et al. 2009). The reactors for the fast (off-line) pyrolysis of biomass to produce bio-oil or fuel gases is summarized by Bridgewater (Bridgwater 2008), estimated in terms of product yield, feed size, input gas, complexity and so on (Table 2-2). Compared to the fixed bed reactors, the fluidized bed reactor is determined to be one of the promising technologies for biomass thermal conversion due to the high-efficient heat transfer and ease of scale-up, which has potential for commercial practice (Garcia, et al. 1995; Islam, et al. 1999; Mohan, et al. 2006; Park, et al. 2008; Zheng, et al. 2008).

Table 2-2: the characteristics of the fast (off-line) pyrolysis reactors of biomass (Bridgwater 2008)

Reactor	Status*	Liquid yield wt%	Feed size	Input gas	Complexity	Scale-up
CFB	Pilot	75	Medium	High	High	Easy
Fluidized bed	Demo	75	Small	High	Medium	Easy
Rotating cone	Pilot	65	Very small	Low	High	Hard
Ablative	Lab	75	Large	Low	High	Hard
Vaccum	Demo	60	Large	Low	High	Hard
Auger	Lab	65	Small	Low	Low	Easy
Entrained gas flow	Lab	65	Small	High	High	Easy

*: Demo scale is estimated to be 200-2000 kg/h, pilot scale is 20-200 kg/h and lab scale is <20 kg/h.

The outstanding contribution on study of cellulose pyrolysis in the fluidized bed reactor was made by the research group led by Scott and Piskorz in the University of Waterloo in Canada (Scott and Piskorz 1982; Scott and Piskorz 1984; Piskorz, et al. 1986; Piskorz, et al. 1988; Piskorz, et al. 1989; Radlein, et al. 1991; Piskorz, et al. 2000). A bench scale atmospheric pressure fluidized bed unit using sand as the fluidized solid with the feeding rate of 30 g/h of biomass was designed to investigate the yield of liquid product at different temperatures in an inert nitrogen atmosphere with an apparent vapor residence time of approximately 0.5 s (Scott and Piskorz 1982). Piskorz (Piskorz, et al. 1986) reported the pyrolytic behavior of the two types of cellulose (S&S powdered cellulose with ash content of 0.22% and Baker TLC microcrystalline cellulose with ash content of 0.04%) in the fluidized bed reactor, giving the distribution of the gas, liquid and solid products at the temperature from 450 to 550 ^{o}C summarized in Table 2-3. The yield of organic products in the liquid phase (except water) from the S&S powdered cellulose ranges from 58.58% to 67.81% of the moisture and ash free feed at the temperature from 450 to 550 ^{o}C, reaching the maximum at 500 ^{o}C.

Table 2-3: the summary of the studies on fast (off-line) pyrolysis of cellulose

Author(s)	Sample	Pyrolysis reactor	Conditions		Yield of products (wt%)		
			Temperature (^{o}C)	Residence time (s)	Gas	Liquid [1] (water)	Char
(Mohammed, et al. 1982)	No. 507 filter paper	Screen-heating Pyrex reactor (fixed bed)	400 ~ 1000	0 ~ 30	5.25 ~ 46.97	16.37 ~ 83.35	3.32 ~ 78.37
(Mok and Antal 1983)	Whatman filter paper	Two-zone tubular micro reactor (fixed bed) [3]	800	1 ~ 18	62 ~ 71	--	15 ~ 23
(Graham, et al. 1984)	Avicel pH-102 crystalline cellulose	Downflow entrained bed (fluidized) reactor	750 ~ 900	< 0.6	74.7 ~ 98.1	0.7 ~ 15.8 [4]	--
(Piskorz, et al. 1986; Piskorz, et al. 1989)	S&S powdered cellulose	Fluidized bed reactor	450 ~ 550	0.53 ~ 0.56	8.49 ~ 17.89	68.75 ~ 75.59 (7.35 ~ 10.17)	4.2 ~ 8.53
	Baker TLC crystalline cellulose		500	0.48	5.1	94.7 (4.6)	1.0
(Radlein, et al. 1991)	Commercial SS-144 crystalline cellulose	Fluidized bed reactor	500	< 0.5	7.8	83.3 (10.8)	5.4

	Avicel pH-102 crystalline cellulose		500	< 0.5	3.9	89.6 (6.1)	1.3
(Liao 2003)	Filter paper with ash content of 0.01%	Gravitational feeding reactor (Fixed bed)	300 ~ 1090	0.1 ~ 1.4	1.5 ~ 60.2	6.0 ~ 86.3	1.8 ~ 92.5
(Aho, et al. 2008)	Microcrystalline cellulose powder	Batch-operating fluidized bed reactor	460	<1.5	32.3	47.6 (24.5)	20.1
(Hosoya, et al. 2007)	Cellulose powder from Toyoroshi Co.	Cylindrical furnace and tube reactor (fixed bed)	800	30	12.9	77.1 (5.1)	10
(Shen and Gu 2009)	Microcrystalline cellulose powder	Batch-operating fluidized bed reactor	420 ~ 730	0.44 ~ 1.32	20.1 ~ 42.5	30.6 ~ 72.2	1.03 ~ 47.4

1: the yield of liquid product including water;
2: the pressure of the reactor is 5 psig of helium pressure;
3: the operating pressure in the furnace is 5 atm;
4: including solid product (char);

Comparatively, the yield of organic products from the Baker TLC microcrystalline cellulose at 500 ^{o}C is determined to be 90.1%. Moreover, the yield of char for S&S powdered cellulose at 500 ^{o}C is 3.4%, compared to 1.0% for Baker TLC microcrystalline cellulose. These results confirms that the larger amount of the inorganic salts in the ash content promotes the formation of the condensed structure through the catalytic effects, inhibiting the cracking of the macromolecules and enhancing the yield of solid product (Shafizadeh 1982; Radlein, et al. 1991; Colomba 1998; Liao 2003; Shen and Gu 2009; Shen, et al. 2009). Several years later, the pyrolysis of the two further types of cellulose (commercial SS-144 crystalline cellulose and Avicel pH-102 crystalline cellulose) were also studied in the fluidized bed by Piskorz's co-worker (Radlein, et al.) (Radlein, et al. 1991), presenting the yield of the products in Table 2-3. The temperature 500 ^{o}C, regarded as the optimal condition for producing bio-oil from cellulose in the fluidized bed reactor, gives the yield of organic products of 72.5% for commercial SS-144 crystalline cellulose and 83.5% for Avicel pH-102 crystalline cellulose. The difference should also be attributed to the catalytic effect of inorganic salts in the ash, since the yield of char for commercial SS-144 crystalline cellulose is 5.4% compared to 1.3% for Avicel pH-102 crystalline cellulose.

Recently, Aho (Aho, et al. 2008) conducted the pyrolysis of softwood carbohydrates under the nitrogen atmosphere in a batch-operating fluidized bed reactor, where the quartz sand was used as bed material and the load of the raw material is approximately 10 g. All sand was kept in the reactor by a net at the upper part of the reactor. The evolved vapors were cooled in the four consecutive coolers with the set point of -20 ^{o}C, while between the third and fourth cooler the vapors were passed through a water quench with the pH value of 3 for avoiding the absorption of CO_2. The furnace temperature was kept at 490 ^{o}C until the release of non-condensable gases stopped, while the temperature in the reactor is about 460 ^{o}C. The vapor residence time was estimated to be less than 1.5 s based on the height of the reactor and the actual fluidizing gas velocity. The distribution of the products from cellulose (microcrystalline cellulose powder) is shown in Table 2-3, giving the low yield of organic products of 23.1% and high yield of char as 20.1%. The condensation of the vapors was estimated to be insufficient, while the

values for gases and char can be considered reliable. It should be mentioned that the mass balance of the experiment could not be satisfactorily completed, due to its current reactor set-up (especially the vapor-cooling and liquid-precipitating system).

A similar batch-operating fluidized bed reactor was designed by D.K. Shen, in order to study the fast pyrolysis of biomass and its components with the variation of temperature and vapor residence time under inert atmosphere (Shen and Gu 2009; Shen, et al. 2010; Shen, et al. 2010). No bed material was applied and the load of the raw material is about 5 g. The solid product was captured by the carbon filter, while the evolved hot vapors were cooled through the two U-tubes immersed in ice-water mixture (0 ^{o}C) and dry ice-acetone (-30 ^{o}C), respectively. The distribution of the products from the pyrolysis of microcrystalline cellulose at temperatures between 420 and 730 ^{o}C with a residence time from 0.44 to 1.32 s is given in Table 2-3. It is estimated that the yield of liquid product reaches its maximum of 72.2% at the temperature of 580 ^{o}C with the residence time of 0.44 s. The higher temperature and long residence time promotes the decomposition of the macromolecules and cracking of the volatile, enhancing the yield of gases and reducing the solid product (Shen and Gu 2009).

Graham (Graham, et al. 1984) designed a complicated entrained bed reactor to investigate the fast pyrolysis of cellulose, which had a similar or even higher heating rate than that of fluidized bed. The rapid heat transfer and thorough mixing between the particulate solids and feed are accomplished in two vertical gas-solids contactors: Thermovortactor and Cryovortactor. The biomass or other carbonaceous fuel is rapidly mixed with the hot particulate solids in Thermovortactor. The suspension passed through a downdraft entrained-bed (fluidized) reactor allowing the individual setting of temperatures, and then was quenched by the cold solids in the Cryvortactor and cooled through the cooling coil submerged in a water tank. The solids were then separated in the mass balance filter and the gas was collected in sampling bags. The feeding rate is less than 1 kg/h and the total elapsed time from the Termovortactor inlet to the cryovortactor exit is typically less than 600 ms. The yield of the gas and liquid (heavy fraction including tar and char) products at the temperature from 750 to 900 ^{o}C is shown in Table 2-3. The low yield of

liquid product (less than 20%) is mainly due to the high reactor temperature and the inefficient cooling method. Moreover, the mass balance is not convincing, since the heavy fraction of the vapors may condense on the vessels of Cryovortactor and solid separator (Graham, et al. 1984). It should be noted that the high yield of gases is attributed to the enhanced heat transfer through the pre-mixing between the biomass and solid heat carrier before being fed to the pyolsyis reactor, compared to that of fluidized bed reactor.

The residence time (both solid and vapor) in the fluidized or entrained bed reactors could be narrowly changed (normally less than 1 s), because of the confinement of the minimum gas velocity for the solid fluidization. Therefore, the fixed bed reactors are designed for investigating the effect of not only temperature but also residence time on the yield of products and their specificity (Hajaligol, et al. 1982; Mok and Antal 1983; Liao 2003; Hosoya, et al. 2007). Liao (Liao 2003) designed a fixed bed reactor (quartz tube with a sample-holder in the middle), the temperature of which could be changed from 0 to 1100 ^{o}C. The filter paper shaped as 18*50 mm (about 2 g) is fed gravitationally to the reactor from the top, and the carrier gas (nitrogen) brings the evolved volatiles and some char fragments through the carbon filter. The purified volatiles are then cooled through the three traps consecutively: 1) the mixture of water and ice (0 ^{o}C); 2) the mixture of acetone and dry ice (-30 ^{o}C); and 3) assisting cooling agent (-45 ^{o}C). The yield of the products (gas, liquid and char) at the temperature from 300 to 1090 ^{o}C with the (vapor) residence time between 0.1 to 1.4 s determined by the carrier gas velocity is extensively discussed by Liao (Liao 2003) (shown in Table 2-3), while the mass balance for all the experiments is convincingly located between 96% and 101.5%. With the same vapor residence time (carrier gas velocity), the yield of liquid product complies with a Gaussian distribution with temperature, giving the maximum of 86.29% (including 15.72% water) at around 600 ^{o}C with the residence time of 0.1 s. It is estimated that the long residence time promotes the yield of gases, due to the sufficient secondary reactions of the volatiles. The yield of gases is increased from 1.5% to 60.2% monotonously with temperature (from 300 to 1090 ^{o}C). It needs to be noted that the

duration of each experiment, corresponding to the sample heating-up and holding time, is not specified in the work.

The pyrolysis of cellulose in a tube (fixed bed) reactor made of Pyrex glass is investigated by Hosoya et al. (Hosoya, et al. 2007). Compared to the study of Liao (Liao 2003), the cellulose sample is horizontally fed to the furnace and the carrier gas is not employed which means that the vapor residence time could not be set individually. It is estimated that thirty seconds are enough for completing the pyrolysis since no volatile product formation is observed after a longer pyrolysis time. The evolved volatiles are retained in the reactor with the solid residue during the whole pyrolysis process. After 30 s pyrolysis, the reactor is pulled out from the furnace and cooled with an air flow for 1 min at the room temperature. The tar (liquid product) condensed on the reactor vessel is extracted by *i*-PrOH and water. The amounts of the gaseous, tar and char fractions are determined gravimetrically after pyrolysis and extraction, giving the result at the temperature of 800 ^{o}C in Table 2-3. It should be mentioned that the temperature of the reactor is not evenly distributed during the pyrolysis process, because the bottom of the tube reactor was placed at the center of the cylindrical furnace. Most of the evolved volatiles are condensed at the upper part of the reactor, but not suffered from the vigorous secondary cracking due to the long (solid) residence time. Thus, the yield of liquid product (77.1% including water) is not visibly different from that of Liao's results at the temperature of 810 ^{o}C with the shorter vapor residence time (74.39%) (Liao 2003).

Another Pyrex cylindrical tube (fixed bed) reactor is made by Hajaligol et al. (Hajaligol, et al. 1982), where the cellulose sample is held and heated by the porous stainless screen connected to the brass electrodes of the reactor. The system allows independent variation of the following reaction conditions: heating rates (100-100 000 ^{o}C/s), final temperatures (200-1100 ^{o}C), sample residence (holding) time at final temperature (0-∞ s). Similar to the experimental set-up of Hosoya (Hosoya, et al. 2007), the vapor residence time could not be individually changed while the carrier gas is not employed. Part of the evolved vapors is rapidly diluted and quenched in the reactor vessel during the operation, because most of the gas within the reactor remains close to the room

temperature. The other part of the evolved vapors is purged out of reactor vessel with the helium and cooled down through two downstream traps: 1) U-tube packed with glass wool immersed in dry ice/alcohol (-77 ^{o}C) and 2) the same trap in liquid nitrogen (-196 ^{o}C). The char retained on the screen is determined gravimetrically. The mass balance for each case is around 100%, giving the convincing results of the yield of the products at the temperature 400- 1000 ^{o}C with the sample holding time 0-30 s in Table 2-3. It is concluded (Hajaligol, et al. 1982) that tar yield (liquid product) increases with temperature to a maximum of about 65% at around 700 ^{o}C and then decreases with further temperature increases, since the sample residence time is zero. With the long residence time (for example 30 s), the yield of liquid product at 400 ^{o}C is remarkably increased to 83.35%, due to the sufficient heating-up time for the complete pyrolysis of cellulose. Comparatively, the yield of liquid product at 500 ^{o}C with zero holding time is only 16.37% and the yield of char is 83.63% (where the mass balance is 105%), because of the incomplete decomposition of cellulose.

A two-zone tubular micro reactor (fixed bed) was designed by Mok and Antal (Mok and Antal 1983), to investigate the effect of vapor residence time on the yield of products from cellulose pyrolysis. Zone A is operated for 15 min for complete solid phase pyrolysis, while Zone B is maintained at 700 ^{o}C for vapor phase cracking. The char is determined gravimetrically, and the gases are collected by the replacement of water. Unfortunately, the tar collection is not possible with that apparatus. The results of the product distribution at the temperature of 800 ^{o}C with the vapor residence time 1-18 s are shown in Table 2-3. The long vapor residence time and high pressure (5 atm) promote the secondary cracking of volatiles, enhancing the yield of the gas product.

With regard to the above discussion, it can be summarized that the long vapor residence time could visibly promote the secondary reaction of the volatiles to favor the formation of gases, whatever the pyrolysis reactor is. The yield of liquid products is initially increased with the elevated temperature and then declines with temperature increases for both fluidized bed reactor (Piskorz, et al. 1986; Shen and Gu 2009) and fixed bed reactor (Hajaligol, et al. 1982; Liao 2003). Comparatively, the highest yield of liquid product

(about 90%) from the cellulose pyrolysis in fluidized bed reactor is accessed at the temperature of about 500-600 ^{o}C with a short solid residence time (Piskorz, et al. 1986), while the temperature for obtaining the highest yield of liquid product (about 85%) in fixed bed reactor (Liao 2003) is higher than 600 ^{o}C or even with longer solid residence time (Hajaligol, et al. 1982). This proves that fluidized bed reactor is a promising technology for thermal conversion of biomass to produce bio-oil due to its characteristics of high-efficient heat transfer and low energy input.

However, the condensing method, termed as direct condensing and indirect condensing, is another important factor to influence the distribution of the products. Direct condensing (such as quenching) is defined as the direct mixing of the cold cooling-agent and the hot vapor, giving the efficient heat exchange and precipitation (Scott and Piskorz 1982; Scott and Piskorz 1984; Piskorz, et al. 1986; Bridgwater 2008). The challenge is the selection of the cooling-agent which should be of large specific capacity and insoluble with the constituents in bio-oil. Indirect condensing is that the hot vapors are condensed through the heat exchanger immersed in the cooling agent (Hajaligol, et al. 1982; Liao 2003). Compared to the direct condensing, the indirect condensing method has lower efficiency of heat exchange, but the collected bio-oil (liquid product) is not contaminated by the cooling-agent. Thus, the indirect condensing method is applicable for the bench-scale analytical study, while the fluidized bed reactor equipped with the direct condensing assembly would be potential for the industrial application of bio-oil production.

The specificity of the typical compounds in the gas/liquid products

The volatiles (both condensable and non-condensable) produced from cellulose pyrolysis under moderate or high temperatures are very complicated, most of which have been identified by employing the advanced analytical equipments such as FTIR, GC-MS, HPLC, NMR and so on. A variety of pyran and furan derivatives (C_{5-6} ring-containing compounds), aliphatic oxygenated C_{2-4} organic compounds and light species/gases (such as light hydrocarbons, CO and CO_2) can be obtained, and the extensive lists together with their spectrometric/chromatograghic patterns and the yields are available in the literature,

where the results are remarkably affected by the pyrolytic reactor, operating condition, condensing method and sample sources (Graham, et al. 1984; Piskorz, et al. 1986; Pouwel, et al. 1989; Radlein, et al. 1991; Li, et al. 2001; Liao 2003; Hosoya, et al. 2007; Shen and Gu 2009). Due to the great potential as the feedstock for fuel and chemicals production, some products which are established in good yields (such as levoglucosan, furfural, hydroxyacetaldehyde, acetol, CO, CO_2 and so on) would be vigorously investigated regarding the chemical mechanism for their formation and fractionation, while other products would be briefly discussed.

Pyran- and furan- derivatives (C_{5-6} ring-contained compounds)

The C_{5-6} ring-containing compounds from cellulose pyrolysis are condensable and mainly composed of a variety of anhydrosugar and furan derivatives, among which levoglucosan (1, 6-anhydro-β-D-glucopyranose) are the most prevalent (Byrne, et al. 1966; Shafizadeh and Lai 1972; Schulten and Gortz 1978; Piskorz, et al. 1986; Pouwel, et al. 1989; Antal and Varhegyi 1995; Li, et al. 2001; Lede, et al. 2002; Liao 2003; Hosoya, et al. 2007; Kawamoto, et al. 2008; Shen and Gu 2009). Shafizadeh et al. confirmed that levoglucosan can be obtained in yields from 20% to 60% by weight in their vacuum pyrolysis study of various cellulose samples, while other anhydrosugars (such as 2,3-anhydro-d-mannose, 1,4:3,6-dianhydro-α-D-glucopyranose, 1,6-anhydro-β-D-glucofuranose and 3,4-altrosan) are slightly produced (less than 1% by weight) (Shafizadeh, et al. 1979). Similar results were reported by Piskorz et al. by comparing levoglucosan yields from S & S powdered cellulose (2.1%) and Baker TLC microcrystalline cellulose (25.2%) pyrolysis at the temperature of 500 ^{o}C under atmospheric pressure in a fluidized bed reactor (Piskorz, et al. 1986). Inasmuch as the cellulose samples have somewhat different ash contents, the different levoglucan yield may be due to the well-known effect of inorganic cations in reducing tar yields by promoting other fragments or char formation (Radlein, et al. 1991). Richards and co-workers established the extraordinary influence of salts and metal ions on the productivity of volatiles (especially levoglucosan and hydroxyacetaldehyde), presenting that the addition of alkali and Ca^{2+} cations to ash-free cellulose reduced the yield of levoglucosan while other metal ions (particularly Fe^{3+} and Cu^{2+}) enhanced the yield of

levoglucosan (Essig, et al. 1989; Richards and Zheng 1991). In accord with the findings of Richards's laboratory, Piskorz et al. observed very dramatic increases in the yields of levoglucosan (more than 30% by weight) from various celluloses after a mild sulfuric acid-wash pretreatment (Piskorz, et al. 1989). The profound effects of inorganic substances on the product from carbohydrates were also evidenced by Van der Kaaden through the matrix study on amylase pyrolysis using Curie-point (the apparatus for isothermally heating) pyrolysis, concluding that carbonyl compounds, acids and lactones are released by alkaline and neutral matrices while furans and anhydrohexoses are favored under neutral and acidic conditions (Kaaden, et al. 1983).

The experimental conditions as well as the purity of cellulose and inorganic additions appear to have an important effect on the yield of levoglucosan. The yield of levoglucosan produced from the S &S powdered cellulose pyrolysis in a fluidized bed is increased with the temperature, reaches its maximum at the temperature of 500 ^{o}C and then decreased with the elevated temperature (Radlein, et al. 1991). This is consistent with the results from Shen's work using fluidized bed reactor, giving the maximum yield of levoglucosan at the temperature of 530 ^{o}C (Shen and Gu 2009). A great deal of specific work studying pyrolysis oils produced from Whatman filter paper at the temperature from 400 ^{o}C to 930 ^{o}C in the fixed bed reactor confirmed that the formation of levoglucosan is mainly located at the temperature between 450 ^{o}C and 650 ^{o}C, obtaining the maximum yield at 580 ^{o}C (about 58.37% by weight of pyrolysis oil) (Liao 2003). Moreover, the yield of levoglucosan is decreased with the long vapor residence time at the temperature of 600 ^{o}C, while most of the small fragments (low molecular weight volatiles) are increased notably. These phenomena add the interests in looking inside into the chemical mechanism of the levoglucosan formation and its secondary cracking during the cellulose pyrolysis.

An established standpoint is that the formation of levoglucosan is initiated by disruption of the cellulose chain, primarily at the 1,4 glucosidic linkage in the macromolecule, followed by intramolecular rearrangement of the cellulosic monomer units (Shafizadeh, et al. 1979; Radlein, et al. 1991; Li, et al. 2001; Liao 2003; Shen and Gu 2009). The

actual mechanism of levoglucosan formation remains controversial. Golova favors a free-radical mechanism through the successful validation of the data on the effects of free-radical (Golova 1975). Shafizadeh arguing by analogy with the reactions of model phenyl glucosides prefers a heterolytic mechanism (Shafizadeh, et al. 1979). Essig and Richards (Essig, et al. 1989) proposed that the hydroxyl group (-OH) of free chain ends further depolymerizes the short chain through transglycosylation accompanying with the release of levoglucosan, while Shen and Gu (Shen and Gu 2009) gave the speculative chemical pathway for the formation of levoglucosan involving the free hydroxyl group. Another unsettled issue is whether depolymerization of macromolecule (disruption of cellulose chain) takes place by a concerted "unzipping" process or by random breaking of the cellulose chain. Briodo et al. (Briodo, et al. 1973) found that crystalline cellulose and undergoes a large change in DP before weight loss occurs. Similarly, Basch and Lewin (Basch and Lewin 1973) proposed that if cellulose depolymerized by an unzipping process then the number of free chain ends, as reflected by DP, will influence the initiation rate. Radlein (Radlein, et al. 1991) presented that one cellulose sample which has been heated to 180 ^{o}C for several hours and has a very low DP appears to give an abnormally high yield of levoglucosan. While the unzipping process may well operate at low temperature, there is evidence that it is inapplicable under fast pyrolysis conditions due to the significant amounts of cellobiosan and higher anhydro-oligomers in cellulose pyrolysates (Radlein, et al. 1991). The correlation between the yield of levoglucosan and DP of cellulose sample under fast pyrolysis conditions needs to be specified, attracting the interests for further study.

The usual view on the mechanism of levoglucosan cracking is that the lower molecular weight products are formed by fragmentation of principal intermediates like levoglucosan and cellobiosan as discussed by Pouwels et al. (Pouwel, et al. 1989). Such a scheme is also indicated by the data of Shafizadeh and Lu who showed that similar low molecular weight products (such as furfural, 5-HMF, glycolaldehyde, hydroxyacetone, acetic acid, formic acid and light species) as from cellulose pyrolysis can be formed by direct pyrolysis of levoglucosan (Shafizadeh and Lai 1972), which is consistent with the observation by Hosoya et al. through the NMR identification of levoglucosan pyrolysis

volatiles (Hosoya, et al. 2008). Evans et al. (Evans, et al. 1984) even concluded that both cellulose and levoglucosan were pyrolyzed at various residence times and give similar cracking patterns and products by using a flash pyrolysis-mass spectrometric technique.

However, Richards (Richards 1987) has argued that it is more likely that hydroxyacetaldehyde, known as one of the prominent products from cellulose pyrolysis, forms directly from cellulose by a plausible mechanism involving the dehydration followd by a ring-opening reaction but not from the secondary cracking of levoglucosan. Li et al. (Li, et al. 2001) presented that no detactable hydroxyacetaldehyde is observed by FTIR during levoglucosan pyrolysis in the two-zone pyrolysis reactor, indicating that levoglucosan might not be the major precursor of hydroxyacetaldehyde in cellulose pyrolysis. The two major pathways are then recognized to be active during cellulose pyrolysis: one leading to the formation of levoglucosan as a relatively stable product and the second to yield low molecular products particularly hydroxyacetaldehyde. The experimental studies of cellulose pyrolysis with the addition of inorganic substances show that conditions which result in the selective formation of levoglucosan realize very low yield of hydroxyacetaldehyder and vice versa, confirming the competitive nature of the above two pathways (Piskorz, et al. 1986; Essig, et al. 1989; Pan and Richards 1989; Richards and Zheng 1991; Antal and Varhegyi 1995; Hon and Shiraishi 2001).

Regarding to the notable argument on the relationship between levoglucosan and hydroxyacetaldehyde, Liao (Liao 2003) conducted the pyrolysis of both cellulose and levoglucosan under different temperature and vapor residence time in a fixed bed. For cellulose pyrolysis, the yield of levoglucosan is increased and then decreased with the elevated temperature reaching the maximum at the temperature of 580 ^{o}C, while the yield of hydroxyacetaldehyde is monotoneously increased with the temperature. Under the fixed temperature (610 ^{o}C), the long vapor residence time favors the yield of small fragments (especially hydroxyacetaldehyde) remarkably at the expense of levoglucosan, showing the plausibly “consecutive mechanism” between them. For levoglucosan pyrolysis, no hydroxyacetaldehyde (even some other prevalent volatiles from cellulose

pyrolysis) is detected at the temperature of 610 ^{o}C with the short residence time 0.1 s, confirming the "competitive mechanism" between levoglucosan and hydroxyacetaldehyde. But under the same temperature with the long residence time 1 s, almost all kinds of volatiles from cellulose are released from levoglucosan pyrolysis, enhancing the "consecutive mechanism" between levoglucosan and hydroxyacetaldehyde. The quantitatively similar results are reported by Shen and Gu (Shen, et al. 2009) for cellulose pyrolysis in a fluidized bed reactor at different temperatures and vapor residence times. The published data by Piskorz et al. (Piskorz, et al. 1989) presenting the variation of levoglucosan and hydroxyacetaldehyde yields with temperature are compatible with either mechanism.

The experimental results summarized above plainly reveal the hybrid relationship between levoglucosan and the low molecular weight fragments (particularly hydroxyacetaldehyde) during cellulose pyrolysis: both competitive and consecutive. However, the predominance of the nominal mechanism during cellulose pyrolysis is still ambiguous for specifying the hydroxyacetaldehyde (or other low molecular weight volatiles) formation and the extent of levoglucosan secondary decomposition, due to the widely varied experimental conditions and inorganic additions.

Furfural and 5-hydroxymethyl-furfural categorized as furan derivatives, are another two important $C_{5\text{-}6}$ ring-contained compounds in the products list of cellulose pyrolysis (Piskorz, et al. 1986). Although the yield of these two compounds is less than 1% by weight of fed cellulose, they are notably identified from the pyrolysis oil (GC-MS) spectrum of cellulose (Byrne, et al. 1966; Piskorz, et al. 1986; Pouwel, et al. 1989; Liao 2003; Hosoya, et al. 2007; Aho, et al. 2008; Shen and Gu 2009). The effect of experimental conditions (temperature and vapor residence time) on yield of furfural and 5-hydroxymethyl-furfural is fully discussed by Liao (Liao 2003), presenting that the formation of furfural is notably enhanced by the increased temperature and residence time while the yield of 5-hydroxymethyl-furfural is only increased with the elevated temperature. It is observed that these two compounds could be produced from levoglucosan pyrolysis under the suitable vapor residence time, showing the "consecutive

mechanism" between them. Moreover, furfural is found to be one of the important secondary cracking products from 5-hydroxymethyl-furfural pyrolysis. The commonly accepted standpoint concerning the chemical pathway for furfural and 5-hydroxymethyl-furfural is that levoglucosan or cellulose monomer undergoes ring-opening reaction to the C_6 aliphatic intermediate, followed by hemiacetal reaction between C-2 and C-5 to form furan-ring structure after the formation of acetone-structure on position C-2 through dehydration reactions (Shafizadeh and Lai 1972; Liao 2003). The 5-hydroxymethyl-furfural could be decomposed to furfural together with release of formaldehyde through the de-hydroxylmethyl reaction, furan methanol through de-carbonylation reaction, or 5-methyl-furfural through de-hydroxyl reaction (Shin, et al. 2001; Liao 2003; Shen and Gu 2009). It could be concluded that furfural and 5-hydroxymethyl-furfural are both competitively and consecutively produced with levoglucosan, while 5-hydroxymethyl-furfural is another source for the formation of furfural.

Aliphatic oxygenated C_{2-4} organic compounds

Perhaps the most unusual result noticeably in the compounds from cellulose pyrolysis is the abundance of hydroxyacetaldehyde (glycolaldehyde) and acetol (1-hydroxy-2-propanone) (Shafizadeh and Lai 1972; Piskorz, et al. 1986; Piskorz, et al. 1989; Radlein, et al. 1991; Liao 2003; Hosoya, et al. 2007; Shen and Gu 2009). A survey of literature reveals that these compounds were only occasionally reported as pyrolysis products, and have received very little attention in the sense of being a major product (Mohammed, et al. 1982; Mok and Antal 1983; Graham, et al. 1984). In 1966, Byrne et al. reported hydroxyacetaldehyde as one major components of a group of highly oxygenated products from pyrolysis of cellulose treated with flame retardants, along with glyoxal, pyruvaldehyde and 5-hydroxymethylfurfural (Byrne, et al. 1966). It is perhaps that Pikorz et al. who first called attention to hydroxyacetaldehyde as a major product from rapid pyrolysis of slightly impure cellulose in a fluidized bed reactor, obtaining approximately 18% yield by weight of S & S powdered cellulose (0.22% ash content) and 8% of Baker TLC microcrystalline (0.04% ash content) (Piskorz, et al. 1986). The difference of hydroxyacetaldehyde among diverse celluloses is possibly attributed to the

catalytic effects of inorganic salts in ash. A great deal of careful work on pyrolysis of cellulose treated with salts, neutral or acidic inorganics by Piskorz et al. and Richards' laboratory proves that the formation of hydroxyacetaldehyde is notably favored by the addition of alkali salts (such as NaCl), but inhibited by the addition of acid (such as H_2SO_4) (Essig, et al. 1989; Piskorz, et al. 1989; Radlein, et al. 1991; Richards and Zheng 1991).

Moreover, the study of cellulose (Whatman filter paper) pyrolysis in a fixed bed reactor by Liao (Liao 2003) indicates that hydroxyacetaldehyde is an important compounds in the condensed liquid product, the yield of which is notably increased from 3% to 19% by weight of liquid product with the elevated temperature (450 to 930 ^{o}C). The quantitatively similar result is reported by Shen and Gu (Shen and Gu 2009) studying the cellulose pyrolysis in a fluidized bed reactor under various temperatures and residence times. But the experimental data published by Piskorz et al. (Piskorz, et al. 1989) shows that yield of hydroxyacetaldehyde by weight of fed cellulose is increased with the temperature and starts to decrease at the temperature of 610 ^{o}C. Since the yield of liquid product against temperature is changed compatibly with the yield of hydroxyacetaldehyde (Piskorz, et al. 1986; Piskorz, et al. 1989; Liao 2003; Shen and Gu 2009), the apparent yield of hydroxyacetaldehyde by weight of fed cellulose performs a Gaussian distribution with temperature even though its relevant yield by weight of liquid product is increased with temperature.

Since no other C_2 or C_3 product appears in the same yield as hydroxyacetaldehyde, it is an intermediate or primary products formed early in the decomposition process through monomer ring cleavage. The most acceptable standpoint for hydroxyacetaldehyde formation is proposed by Shafizadeh and Lai (Fig. 2-12) (Shafizadeh and Lai 1972), presenting that hydroxyacetaldehyde, assumed as the precursor for glyoxal, was produced mainly from C-1 and C-2 position of the glucopyranose (Shafizadeh and Lai 1972). This scheme is similar to that proposed by Byrne et al. (Byrne, et al. 1966).

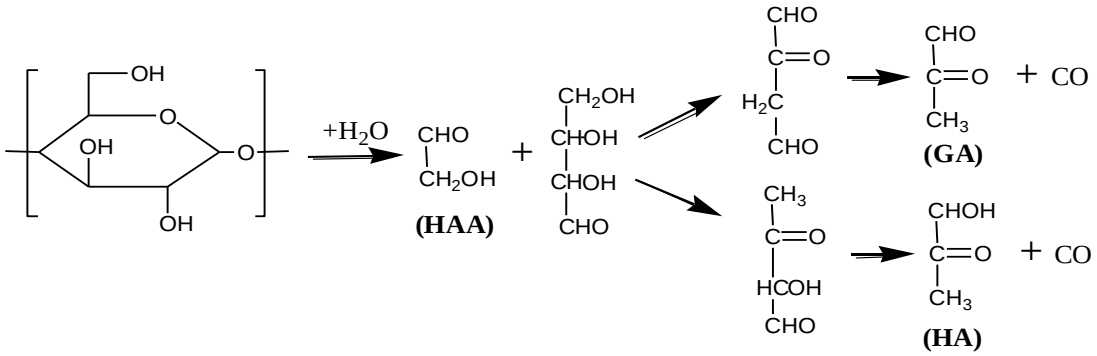

Fig. 2-12: the possible primary cracking of cellulosic monomer proposed by Shafizadeh and Lai (Shafizadeh and Lai 1972)

Through the examination of bond energies in the monomer unit by Frankiewicz (Frankiewicz 1980)and interatomic distance for β-D-glucose by Sutton (Sutton 1958), it was shown that the length for the C-2 to C-3 bond and for C-1 and O-ring linkage is slightly greater than other similar bonds. This finding is confirmed by Madorsky et al. (Madorsky, et al. 1958) who pointed out that the C-O hemiacetal bond on the ring is thermally less stable than C-C bonds. These information offer support to the hypothesis that initial ring cleavage of cellulose monomer tends to occur frequently at these two locations, yielding a two-carbon fragment and a four-carbon fragment, while the two-carbon fragment is rearranged to a relatively stable product, hydroxyacetaldehyde, and the four-carbon fragment can undergo a number of rearrangement of dehydration, scission and decarbonylation to yield a variety of lower molecular weight products (Piskorz, et al. 1986). This chemical pathway for the formation of hydroxyacetaldehyde is well presented in the study of Liao (Liao 2003) and Shen et al. (Shen and Gu 2009). They also suggested that almost all of the positions on the pyran-ring could be contributed to hydroxyacetaldehyde formation, involving the examples on C-2 to C-3 or C-5 to C-6 positions plausibly through the cracking of five carbon fragment from initial cleavage of monomer on the bonds of C-1 to C-2 and hemiacetal C-O. However, this suggestion should be evidenced through the bond energy examination and atomic label technology on the model compound.

Acetol (1-hydroxy-2-propanganone), regarded as another major product, is perhaps firstly reported by Lipska and Wodley (Lipska and Wodley 1969) in their study of isothermal cellulose pyrolysis at 315 ^{o}C. Moreover, some of cellulose fast pyrolysis studies have also evidenced the acetol as a major component in the products. For instance, Hosoya et al. (Hosoya, et al. 2007) obtained the acetol (in the *i*-PrOH-soluble fraction) yield of 1.1% by weight of fed sample from the cellulose pyrolysis at the temperature of 800 ^{o}C in a sealed tube. Two cellulose samples pyrolysed at the temperature of 500 ^{o}C in a fluidized bed reactor by Piskorz et al. (Piskorz, et al. 1986) gave the acetol yield of 3.2% for S & S Powdered cellulose and 0.7% for Baker TLC microstalline cellulose by weight of fed sample, which is possibly due to the well-known effect of inorganic salts. Meanwhile, the authors (Piskorz, et al. 1986) observed that the acetol yield from S & S Powdered cellulose pyrolysis is notably increased with the temperature. This phenomenon is also evidenced by the work of Liao (Liao 2003) studying cellulose pyrolysis in the fixed bed reactor and the fluidized bed reactor respectively, obtaining the range of acetol yield by weight of liquid product from 0.8% to 6% at the temperature from 450 ^{o}C to 930 ^{o}C.

In 1972, Shafizadeh and Lai (Shafizadeh and Lai 1972) proposed the possible chemical pathway for acetol formation from levoglucosan decomposition as the rearrangement of the four-carbon fragment from the primary pyran-ring cleavage, while the other two-carbon fragement might be the precursor for hydroxyacetaldehyde (Fig. 2-12). The similar reaction scheme is reported by Byrne et al. in 1966 (Byrne, et al. 1966) and proposed again by Piskorz et al. (Piskorz, et al. 1986) in 1986. Meanwhile, the pyruvaldehyde was also proposed to be formed through the rearrangement of the four-carbon fragment, competing with the formation of acetol (Fig. 2-12). It could be found that enol-structure from the dehydration between the conjunct carbon is the intermediate for the acetone-structure, while the dehydration is between C-5 and C-6 for acetol formation and between C-4 and C-5 for pyruvaldehyde formation. According to Benson's rules on energy grounds (Benson 1976), acetol should be favored over the alternative possibility of pyruvaldehyde. This speculation is evidenced by Piskorz (Piskorz, et al. 1986), Liao (Liao 2003) and Shen and Gu (Shen and Gu 2009) studying

cellulose fast pyrolysis in fixed bed reactor or fluidized bed reactor, obtaining higher yield of acetol over pyruvaldehyde. Moreover, other chemical pathways for acetol and pyruvaldehyde formation from the five-carbon fragment or ring-opened six-carbon intermediate are proposed by Liao (Liao 2003), which are then summarized in levoglucosan secondary cracking pathways by Shen and Gu (Shen and Gu 2009). However, the prevalent one for their formation, which might be affected by experimental conditions, is not specified, while their secondary cracking to CO and aldehyde-compounds could be readily determined.

Among a number of the detectable pyrolysis products from cellulose, some products, such as acetic acid, aldehyde, methanol, formaldehyde and so on, are less frequently discussed in the literature due to their low yields (Hajaligol, et al. 1982; Funazukuri 1983; Mok and Antal 1983; Graham, et al. 1984; Piskorz, et al. 1986; Radlein, et al. 1991; Liao 2003; Shen, et al. 2009). In an investigation of the formation of acidic product, Kang et al. (Kang, et al. 1976) proposed a mechanism of hydration of ketene which is formed from the dehydration of alcohol-aldehyde structure. This reaction scheme for carboxyl group formation was well-established by the following researchers (Piskorz, et al. 1986; Piskorz, et al. 1988; Radlein, et al. 1991; Liao 2003; Hosoya, et al. 2007; Shen and Gu 2009; Shen, et al. 2010), most of whom did not specify its position on the pyran-ring. The possible chemical pathways for cellulose primary reactions and volatile secondary cracking are systematically summarized by Shen and Gu (Shen and Gu 2009), giving a number of pathways for the formation of these low molecular weight oxygenated compounds.

Light species/gases

CO and CO_2 are regarded as the most dominant gas species in the gaseous product from cellulose pyrolysis, accounting for approximately 90% by weight of total gas products (Hajaligol, et al. 1982; Mohammed, et al. 1982; Funazukuri 1983; Mok and Antal 1983; Graham, et al. 1984; Piskorz, et al. 1986; Liao 2003; Aho, et al. 2008; Shen and Gu 2009). Hajaligol et al. presented that above 750 ^{o}C CO (more than 15% by weight of the fed) was the most abundant gaseous product from rapid pyrolysis of cellulose in the

screen-heating reactor, while CO_2 (around 3% by weight of fed) was the second abundant species in gaseous product (Hajaligol, et al. 1982). The result is agreed by Graham (Graham, et al. 1984) that CO is observed as the single most prevalent gas species with the yield of 63% mole percent of the product gas at the reaction temperature of 700 ^oC in the entrained down-flow reactor. Comparatively, Aho et al. (Aho, et al. 2008) obtained the higher yield of CO_2 than that of CO from the cellulose fast pyrolysis in a fluidized bed reactor at the temperature of 460 ^oC. The above phenomena are all evidenced by Piskorz et al. studying cellulose fast pyrolysis under the temperature of 450 ^oC, 500 ^oC and 550 ^oC in a fluidized bed reactor (Piskorz, et al. 1986), finding that CO_2 is predominant over CO in the gaseous product as the reaction temperature is lower than 500 ^oC, but above 500 ^oC CO turns to be dominant over CO_2. The different result is reported by Shen and Gu (Shen and Gu 2009) studying cellulose pyrolysis in a fluidized bed reactor, observing that the yield of CO is dominant over that of CO_2 in spite of the reaction temperature. Although the predominance of CO and CO_2 in gaseous product from cellulose pyrolysis against the variation of temperature is still controversial, the yield of CO is confirmed to be enhanced by the elevated reaction temperature while that of CO_2 is slightly changed (Hajaligol, et al. 1982; Piskorz, et al. 1986; Radlein, et al. 1991; Li, et al. 2001; Liao 2003; Shen and Gu 2009). The established explanation is that CO_2 is the primary product mainly formed at the low temperature stage, while CO is produced of large proportion from secondary tar decomposition steadily enhanced by the increased temperature.

Mok and Antal (Mok and Antal 1983) investigated the effect of residence time on the yield of main gas products from cellulose pyrolysis at the pressure of 5 psig, concluding that CO_2 formation was notably enhanced by the longer residence time while CO was inhibited. The different result is reported by Liao (Liao 2003) that CO is remarkably favored by the longer residence time while CO_2 is changed slightly, which is further confirmed by Shen and Gu (Shen and Gu 2009). Evans et al. (Evans, et al. 1984) proposed that carboxyl group formed through hydration of ketene structure is the precursor for producing CO_2, while CO is mainly produced through the decarbonylation reaction of aldehyde-type species. Since the ketene structure, which is related to the

formation of acidic compounds (containing carboxyl group), is mainly formed during the low temperature stage, CO_2 is approved to be the primary product of cellulose pyrolysis, and thus it is not remarkably influenced by reaction temperature. Comparatively, high reaction temperature favors the vigorous secondary tar cracking reactions, especially the carbonyl-group containing fragments, in order to enhance the formation of CO steadily and rapidly. This reaction mechanism is summarized from the results of the researchers (Evans, et al. 1984; Piskorz, et al. 1986; Radlein, et al. 1991; Li, et al. 2001; Liao 2003; Hosoya, et al. 2008; Shen and Gu 2009), however the preference of the carbon on the pyran-ring for CO and CO_2 formation is not specified. From the study of thermal decomposition of levoglucosan, Shafizadeh and Lai (Shafizadeh and Lai 1972) suggested that CO_2 was produced primarily from C-1 and C-2 position as well as hydroxyacetaldehyde, while the production of CO was less specific, but the information for cellulose pyrolysis is not ruled out.

It needs to be noted that the mole fraction of hydrogen (H_2) is also important as well as CO and CO_2 and constitutes approximately 21% of the product gas at the reaction temperature of 900 ^{o}C in the study of Garham et al. (Graham, et al. 1984). Quantitatively similar result is reported by Hajaligol et al. (Hajaligol, et al. 1982), also finding that the yield of H_2 is noticeably increased at the high temperature (more than 800 ^{o}C), while no hydrogen is observed at the low reaction temperatures. This implies that high reaction energy is required for the formation of hydrogen through the secondary tar cracking reaction. Li et al. (Li, et al. 2001) proposed that formaldehyde is precursor for hydrogen formation, together with the evolution of CO through the secondary cracking at around 550 ^{o}C. The same chemical scheme is proposed again by Liao (Liao 2003), Hosoya (Hosoya, et al. 2008) and Shen and Gu (Shen and Gu 2009), also giving the possible chemical pathway for hydrocarbons formation through the decarbonylation of aldehyde-type compounds together with the production of CO. It is also observed that both hydrogen and hydrocarbons formation are favored by the elevated temperature, confirming the enhancement of temperature on the secondary tar cracking reactions proposed above together with the evolution of CO. Since hydrogen is the important synthesis gas for methanol and other synthesis, the new methods coupled with thermal

technology but with low heating energy input, such as catalytic hydrothermal conversion technology (Watanabe, et al. 2002; Osada, et al. 2004; Hao, et al. 2005), are attracting global interests to specify the hydrogen formation from cellulose.

The products established in good yield from cellulose pyrolysis are extensively discussed in the above studies, involving a large number of plausible chemical pathways for the primary reactions and secondary tar cracking. It is commonly accepted that levoglucosan is the most prevalent product in the primary volatiles from cellulose pyrolysis, which could be further decomposed into various low molecular weight compounds (C_{2-4} compounds or light gases). However, the preference of the various primary reactions and secondary tar (especially levoglucosan) cracking reactions under widely varied experimental conditions with or without the catalysts needs to be further determined, in order to identify and promote the specific compound formation.

2.3.2 Hemicellulose

There are some other technologies (catalytic hydrolysis and enzymatics) to convert hemicellulose to value-added chemicals or fuel gases (such as H_2) (Goodwin and Rorrer 2009; Hakka and Jumppanen 2009), but the pyrolysis of xylan is of some practical importance because thermochemical technology is one of the most promising methods for utilization of biomass. Therefore, the laboratories led by Shafizadeh, Antal, Richards and Simkovic should be greatly appreciated for their great contributions on the off-line pyrolysis of hemicellulose (especially on xylan and the related model compounds) (Shafizadeh and McGinnis 1971; Shafizadeh, et al. 1972; Shafizadeh, et al. 1972; Stevenson, et al. 1981; Richards and Shafizadeh 1982; Simkovic, et al. 1987; Essig and Richards 1988; Simkovic, et al. 1988; Ponder and Richards 1990; Antal, et al. 1991; Ponder and Richards 1991; Simkovic, et al. 1995), concerning the distribution of the gas, liquid and char products, the chemical pathways for several typical compounds formation and effect of the addition of alkaline salts, metal ions and acidic compounds.

Xylan polysaccharides and model compounds have been considered in some cases,, which would be vigorously discussed in the following parts. it has been shown that degradation takes place in the temperature range 473-573 K (Simkovic, et al. 1987; Bilbao, et al. 1989; Varhegyi, et al. 1989; Simkovic, et al. 1995) or even lower (Ramiah 1970; Bar-Gadda 1980). For high temperatures (mostly in off-line pyrolysis studies), xylan pyrolyis products are mainly volatiles with solid char yields variable from about 20 to10%, depending on the heating rate, temperature and residence time (Shafizadeh, et al. 1972; Simkovic, et al. 1988; Ponder and Richards 1991). The following parts will be concentrated on the pyrolysis of xylan, due to its prevalent role in hemicellulose of hardwood, since less studies are reported for pyrolysis of mannose as the prevalent monomer in hemicellulose of softwood (Hosoya, et al. 2007).

Xylan chains are commonly 1,4-β-linked xylopyranose and usually carry abundant side chain(s) composed of L-arabinofuranose and/or uronic acid groups, while the details concerning the chemical structure of hemicellulose and xylan in different biomass is extensively discussed in (Dumitriu 2005). Thermal analysis of α-D-xylose and several xylopyranosides (methyl β-D-xylopyranoside), selected as model compounds, was conducted by Shafizadeh in 1970s (Shafizadeh, et al. 1971; Shafizadeh, et al. 1972), showing that heating of these molecules results in cleavage of the glycosidic group, polymerization of the glycosyl units, and decomposition of the sugar moiety within a narrow range of temperature. Later, the decomposition of the α-D-xylose and several xylopyranosides with the addition of zinc chloride was further analyzed and compared with the pyrolysis of 4-O-methylglucuronoxylan and O-acetyl-4-O-methylglucuronoxylan (which have different substituting groups or glycosides on the xylan backbone-chain) by Shafizadeh (Shafizadeh, et al. 1972). The pyrolysis experiments in a fixed-bed reactor at the temperature of 300 ^{o}C were carried out before and after addition of 10% zinc chloride for all samples, and the products were isolated as the char residue, a tar fraction which condensed at room temperature, a liquid fraction (aqueous pyrolysates) that was collected in a dry ice-acetone trap and carbon dioxide which was recovered as barium carbonate. It needs to be notified that CO, H_2 and hydrocarbons are exclusive in the mass closure of all pyrolysis products. The data

shows that, in all case, the addition of zinc chloride resulted in a decrease in the tar fraction but an increase in aqueous fraction and char. Without zinc chloride, the tar fraction of α-D-xylose (50.2% by weight of sample) is notably higher than that of 4-O-methylglucuronoxylan (15.7%) and O-acetyl-4-O-methylglucuronoxylan (33.1%), while the other three fractions of α-D-xylose is lower, probably due to the abundant substituting groups and glycosides on the xylan chain which may enhance the reactivity of molecules (Dumitriu 2005).

The composition of the products obtained from pyrolysis of α-D-xylose and methyl β-D-xylopyranoside at 500 ^{o}C, before and after treatment with zinc chloride, was determined by analysis of the liquid condensation product (aqueous pyrolysate) for qualitative analysis and by GPC (gel permeation chromatogram) of the pyrolysis products for quantitative investigations (Shafizadeh, et al. 1972). Pyrolysis of the tar fraction from α-D-xylose condensation gave a more complex mixture of volatile products containing large amounts of acetic acid (1.6%) and indicating a more-random breakdown and rearrangement of the molecule. It is evidenced that the pyrolysis volatiles (other than methanol, possibly derived from the methyl group linked to the xylan chain) consist mainly of 2-furaldehyde (5.8% for α-D-xylose and 2.4% for methyl β-D-xylopyranoside) and water, both of which are substantially increased by the addition of zinc chloride in all cases.

Complex mixtures of volatile products were also obtained on pyrolysis of 4-O-methylglucuronoxylan and O-acetyl-4-O-methylglucuronoxylan as such, or on addition of zinc chloride or sodium hydroxide at the same pyrolysis temperature of 500 ^{o}C. The formation of methanol in the mixtures (1.3%) can be attributed to the methyl group on the 4-O-methylglucuronic acid side-chain in the xylan polysaccharides, which is mainly inhibited by the addition of zinc chloride (1.0%), but enhanced by addition of sodium hydroxide (2.1%). Similarly, the high yields of acetic acid (10.3%) from O-acetyl-4-O-methylglucuronoxylan could be related to the abundant acetyl groups in the original material, which is notably inhibited by addition of both zinc chloride (9.3%) and sodium hydroxide (3.4%). For both samples, the formation of 2-furaldehyde, water and

char is enhanced by addition of zinc chloride, while that addition of alkali has resulted in increased fragmentation of molecule giving the increase of water and carbon dioxide but inhibition for 2-furaldehyde formation. However, comparison of the products formed from pyrolysis of levoglucosan and xylans indicate that the alkaline-framentation products of xylans are produced through more-extensive rearrangement or disproportionation reactions (Shafizadeh and McGinnis 1971; Shafizadeh, et al. 1971; Shafizadeh and Lai 1972; Shafizadeh, et al. 1972). By comparing the pyrolysis products of α-D-xylose, methyl β-D-xylopyranoside, xylan and their random-condensation products, it can be seen that substitution of the xylosyl units produce a quantitative variation of the products by changing the reactivity of different positions and influencing the patterns of the competitive, pyrolytic reactions, while the dehydration reactions are catalyssed by acidic conditions and alkali promote the fragmentation and rearrangement, enhancing the formation of char and water.

Later, the thermal degradation of methyl β-D-xylopyranoside with and without addition 1% sodium chloride at the temperature of 280 ^{o}C for 30 min was investigated by Ponder and Richards (Ponder and Richards 1991). The distillate fractions (namely, -50 ^{o}C condensates after removal of room temperature condensates as defined in (Shafizadeh, et al. 1972)) are predominantly water for both cases. Pyrolysis of xylan containing added sodium chloride resulted in increased yields of the one-, two- and three-carbon compounds in distillate at the expense of anhydrosugar (such as 1,4-anhydro-α-D-xylopyranose) yield in the tar fraction (reduced from 5.7% to 0.3%). These products are the same as those favored by the presence of sodium chloride in the pyrolysis of cellulose (Essig, et al. 1989). However, the yield of char from xylan pyrolysis is not notably affected by the addition of sodium chloride (from 48.2% to 43.1%), both of which are much higher than that (about 10%) obtained in the study of Shafizadeh (Shafizadeh, et al. 1972) because of the different reaction temperatures.

The 2-furaldehyde is formed by xylan pryolysis with or without sodium chloride (0.2% and 0.5%), but the influence of addition of sodium chloride is as noticeable as that with added zinc chloride (Shafizadeh and Lai 1972). A mechanism whereby 2-furaldehyde

can arise in the acid degradation of xylose has been proposed by Antal et al. (Antal 1985), and can be extrapolated to the pyrolysis of a xylan. This mechanism is only likely to apply to free xylopyranosyl cations derived from non-reducing end group and to in-chain scission products which are 1,4-linked and/or 1,3-linked, since the formation of the O-2 to C-5 bond required by this mechanism is sterically unlikely for a xylosyl cation linked at position 2. Another mechanism where 2-furaldehyde can be enhanced in the xylan pyrolysis with addition of zinc chloride was elucidated by Shafizadeh (Shafizadeh, et al. 1972), through the analysis of resulting volatiles from pyrolysis of several substituted phenylβ-D-xylopyranoside (Fig. 2-13). The glycoladhehyde was detected in the distillated fractions from the pyrolysis of xylan with addition of sodium chloride, while no glycoaldehyde was found in the study of xylan pyrolysis with or without added zinc chloride at the temperature of 500 ^{o}C. Conversely, the acetic acid as well as methanol from xylan pryolysis without sodium salt at 300 ^{o}C can not be detected in the distillate fraction, while large amounts of acetic acid are formed in the volatiles from xylan pyrolysis with and without added zinc chloride at the temperature of 500 ^{o}C.

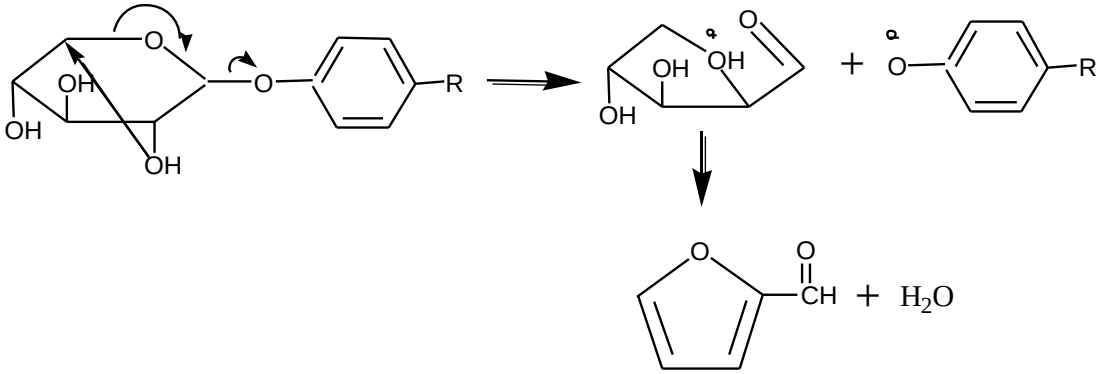

(2-furaldehyde)

Fig. 2-13: the chemical pathways for 2-furaldehyde formation from substituted phenyl β-D-xylopyranoside

It needs to be noted that the 3-hydroxy-2-penteno-1,5-lactone, as a marker compound from xylan in pyrolysis of biomass materials, was also evidenced in the tar fraction of xylan pyrolysis at 300 ^{o}C(Ponder and Richards 1991), which is promoted by the addition of sodium chloride. This compound previously reported as a product of xylan pyrolysis

by Miyazaki (Miyazaki 1975), and subsequently accepted by later workers (Ohnishi, et al. 1977; Pouwel, et al. 1987). The tar components listed in (Ponder and Richards 1991) accounts for less than one third of the total tar, and relevant analysis suggested the presence of a variety of oligomers (such as xylosylanhydroxyloses). However, most of these compounds in tar fraction cannot be identified in the study of Shafizadeh (Shafizadeh, et al. 1972), which might undergo thorough secondary cracking at the high temperatures.

In 2007, the pyrolysis of main chemical components in biomass, including commercial xylan, is individually investigated by Hosoya et al. (Hosoya, et al. 2007) employing a fixed bed reactor at the temperature of 800 ^{o}C for 30 seconds. The gas yield of xylan is 14.1%, while the liquid yield (both aqueous fraction and tar fraction) is 54.3% and the char yield is 20.1%. The experimental data is comparably similar as that from Shafizadeh (Shafizadeh, et al. 1972). Most of the compounds identified in the liquid fractions from xylan by Shafizadeh (Shafizadeh, et al. 1972) are also quantitatively determined by Hosoya et al., such as hydroxyacetone, acetic acid, and 2 furaldehyde. However, the chemical mechanisms for these compounds formation are not specified, as well as the effect of the catalyst addition on the products distribution.

The above studies, mostly in fixed-bed reactors, evidenced some of the typical products from the pyrolysis of xylan and its related model compounds, considering the effect of addition of chloride salts and alkaline catalysts. Compared to cellulose, the volatiles in liquid fraction are not extensively identified, and the effect of experimental conditions and reactors is not well discussed. For gaining the further information about the nature of the reactions involved in xylan pyrolysis, the studies in fast pyrolysis reactor (fluidized bed reactor recommended) should be conducted under different experimental conditions. This helps to figure out the possible chemical pathways for its primary decomposition and secondary cracking of volatiles, giving the systematical reaction mechanism similar as the precedent of cellulose proposed by Shafizadeh and Lai (Shafizadeh and Lai 1972), Richards et al. (Richards 1987; Pan and Richards 1989; Richards and Zheng 1991) ,

Piskorz et al. (Piskorz, et al. 1988; Piskorz, et al. 1989; Radlein, et al. 1991) and Liao (Liao 2003).

2.3.2 Lignin

Pyrolysis-gas chromatography-mass spectrometry (Py-GC-MS) has been applied by Obst (Obst 1983) to study the pyrolysis of the samples of loblolly pine softwood and white oak hardwood, as well as their respective isolated milled-wood lignins (MWLs). In the case of loblolly pine, more than 50 phenolic compounds were found, including guaiacoal, 4-methylguaiacol, 4-vinylguaiacol, vanillin, coniferaldehyde and coniferul alcohol. White oak yielded syringol, 4-methylsyringol, syringaldehyde, acetosyringone, sinapaldehyde and some guaiacyl compounds. The corresponding milled wood lignins also yielded the same type of compounds. The author did not report the quantitative results but noted that more vanillin than guaiacol was produced when pyrolysing MWL than white oak wood. It was believed that the lignin isolation method caused structural changes that produced higher yields of the above-mentioned compounds.

Pyrolysis-gas chromatography coupled to a molecular beam mass spectrometer (Py-GC-MBMS) has been employed by Evans et al. (Evans, et al. 1986) for the study of different wood lignin types and isolation methods. Pyrolysis runs were generally carried out at 900 ^{o}C with argon as the sweeping gas. Monolignols were predominant among the phenolic products. Softwood lignins yielded important amounts of coniferyl alcohol, whereas sinapyl alcohol was found after hardwood lignin pyrolysis. Herbaceous lignin pyrolysis (e.g., bagasse) gave coumaryl alcohol and vinyl phenol as the most abundant volatile compounds. Vinyl phenol was attributed to further degradation of coumaryl alcohol. These compounds were indicative of primary lignin fragmentation reactions. The lignin alcohol precursors are difficult to isolate because of their tendency to polymerize. This finding also indicates that such primary phenols can be obtained even at high pyrolysis temperature, but under a high vacuum, a small sample size and a fast heating rate. The produced phenols were found in the following order: coniferyl, sinapyl and coumaryl acohols, methoxyphenols, alkyl derivatives of phenol and

dihydroxybenzenes. Light and non-phenolic species evolved in the following order: formaldehyde, methanol and methane. Formaldehyde and methane generation coincided with the evolution of coniferyl alcohol and dihydroxybenzene, respectively. A relationship was also found between the lignin isolation procedure and the volatile phenolic composition. Monolignols were predominant in native or milled wood lignins, while guaiacol, syringol and lighter phenols were important in more severe lignin isolation methods (e.g., Krate, organosolv lignins).

Faix et al. (Faix, et al. 1987) performed the pryolysis-gas chromatography-mass spectrometry (Py-GC-MS) of beech, spruce and bamboo species and their isolated milled wood lignins. They identified the same compounds reported by Obst (Obst 1983). Some benzene and alkyl derivatives were also found. Analytical pyrolysis followed by analysis of volatile compounds by gas chromatography equipped with a flame ionization detector (Py-GC-FID) enabled the quantification of the condensed volatile compounds in a liquid nitrogen trap. In total, 75 compounds were identified and most of them were quantified using response factors from authentic compounds. Interestingly, the analytical pyrolysis of beech wood species yielded coniferyl alcohol and sinapyl alcohol in higher amounts than guaiacol and syringol, respectively. Related compounds preserving carbonyl and double bond functionalities like coniferaldehyde and sinapaldehyde were also found in appreciable quantities in the three wood samples. This quantification confirmed by the observation made by Obst (Obst 1983) that more alkyl guaiacyl and syringyl derivatives are obtained from pyrolysis of MWL than from the whole wood sample. These findings indicate that aliphatic hydroxyl and carbonyl functionalities may be preserved and not eliminated from the propanoid side chain by dehydration and decarbonylation reactions, respectively, as Fenner and Lephardt (Fenner and Lephardt 1981) found in their experiments.

Alen et al. (Alen, et al. 1996) performed an analytical pyrolysis of an air-dried, bark-free sawdust of Scots pine with 105-125 μm particle size. Pyrolysis was conducted at 300 ^{o}C, 400 ^{o}C, 600 ^{o}C, 800 ^{o}C and 1000 ^{o}C at a heating rate of 1000 ^{o}C/s. The main products formed at 400 ^{o}C wer phenolic aldehydes and alkyl guaiacols, while at 600 ^{o}C phenolic

aldehydes were converted into catechol and alkylphenols. High temperatures (800 ^{o}C and 1000 ^{o}C) resulted in an increase of aromatic hydrocarbons while phenolic aldehydes and guaiacols yields were considerably reduced. The results were in agreement with those obtained earlier by Elliott about the dependence of phenolic composition yield on pyrolysis temperature.

The vacuum pyrolysis of lignin derived from steam explosion of wood in a fixed bed reactor was carried out by Pakdel et al. (Pakdel, et al. 1992), employing GC-MS for characterizing the evolved volatiles. The results showed a significant oil yield increase from 34.5% to 42.7% by weight of feedstock as the pyrolysis temperature was increased from 400 ^{o}C to 465 ^{o}C, which is an indication that the ideal temperature to obtain a maximum yield of oils from the Iogen lignin material is probably in the range of 450 ^{o}C to 465 ^{o}C. The gas analysis exhibited that carbon dioxide, carbon monoxide and methane were the major components of the gaseous phase. The charcoal is significantly produced during the thermal decomposition of lignin, giving the yield of 38% at temperature of 465 ^{o}C and 44.4% at 400 ^{o}C. The calorific value of the charcoal is substantially higher than that of the feed stock, which is an asset if burned for energy generation. A detailed GC-MS analysis of 7 chromatograms fractions were exhibited, including the saturated and aromatic hydrocarbon mixtures, phenolic, aldehydic, ketonic and alcoholic compounds with increasing polarity form low polar methoxy benzene to high polar diphenolic and aldehydic compounds. However, the compounds with high polarity or high molecular weight could not be analyzed by GC-MS in the study, but suggested to be determined by Gel-permeation chromatography, HPLC/MS and NMR.

The gasification of milled wood lignin under the pyrolysis conditions (N_2/600 ^{o}C/50-120 s) in a closed ampoule reactor was carried out by Hosoya et al. (Hosoya, et al. 2008; Hosoya, et al. 2008), employing GC for gas analysis and NMR for tar analysis. It is obvious that the char yield is reduced from 50% to 44% with the residence time from 50 to 120 s, while the gas products are increased. The tar fraction is not visibly changed with the residence time. At 50 s, the tar fraction contains the primary pyrolysis products with the guaiacyl-unit, such as the aromatic structure existing in the original lignin.

Most of these primary products disappeared at 60 s. By contrary to this, the signals characterized to aliphatic alkyl and carbonyl groups did not change so much during 50-120 s. These spectral changes suggest that the O-CH_3 bond cleavage occurs vigorously in the period between 50 s and 60 s, while this reaction does not reduce the amount of the aromatic compounds in the tar fractions. This is consistent with the almost constant yields of the tar fraction in the period: 31.7% (50 s) to 27.7% (120 s). Conversion of the guaiacyl-type aromatic ring to o-cresol and catechol-types during pyrolysis is extensively reported in (Hosoya, et al. 2008). The secondary char formation also progressed in the period (50-60 s). The O-CH_3 bond homolysis would relate to the char formation of the lignin-derived tar components through the condensation occurred in the low-temperature stage (Nakamura, et al. 2007). However, the char formation from lignin, both primary and secondary, is not systematically presented in the literature.

Since Freudenderg and Neish (Freudenberg and Neish 1968) proposed the possible lignin structure extracted from different biomass, some other workers carried out pyrolysis studies on model compounds which have structural features that closely approximate the major linkages and functionalities in lignin, in order to obtain more specific experimentation relating lignin structure to devolatilization mechanisms. The pyrolysis of single/monomeric model compounds (e.g., methoxy phenols) is important to determine the thermal stability of the intermediate compounds formed during lignin pyrolysis. Experiments on guauacol pyrolysis at 350 ^{o}C by Klein (Klein 1981) produced catechol, methane, phenol and carbon monoxide as the main products. Catechol and methane yields were in almost stoichiometric amounts, as well as phenol and carbon monoxide. As proposed, demethylation of guaiacol yielded catechol. In addition, carbon monoxide and phenol were produced by demethoxylatoin of guaiacoal. Catechol yield was five times higher at 450 ^{o}C than at 300 ^{o}C. He also studied the pyrolysis of substituted phenols to determine the influence of the group functionalities on the thermal stability of the aromatic unit. Syringol, isoeugenol, vanillin, anisole, veratrole, acetophenone and Cinnamaldehyde were pyrolysed at 300-500 ^{o}C in a small batch reactor. Syringol and isoeugenol decomposed in a rather similar was as guaiacol. It was observed that substitution in the guaiacylic ring caused little influence on the pyrolysis mechanism of

these compounds. On the other hand, anisole pyrolysis yielded a wider product spectrum than the guaiacolic model compounds. The higher temperature required for anisole pyrolysis than for guauacol decomposition is indicative of the higher reactivity of guaiacol which was provided by the phenolic HO-group substituent.

Veratrole behaved like anisole during thermal decomposition. Guaiacol was one of the major pyrolysis products but was further decomposed to yield catechol and phenol. A concerted reaction between adjacent substituent groups was proposed as the mechanism for the generation of o-cresol from veratrole in a similar way to the production of phenol from guaiacol. Compounds with carbonyl functionalities such as benzaldehyde, vanillin, acetophenone and cinnamaldehyde reacted mainly via decarbonylation. Vanillin showed higher reactivity than benzaldehyde, attributed to electronic effects by the methoxyl and hydroxyl substitutions in the aromatic ring. Comparison of acetophenone and benzaldehyde pyrolysis indicated that the terminal C=O groups (aldehydes) were more reactive than C=O groups in α- or β-position (ketones). Cinnamaldehyde pyrolysis yielded phenol and alkyl phenols. Dimers were also produced, probably by Diels-Alder addition of two cinnamaldehyde molecules. Cinnamyl alcohol generated water, methanol, cinnamaldehyde, allylbenzene, cresols and dimmers. Water and methanol by C_β-C_γ bond cleavage. Cinnamaldehyde was the product of a H-abstraction from the corresponding alcohol. Interestingly, allylbenzene formation from cinnamyl alcohol can probably serve as a model for the production of allyl syringal and eugenol in wood and lignin pyrolysis. It can therefore be assumed that terminal HO-groups in the propanoid chain of the lignin monomer units yield allyl syringol and eugenol upon pyrolysis, while HO-functionalities in β-position yield *cis* and *trans*-1-propenylsyringol and *cis* and *trans*-1-propenyleugenol. Dehydration of HO-groups in the alkyl chain of different species of wood and lignin samples resulting in similar unsaturated compounds has also been reported by Faix et al. (Faix, et al. 1988) and Fenner and Lephardt (Fenner and Lephardt 1981).

Vuori and Bredenberg (Vuori and Bredenberg 1987) have studied the pyrolysis of guaiacol at 350-400 ^{o}C and reaction times from 0.5 to 4 h. Influence of tetralin as a

hydrogen donor agent was also evaluated in their study. Yields of catechol at 350 ^{o}C at reaction times from 0.5 to 2 h were similar. When the pyrolysis temperature was increased to 375 ^{o}C and 400 ^{o}C, catechol was formed at shorter residence times. At 375 ^{o}C, guaiacol pyrolysis also generated single phenol at the expense of catechol and o-cresol yields. At 400 ^{o}C, catechol and phenol predonated over the other products. It was noted that reaction time and temperature conditions were important for the formation of catechol and phenol from guaiacol pyrolysis. It was suggested that phenol was produced from guaiacol via a catechol intermediate. Masuku et al. (Masuku, et al. 1988) studied the thermal decomposition of 4-propylguaiacol. The reaction temperatures were 350 ^{o}C and 375 ^{o}C with a reaction time of 20-120 min. High yield of 4-propylcatechol was obtained. This indicates that the alkyl chain was more resistant to thermal degradation than the C-OCH_3 bond. Methyl-propylcatechol was also produced, with higher selectively at lower temperatures. Formation of this compound was attributed to the ring methylation of 4-propylcatechol. This type of reaction was highly improbable for guaiacol according to Masuku (Masuku 1991). These two observations suggest that alkyl chain may increase the reactivity of the aromatic ring, likely by the electron donation effect, as suggested by Korobkov et al. (Korobkov, et al. 1988).

Masuku (Masuku 1991) also studied the pyrolysis of dimethoxyphenols in a batch reactor from 250 ^{o}C to 325 ^{o}C and reaction times of 2-6 h. Syringol mainly yielded 2,3-dihyeroxyanisole, 2,3-dimethoxyphenol and small amounts of guaicol and methyguaiacol at 250 ^{o}C. Product composition was considerably more complex as the temperature increased. A variety of di and tri-hyderoxybenzenes were found at 275 ^{o}C and above. At this temperature, guaiacol and methyguaiacol yields were increase considerably with a decrease in 2,3-dihydroxyanisole production. Dihydroxyanisole and methyguaiacol yields decreased with the reaction time, whereas guaiacol yield increased. Reactivities of the model compounds studied followed the order of: 2,3-dimethoxyphenols, 2,6-dimethoxyphenols and 3,5-dimethoxyphenols, because of the steric effect.

Results of lignin pyrolysis by Domburg et al. (Domburg, et al. 1972) showed that ether bonds were cleaved during the first pyrolysis stage. The same authors studied the thermal decomposition of model compounds having β-ether bonds to simulate the softwood lignin structure (Domburg, et al. 1974). The pyrolysis of model compound 1 (Fig. 2-14 (1)) showed that the dimer was thermally unstable and volatile products were generated at temperature as low as 120 ^{o}C with a maximum rate at 210 ^{o}C and 370 ^{o}C. Guaiacol was the most abundant compound detected during pyrolysis at 180 ^{o}C, 200 ^{o}C and 300 ^{o}C. At 200 ^{o}C, other phenolic compounds including vanillin, eugenol and alkylguaiacols were also found. At this temperature 30% of the β-ether bonds were cleaved. The pyrolyzate produced at this temperature contained only 6.2% of guaiacol. This suggests that guaiacol underwent secondary reactions and produced an unidentified intermediate compound. β-ether cleavage took place in parallel to the appearance of water by dehydration of the aliphatic HO-groups in α-position. However, the authors indicated that these reactions were not interrelated. At 200 ^{o}C, only 10% of the sample preserved aliphatic HO-groups, whereas 70% of the ether bonds were still present. Dehydration gave rise to alkenyl-guaiacols such as eugenol, isoeugenol and alkyl guaiacols like propyl, ethyl and methylguaiacol by further hydrogenation. Guaiacol was produced by cleavages of the aryl and alkyl and aryl ether bonds. Vanillin and acetovanillone were also detected in appreciable quantities at the 200-300 ^{o}C temperature range.

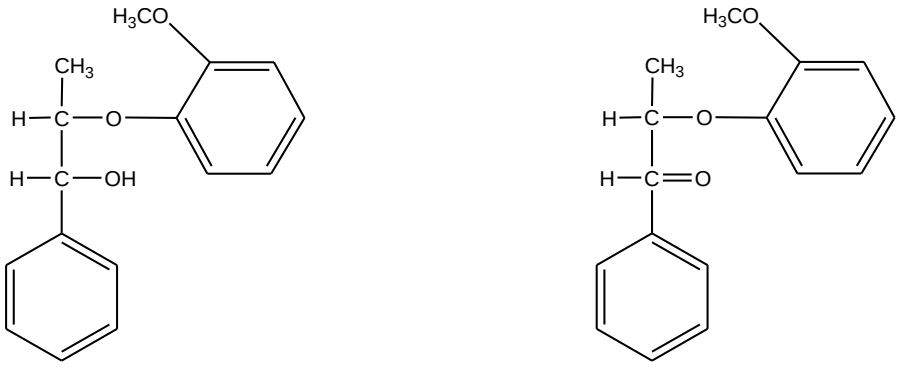

(1) (2)

Fig. 2- 14: the lignin-related model compounds for investigating the cleavage of ether bond during the pyrolysis of lignin (Domburg, et al. 1972)

Thermal decomposition of model compound 2 (Fig. 2-14 (2)) yielded volatiles at 260 ^{o}C with a maximum weight-loss rate at 300 ^{o}C and 400 ^{o}C. This demonstrated the higher stability of this compound compared with compound 1. Increasing yields of acetovanillone, ethylguaiacol and guaiacol were found at 300 ^{o}C and above. The presence of acetovanillone indicated the splitting of the γ-β carbon bond in the propyl chain. This compound was found at a low concentration during pyrolysis of compound 1. β-ether and γ-β carbon bond cleavages were the major reactions of compound 2 leading to vanillin and acetovanillone production, whereas β-ether cleavage and dehydration yielded eugenol, isoeugenol and guaiacol in model compound 2. Aliphatic and aromatic hydroxyl groups contributed to the thermal instability of the compounds, since the aliphatic HO-groups were easily eliminated as water. However, the specific role for the aromatic HO-groups affecting the dimmer's reactivity was not identifed.

Liu et al. (Liu, et al. 1997) studied the possible mechanism of wood liquefaction in phenol. They used a guaiacylglycerol-β-guaiacyl ether (GG) dimmer as the lignin model compound. A GG: Phenol: water mixture in the weight ratio of 1:3:3 was heated in a 3ml autoclave up to 120 min at 250 ^{o}C. Based on their results, liquefaction of GG in the presence of phenol produced low molecular weight intermediates which further reacted with phenol or with each other and transformed into polymeric products. More than 50 products were found by GC-MS. Guaiacol and a variety of dimmers were the main products of GG thermal degradation. The structures and yields of these intermediates suggested hemolytic cleavage of β-O-4 linkage. Production of guaiacol corresponded well with the consumption of GG, suggesting that guaiacol was derived directly from the cleavage of β-O-4 linkages. The authors indicated the possible mechanism involving the cleavage of β-O-4 linkage of GG produced coniferyl alcohol and guaiacol as intermediate. The rapid decrease of the alcohol indicated its great reactivity towards conversion into other substances. This reactivity was attributed to the presence of the side chain double bond in conjugation with the aromatic ring which favored radical formation and coupling.

Some other dimeric and trimeric compounds containing a variety of functional groups (such as carbonyl, hydroxyl and alkyl) and different monomeric linkages (particularly aryl-O-alkyl ether lingkage) were used by the authors to study the thermal stability of different bonds/linkages in lignin and the origin of its primary pyrolysis products, which is extensively reviewed by (Amen-Chen 2001), such as phenethyl-phenyl ether (Klein 1981), diphenylpropane (Gilbert and Gajewski 1982), dibenzyl ether (Korobkov, et al. 1988), guaiacol-glycerol-β-guaiacyl ether (Brezny, et al. 1983), veratrylglycol-β-guaiacyl ether (McDermott, et al. 1986), guaiacylglycerol-β-propylphenyl ether and veratrylglycerol-β-propylphenyl ether (Kuroda 1994). The pyrolysis of the model compounds may demonstrate the effect of each functionality and linkage during thermochemical conversion involving quantities of possible chemical reaction, but it does not demonstrate the complexity of whole lignin pyrolysis. The studies should be further compared and summarized to give a commonly established standpoint on pyrolysis of lignin monomeric and the cleavage of the typical linkage among the monomers.

Despite of the extensive work in lignin pyrolysis that has been done, a comprehensive hypothesis of lignin pyrolysis is desirable because it would allow the development of applied pyrolysis processes based on an understanding of the chemistry involved and thereby allow the selection of optimal conditions, or perhaps lead to methods where the chemistry can be effectively controlled. A comprehensive hypothesis hypothesis should include the following areas: 1) experimentation using well documented and representative samples of biomass and lignins that are representative of native lignin; 2) determination of the mechanisms of the solid phase pyrolysis reaction to improve the kinetic model, involving the information of the formation of typical volatile and secondary cracking of the primary pyrolysis products; 3) the formation of char both primary and secondary by determining the variation of the functionalities in the solid residue and precursor for the condensation reactions; 4) a determination of the relationship of lignin pyrolysis studies to the question of whole biomass pyrolysis and a determination of the inter-relationship with cellulose and hemicellulose.

2.4 The interactions among the components of wood

Wood constituent polymers, i.e. polysaccharides (cellulose and hemicellulose) and lignin, are pyrolyzed in different ways. Wood polysaccharides form anhydraosugars, furans, aldehydes, ketones and carboxylic acids as their primary volatile products, while the volatiles from lignin mainly consist of the low molecular weight aromatic compounds with guaiacyl-units or phenolic-units in case of wood lignins. To date, many researchers have extensively studied the pyrolysis of the real biomass and proposed reaction models by assuming that pyrolysis of the main chemical components (cellulose, hemicellulose and lignin) takes place independently without interactions among the three components (Alen, et al. 1996; Miller and Bellan 1997; Teng and Wei 1998; Orfao 1999; Manya, et al. 2004). They stated that pyrolysis of biomass can be explained based on a linear superposition of that of the three components. Yang et al. (Yang, et al. 2006) presented that the pyrolysis of the synthesized biomass samples containing two or three of the biomass components indicated negligible interaction among the components. A computational approach was made firstly to predict the weight loss of a synthesized biomass from its composition in cellulose, hemicellulose and lignin, and secondly to predict the proportions of the three components of a biomass. The results calculated for the weight loss of the synthesized biomass are quite consistent with the experimental results. However, results for predicting the composition of the biomass in terms of cellulose, hemicellulose and lignin were not very satisfactory, possibly due to the ignorance of interactions among the components.

From the morphological view of the woody plant cell-wall, the main chemical components (cellulose, hemicellulose and lignin) would not perform individually without the intrinsic interactions during the pyrolysis of the whole biomass system (Fengel and Wegener 1984; Dumitriu 2005; Hosoya, et al. 2007; Dammstrom, et al. 2009). The interactions among the chemical components of woody biomass under pyrolytic conditions are of growing interests during recent years, in order to gain better understanding of the pyrolytic mechanism of the whole biomass system and reveal the essential chemical pathways for the evolved volatiles (Hosoya, et al. 2007; Worasuwannarak, et al. 2007; Wang, et al. 2008; Couhert, et al. 2009).

Hosoya et al. (Hosoya, et al. 2007) investigated cellulose-hemicellulose and cellulose-lignin interactions during pyrolysis at gasification temperature of 800 oC for 30 s in a tube reactor, while a cellulose sample mixed with hemicellulose (2:1, w/w) was prepared by grinding cellulose-hemicellulose mixture in mortar and a cellulose sample mixed with milled wood lignin (MWL) (2:1, wt/wt) was prepared by adding cellulose to the 1,4-dioxane solution (0.5 ml) of MWL followed by evaporation of the solvent. In the cellulose-hemicellulose pyrolysis, the experimental and estimated yields were not different so much although the tar (total) yield tended to decrease slightly with small increase in the char yields by mixing. The results indicate that cellulose-hemicellulose interaction is not significant in gas, tar and char yields. In the cellulose-MWL pyrolysis, more significant deviations were observed between the experimental and estimated yields of char and tar fractions; char yield decreased with the increasing yield of the tar total fraction by mixing. Tar composition was also substantially affected by mixing cellulose with MWL, presenting that the yield of the i-PrOH-soluble fraction substantially increased from 52.1% to 68% while the yield of water-soluble fractions substantially decreased from 14.5% to 2.8%. These results suggest that nature of the tar fraction is significantly altered from the water-soluble to i-PrOH-soluble products by the mixing of cellulose with MWL. Moreover, the interactions among the components for the characteristic secondary char-forming were also investigated, involving the photographs of the reactors after pyrolysis and tar extraction (Hosoya, et al. 2007). The wood polysaccharide samples form the secondary char at the upper side of the reactor while vapor phase carbonization of the products from lignin leads to the formation of secondary char from the bottom to upper side continuously. In cellulose-hemicellulose pyrolysis, these char-forming behaviors were explainable as combined behaviors of the individual cellulose and hemicellulose pyrolysis. On the other hand, the cellulose –MWL pyrolysis substantially reduced the vapor phase secondary char formation from MWL.

With the characterization of the compositions in tar by GC-MS, GPC and NMR, it was found that the experimental yield of levoglucosan and 1,6-anhydro-β-D-glucofuranose is similar as the estimated value in the cellulose-hemicellulose pyrolysis. These values are

substantially different in the cellulose-MWL pyrolysis, where levoglucosan yield is enhanced while 1,6-anhydro-β-D-glucofuranose production is visibly inhibited. Thus, lignin may affect these anhydrosugars formation differently, because of the different formation mechanisms of these anhydrosugars. As for MWL-derived products, formation of guaiacol, 4-methylguaiacol and 4-vinylguaiacol was enhanced in the presence of cellulose. Effects on other products were very small. Although detailed mechanism is unknown at present, these results are considered to be related to the inhibition of the vapor phase carbonization of the MWL-derived products.

Later then, Hosoya and his co-workers (Hosoya, et al. 2009) extended their research on interactions between cellulose and lignin at 600 ^{o}C under different pyrolysis times (40-80 s) in two type's reactors. Reactor A is for investigating the vapour phase interactions, where cellulose and lignin are separately placed at the bottom. Reactor B is for investigating the solid-liquid phase interactions, where cellulose mixed with lignin is placed at the bottom. In 40s, the lignin and cellulose samples formed solid char in the inner sample holder and the bottom of the reactor, respectively. Secondary char from lignin was also observed around the reactor wall in 80 s. This secondary char formation was effectively inhibited in co-pyrolysis with cellulose. Since the solid/liquid-phase interaction is not effective in the type A reactor, this inhibitory effect arises from the vapor-phase interaction. Similar inhibition of the secondary char formation was observed also in type B reactor. In 40 s, the tar yield increased from 45.7% (estimated) to 55.1% (experimental) with the suppressing formation of char (32.5-28.3%) and water (16.7-11.6%) in the type B reactor. The influences in the type A reactor were comparatively small. The water yields were usually correlated with the char yields, since dehydration is a main process in char formation. These influences suggest that the solid/liquid-phase interaction in the early stage of pyrolysis (primary pyrolysis stage) enhances the tar formation instead of water and char.

In cellulose pyrolysis, gas yield increased from 5.0% to 31.1% with the decreased yield of tar from 54% to 29.3% under 40 s and 80 s, although the char yields were not so different (17.7% to 17.0%). Thus, gasification of the cellulose derived tar components

proceeded in this period. Contrary to this, gas formation from lignin was comparatively small. Under co-pyrolysis conditions, the experimental gas yields (80 s) (type A: 31.4%, type B: 28.9%) were greater than the estimated one (24.2%), while the estimated and experimental gas yields in 40 s were similar (type A: 4.7%, type B:5.0%, estimated: 5.0%). Accordingly, gas formation in the period of 40-80 s (secondary reaction stage) was accelerated in co-pyroysis. It needs to be noted that the vapor-phase interactions were significant at a longer pyrolysis time of 80 s when the methoxyl groups of the lignin-derived volatiles were cleaved homolytically. The vapor-phase interactions accelerated the gas formation from the cellulose-derived volatiles with suppressing the vapor phase char formation of the lignin-derived volatiles. The yields of methane and catechols from lignin also increased greatly instead of the formation of o-cresols. Most of these influences are explained with a proposed interaction mechanism, in which the cellulose-derived volatiles act as H-donor while the lignin-derived volatiles (radicals) act as H-acceptors. Although the interactions between the cellulose and lignin in both solid/liquid- and vopor-phase are extensively investigated, the results could not interpret the intrinsic mechanism of the interaction among the components in the real wood system because of the ignorance of the inter-linkages and morphological relationship between the chemical components.

Time profile of evolution rates of gas and tar in steam gasification of model biomass samples at the temperature of 673 K were examined by Fushimi et al. (Fushimi, et al. 2009) using a continuous cross-flow moving bed type differential reactor to elucidate the interaction among the major biomass components (cellulose, xylan and lignin) during gas and tar evolution. Two types of model biomass samples (sample A: mixture of cellulose (65%) and lignin (35%) with a ball-mill for 5 h; sample B: mixture of cellulose (50%), xylan (23%) and lignin (27%) with a ball-mill for 5 h) were used for the experiment. In steam gasification of sample A, the evolution of water-soluble tar and gaseous products (CO, H2, CH4 and C2H4) are significantly suppressed by the interaction between cellulose and lignin. The primary (initial) decomposition of lignin is hindered by the interaction with pyrolysate of cellulose, which is different from the result from Hosoya et al. (Hosoya, et al. 2009). Then the CO2 evolution appreciably enhanced and the

evolution of water-soluble tar delays. These results may imply that the volatilization of water soluble tar derived from cellulose is suppressed by lignin and then the decomposition of char derived from polymerized saccharides and lignin takes place, emitting mainly CO2. From the results using sample B, it was found that the addition of xylan greatly enhances the evolution of gases (CO, H2, CH4 and C2H4) and accelerates the evolution of water-soluble tar and CO2, implying that the enhancement of decomposition of water-soluble tar into gases and/or xylan decomposes into gases without significant interaction with cellulose or lignin. In addition, yields of the major tar components (levoglucosan, furfural and 5-methylfurfural) were measured using HPLC. It was observed that the interaction among cellulose, xylan and lignin suppresses the evolution of levoglucoasan and significantly increases the evolution rate of 5-methylfurfural. There is an insignificant influence of interaction among cellulose, xylan and lignin for furfural evolution.

In order to establish a link of the pyrolysis gas yield from the biomass and its main compositions, experimental flash pyrolysis of several biomasses and the model compounds (xylan, cellulose and lignin) at a temperature of 950 ^{o}C with a gas residence time of about 2 s was carried out by Couhert et al. (Couhert, et al. 2009) using an entrained flow reactor (EFR). The synthesized biomass by mixing the three components is described as simple mix where the products are mixed in equal mass proportion with a spatula in a container, and intimate mix where the components were mixed and then co-ground to thin elements using a laboratory ball mill. During the pyrolysis of simple mixes, the three components devolatilized separately. Interactions are likely to occur outside the particles. During the pyrolysis of intimate mixes, reactions can occur outside the particles in the same way as during the pyrolysis of simple mixes but additional interactions may occur inside the particles. As one component devolatilizes inside the particle, it is submitted to an atmosphere with very high concentrations in gas and condensable vapors; the gases formed are in close contact with the solids of other components. There are also probably interactions inside the particles because CO2 yield of intimate mix is higher than CO2 yield of simple mix. An attempt was then made to predict gas yields of any biomass according to its composition, but an additivity law does

not allow the gas yields of a biomass to be correlated with its fractions of cellulose, hemicellulose and lignin. It is concluded that interactions occur between compounds and that mineral matter influences the pyrolysis process.

We have to admit that the interactions among the components of wood under pyrolysis conditions are insufficiently investigated in the literature. Some issues concerning the interactions among components need to be further addressed for gaining better understanding of the pyrolysis of whole biomass system: 1) the sample preparation to simulate/reveal the possible relationships among the components in the real biomass; 2) the effect of experimental conditions (temperature, residence time, pressure and so on) and pyrolysis reactor type on the interactions among the components during pyrolysis; 3) specificity of the chemical mechanisms of the interactions among the components in vapor-phase, solid/liquid-phase or morphological-phase; 4) the quantification of the interactions on the yield specific products (such as proposing some interaction coefficients), which could be incorporated into the multi-component kinetic model for the whole biomass pyrolysis.

2.5 Summaries

With regard to the extensive discussion on both on-line and off-line pyrolysis of the main components of woody biomass and the interactions among them, the development and challenges of the issues can be summarized:

To on-line pyrolysis, the main mass loss stage(s) of the components of woody biomass versus temperature is well presented, together with the corresponding evolution of the volatiles. The proposed kinetic models for the component pyrolysis are mostly correlated with the separate/consecutive mass loss stage(s), which could give good fitting with the mass loss curve of the solid from TGA. However, the specific chemical reactions during the component pyrolysis are not well incorporated in the current kinetic models, leading to the inability to track the formation of the typical products.

To off-line pyrolysis, the products established in good yield from cellulose pyrolysis are extensively discussed in the above studies, involving a large number of plausible chemical pathways for the change of molecule structure and tar cracking reactions. However, the primary rearrangement/cracking of the supramolecule of cellulose, as well as the relationship between the light species and the primary fragments, is not systematically specified, which could be determined by the yield of compounds varied with the experimental conditions. For hemicellulose (mainly xylan), lignin and their relevant model compounds, the off-line pyrolysis involving the yield of the products and possible chemical pathways for the typical compound formation is mostly investigated by employing the fixed-bed system (such as plug-in furnace) and entrained flow gasifier. More knowledge concerning off-line pyrolysis from fluidized-bed pyrolysis system which has the advantages of high heating rate, efficient heat transfer, low energy in-put and easy scale-up is required. This helps to evidence the reactions of macromolecular rearrangement, the formation of the primary products and their cracking reactions systematically.

The interactions among the main chemical components of woody biomass under pyrolytic conditions are remarkably evidenced in terms of the yield of products and variation of the specific compositions. This implies that the interactions among the components should be significantly considered for gaining better understanding of the pyrolysis of the biomass system. It needs to be noted that the synthesized sample composed of the mixture of two or three components is mostly tested in the fixed bed reactor or entrained flow pyrolyzing furnace, but the information about the interactions among the components in fluidized-bed reactor is not available in the literature. Moreover, the knowledge concerning the interactions among the components of woody biomass during on-line pyrolysis needs to be fulfilled, to determine the variation of the mass loss process and evolution of the volatiles.

In order to consolidate the above findings and fill the relevant knowledge gap, the on-line and off-line pyrolysis of the sample of hemicellulose, cellulose, lignin and “synthesized biomass” samples composed of mixed two or three components would be intensively

investigated employing TGA coupled with FTIR and a fluidized-bed fast pyrolysis system in this work. According to the experimental results from both on-line and off-line pyrolysis studies, the chemical pathways of the component pyrolysis involving the changes of macromolecular structure and the fragment cracking would be systematically proposed, which is beneficial for improving the current kinetic model/mechanism. The interactions among the components in terms of solid mass loss, yield of products and variation of typical compounds in liquid and gas products would be remarkably specified through the on-line pyrolysis and off-line pyrolysis of the synthesized samples, in order to gain the better understanding the pyrolytic behavior of the whole biomass system.

Chapter 3: Methodology

3.1 Introduction

In order to gain the better understanding the pyrolytic mechanism of the individual component of woody biomass (hemicellulose, cellulose and lignin) and their interactions under the pyrolytic conditions, both on-line and off-line pyrolysis studies of the components and the "synthesized biomass" sample were carried out by employing TGA coupled with FTIR and a fluidized-bed fast pyrolysis system. The methodology of this study involving the selection of the model components, the preparation of the samples, the on-line and off-line pyrolysis system, experimental procedure and analytical method is briefly presented in Fig. 3-1, and is discussed in details in the following parts.

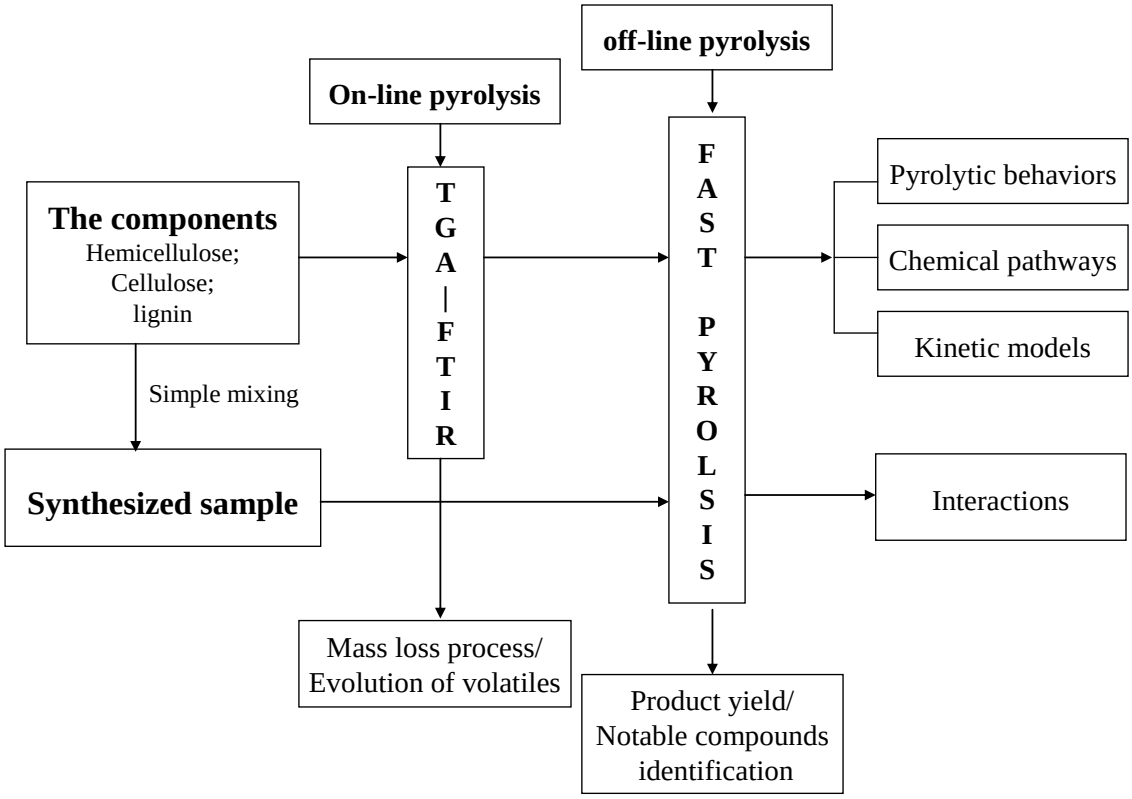

Fig. 3-1: the schematics of the methodology of this study

3.2 Materials

3.2.1 Cellulose

Woody biomass is a complex material, mainly composed of hemicellulose, cellulose and lignin in addition to extractives (tannins, fatty acids, resins) and inorganic salts. Cellulose is the most important element in biomass due to its large proportion. Cellulose forms the framework of the biomass cell walls which are composed of the cohesive, interlaced cellulosic microfibrils matrix deposited by hemicellulose, lignin, proteins and pectins (Keegstra, et al. 1973; Goodwin and Mercer 1983). The cellulose has crystalline and amorphous zones according to the microfibrils periodically or randomly distributed along the orientation of cellulose fibrils. The amorphous zone is more active than the crystalline zone, adding to the complexities in thermal decomposition of cellulose (Severian 2008). It is found that the primary structure of cellulose is a linear homopolymer of glucopyranose residues linked by β-1, 4- glycosidic bonds, while the glucopyranose comes from the hemiacetal reaction of D-glucose between C-1 and C-5 positions (Fig. 3-2) (Charlton, et al. 1926; Chu and Jeffrey 1968). The degree of polymerization of the native celluloses (*n*) depends on the source and is considered to be from 6000 to 8000 for those from woods (Severian 2008).

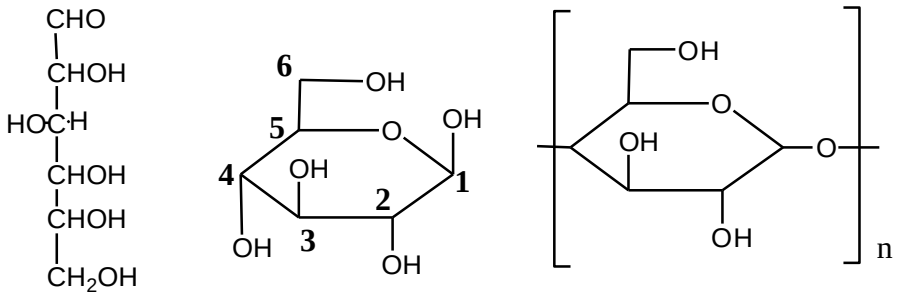

1 (D-Glucose) **2 (Glucopyranose)** **3 (Cellulose monomer)**

Fig. 3-2: the chemical structures of D-glucose, glucopyranose and cellulose monomer

The sample tested in the experimental work is the crystalline cellulose from Sigma Chemical Company, and prepared as the white powder with average diameter of 200 μm.

According to the elemental analysis, the content of C, H, S, N and O is 44.97%, 6.196, 0.096, 0.016% and 48.715% respectively. The chemical formula for this sample polymer could be approximated as $(C_6H_6O_5)_n$, confirming the linearly polymerized structure of the glucopyranose linked by β-1, 4- glycosidic bonds (Severian 2008). The sample powders were dried in the furnace with the temperature around 100 ^oC for 2 hours before the experiment.

3.2.2 Hemicellulose

Hemicellulose, constituting 20-35% (mass) of woody biomass, is the least stable composition among wood components. It is primarily composed of xylans and mannans (Blasi and Lanzetta 1997; Spearpoint 1999). A common standpoint presents that cellulose microfibrils are coated with the hemicellulose in the primary cell wall of the plant, which prevents the flocculation of the cellulose microfibrils (Dammstrom, et al. 2009). Hemicellulose is considered to cross-link cellulosic polymers, lignin and pectins, providing the structural support to the secondary cell wall in plant (Severian 2008).

The model compound representing the hemicellulose in woody biomass for the experimental study is O-acetyl-4-O-methylglucurono-xylan extracted from beech, which is the commercial product from Sigma Chemical Company. The hardwood hemicellulose are mainly composed of xylans, linearly constituted of 1, 4 linked β-xylopyranosyl units (Severian 2008). The 4-O-methylglucurono-xylan from beech gives a xylose-to-uronic ratio of 8:1, i.e. every eighth xylopyranosyl unit is substituted by the 4-O-methylglucuronic acid unit linked to xylan chain through (1,2) linkage (Sandford and Baird 1983). It is also estimated that acetyl group content varies from 8 to 14 % in every 8-xylose units, normally representing 3-7 acetyl groups which are linked to C_2 (sometimes C_3). The above findings imply the speculative chemical structure of the hemicellulose sample (O-acetyl-4-O-methylglucurono-xylan) in Fig. 3-3, which also exhibits the detailed substituting positions of the acetyl groups and 4-O-methylglucuronic acid (4-O-MeGlcA) unit to the xlyan chain. Compared to cellulose, the degree of polymerization of the xylan units is very low, less than 200.

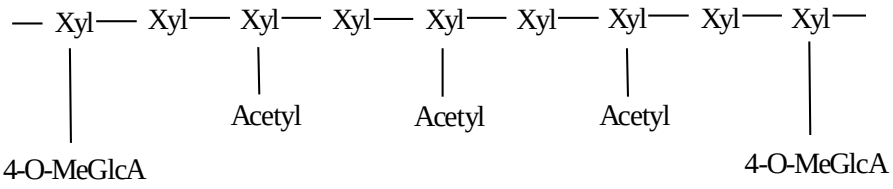

(1) O-acetyl-4-O-methylglucurono-xylan

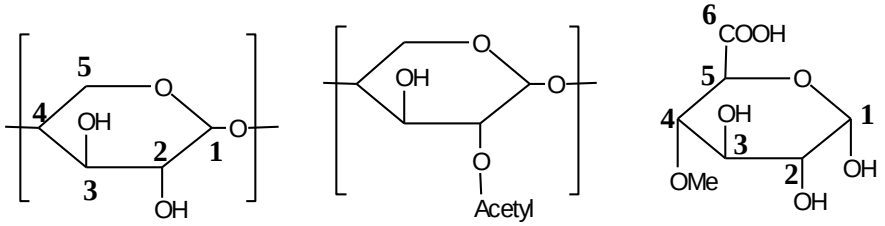

(2) Xylan unit **(3) O-acetyl xylan** **(4) 4-O-MeGlcA**

Fig. 3-3: the chemical structures of the hemicellulose sample and its side–chain unit

The xylan-base hemicellulose sample was prepared as the white powder with average diameter of 200 μm, and the content of C, H, S and O is analyzed to be 40.8, 6.38, 0.26 and 41.01% respectively. The sample powders are dried in the furnace with the temperature around 100 ^{o}C for 2 hours before the experiment.

3.2.3 Lignin

Lignin is one of the principal components which accounts for 18-40 wt% of the dry wood, depending on the wood species (Amen-Chen 2001). Compared to cellulose and hemicellulose, lignin has a complex three-dimensional polymeric structure with various functions attached to the aromatic rings (Pakdel, et al. 1992). The chemical structure of lignin can be described as an irregular polymer of various phenolic-C_3 alkyl side-chain (-$\mathbf{C_\alpha}$-$\mathbf{C_\beta}$-$\mathbf{C_\gamma}$) monomeric (C_9) units (Evans, et al. 1986). The lignin from softwood and hardwood is varied by the number of methoxy groups on the phenolic ring, therefore softwood lignin is formed from the guaiacol-type units (**R1** = H in Fig. 3-4a) while hardwood lignin is from both guaiacol-type units and syrigol-type units (**R1** = OCH_3 in Fig. 3-4a). It is reported that the diversity of the side-chain structure from guaiacol-type units (**R2** = **2, 3, 4, 5** and **6** in Fig. 3-4a) is more abundant than that from syringol-type

units (**R2 = 1 or H** in Fig. 3-4a) (Sjostrom 1993; Jiang 2001), resulting in the vigorous evolution of guaiacol-derivatives as the primary products from woody lignin pyrolysis.

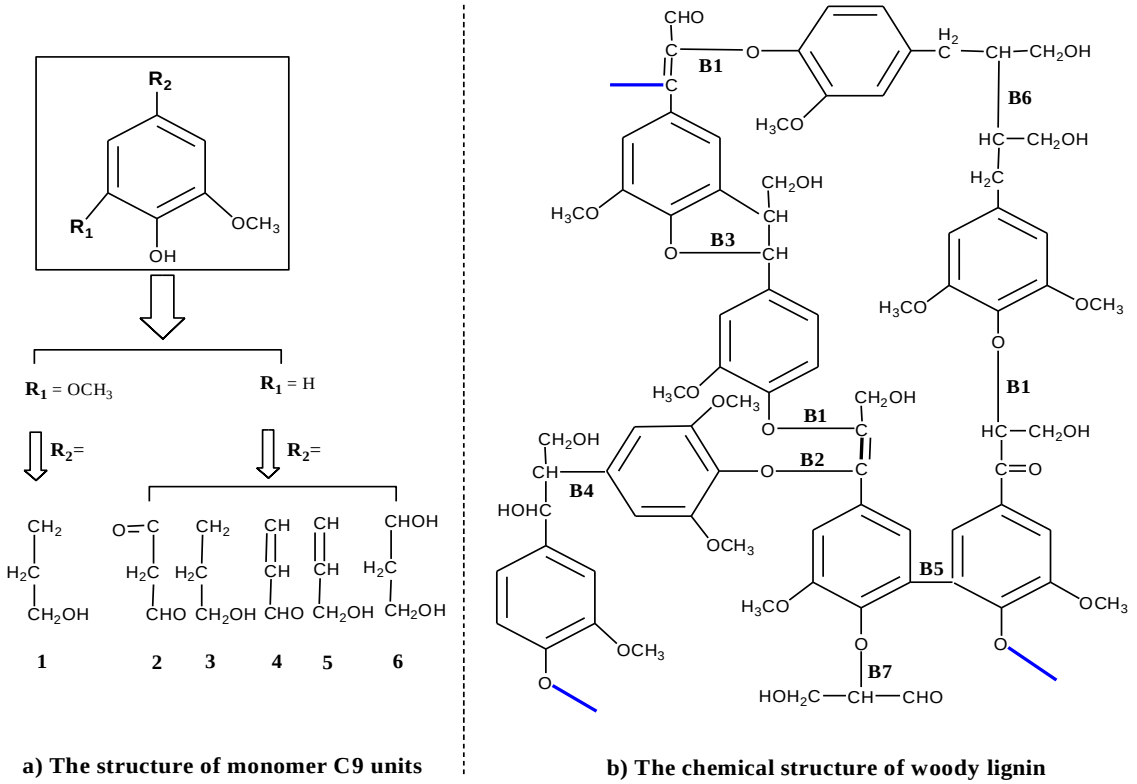

a) The structure of monomer C9 units

b) The chemical structure of woody lignin

Fig. 3- 4: the chemical structure of lignin and its C9 units

Unlike cellulose and hemicellulose, lignin has several different types of linkages between the monomeric (C_9) units. The amounts of the major linkage in typical softwood and hardwood were estimated in Table 3-1 by Alder (Adler 1977). A polymeric structure of woody lignin is proposed in Fig. 3-4b with regard to the linkage distribution and various side-chain structure from different aromatic types (guaiacol-type and syringol-type). It is noticeable that the (β- and α-) alkyl aryl ether linkage (**B1** and **B2**) is the most important linkage, accounting for ~60% of the total polymeric linkages of lignin. This type of linkage is believed to be more reactive than C-C bonds, playing the key role in the primary pyrolysis reactions to form the phenolic hydroxyl group through the H-abstraction of the phenoxy free radical from the cleaved alkyl side-chain (Benson 1978). The structure of phenylcoumaran (**B3**) is composed of the aryl-alkyl-aryl linkage (**B5**) and α-alkyl aryl ether linkage, exhibiting the similar proportion as biphenyl linkage

(**B4**) in both types of wood. The β-β alkyl linkage (**B6**) and glyceraldehyde-2-aryl ether linkage (**B7**) occupy the lowest proportion in the lignin inter-unit linkages for both woods. However, glyceraldehyde might be a considerable H-donor for the formation of phenolic hydroxyl via the cleavage of **B7**, also acting as an important source for generating the free volatile species.

Table 3-1: types of bonds between the monomeric (C9) units in softwood and hardwood lignin (Adler 1977)

Bond type	Assignment in Fig. 3-4	Softwood (Spruce)*	Hardwood (Birch)*
β-Alkyl aryl ether	**B1**	48	60
α-Alkyl aryl ether	**B2**	6-8	6-8
Phenylcoumaran	**B3**	9-12	6
Biphenyl	**B4**	9.5-11	4.5
Aryl-alkyl-aryl linkage	**B5**	7	7
β-β Alkyl linkage	**B6**	2	3
Glyceraldehyde-2-aryl ether	**B7**	2	2

*: values are in frequency per 100 C_9 units.

The lignin samples tested in the experiments, know as kraft lignin, are produced from wood pulping process. According to elemental analysis, the content of C, H, S, N and O is 52.74%, 3.97%, 0.7%, 0.08% and 34.55% respectively. Compared to native wood lignin, kraft lignin is less reactive due to the structural changes (such as the increase of the free phenolic groups and carbon-carbon linkages) during the pulping process (Evans, et al. 1986; Froass and Ragauskas 1996). The samples are grinded into particles less than 200 μm diameter and then dried in furnace with temperature around 100 ^{o}C for 2 hours before the experiment.

3.2.4 "Synthesized biomass" sample

Crystalline cellulose, xylan-based hemicellulose and kraft lignin described above are used to prepare the "synthesized biomass" sample. The utilized component powders are selected under 200μm. The "synthesized biomass" sample composed of the two or three components is prepared as the following way: the components are mixed according to the mass proportion with a spatula in a container. Through this simple mixing method, the mixed particles blown into fluidized bed reactor may be in contact but will be essentially dispersed in the gas phase, favoring the interactions in vapour-phase (Couhert, et al. 2009; Hosoya, et al. 2009).

3.3 TGA-FTIR analysis

Thermogravimetric analyzer (Mettler Toledo TGA/SDTA 8951E) is coupled to the FTIR spectrophotometer (Netxus 670, Nicolet) to investigate the mass loss of solid sample and evolution of volatile against temperature during the on-line pyrolysis process (Fig. 3-5). The heating rate of the thermogravimetric analyzer could be set from 0 to 100 K/min, while the temperature of the TGA furnace could be heating from room temperature to less than 1200 ^{o}C.

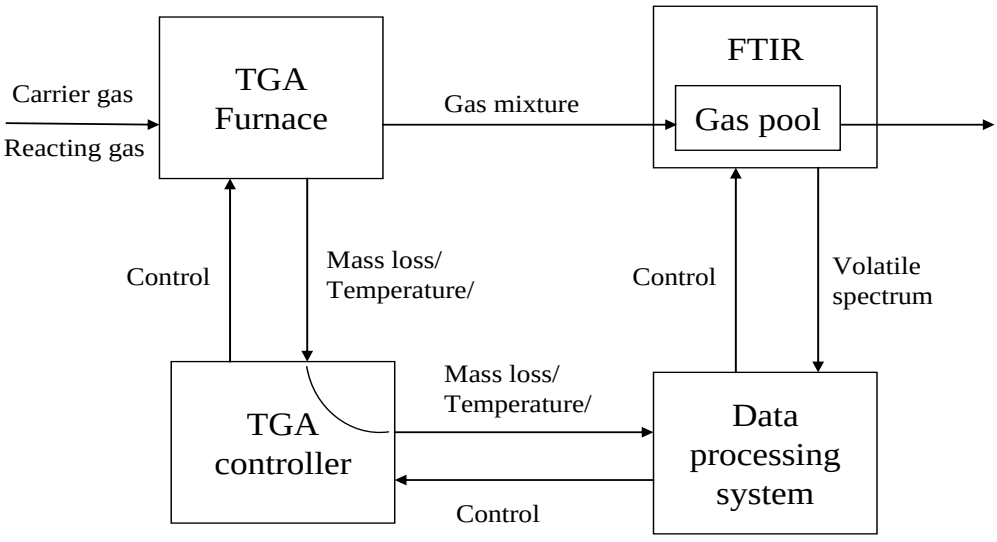

Fig. 3-5: the schematics of TGA-FTIR system

The atmosphere for the pyrolysis of the solid sample in TGA furnace could be adjusted by the flow of reacting gas (inert as nitrogen, reductive as hydrogen or oxidative as air), while the carrier gas is ordinarily set as Nitrigen. The spectral range of the FTIR spectrophotometer is from 27000 to 15 cm^{-1}, while the highest resolution of the spectrum could reach 0.09cm^{-1}.

For the TGA-FTIR experiment, the temperature range of the TGA furnace with the fixed heating rate would be set before the run. The reacting gas and carrier gas are all nitrogen to maintain the inert atmosphere, and the flow rate is set to be 60 ml/min. The mass load of the sample for the TGA experiment is less than 5 mg to avoid the possible temperature gradient in the sample and ensure the kinetic control of the process (Blasi, et al. 2001). The FTIR is connected to TGA by a flow cell which is heated to 180 ^{o}C before the TGA runs, in order to prevent condensation of the produced gases on the cell wall. The FTIR spectrometer is set to collect 32 interferograms at a resolution of 4 wavenumbers with a scanning rate of 0.6329 cm/s and the spectral range is set to be 4000-400 cm^{-1}. The FTIR spectrometer starts 1 minute before the TG experiment. At a nitrogen flow rate of 60 ml/min, about 52.05 s is required to completely fill the cell volume of the spectrometer. Thus, there is a two-minute lag between the TGA result and the corresponding spectra, and the spectrometer should stop scanning about 1 min after the accomplishment of TGA experiment.

The on-line mass loss data of the solid sample against the elevating furnace temperature/time is sensitively recorded by the data processing system through the TGA controller. Meanwhile, the interferograms are collected during the whole pyrolysis process and post-processed to obtain the absorption spectra against time and the corresponding evolved gas profiles (EGP), functional group profile (FGP) and specific gas profile (SGP). The variation of evolution of volatiles against time is qualitatively determined, since the quantification of the profiles is still the limitation for the current FTIR technology. With the help of the relevant software, the mass loss curve of the solid sample from TGA could be correlated with the absorption spectra from FTIR, in order to gain the information about the evolution of volatiles against temperature or the

mass loss stage(s). The quantitative determination of the evolution of volatiles is not available by the TG-FTIR analysis

3.4 The fast pyrolysis experiment

3.4.1 The fast pyrolysis unit

The fast pyrolysis unit, is composed of a feeding system, pyrolysis system, carbon filter, vapour-condensing and gas storage, as shown in Fig. 3-6. The reactor is a quartz tube (diameter of 15mm, length of 1200 mm and thickness of 2 mm) heated by the carborundum heater with the power of 8 kW, while there is a 4 mm gap to ensure the same temperature in the tube and heater. Temperature is not evenly distributed within the heater and the difference between the distributed points decreases at higher temperature (Fig. 3-7). Hereof, the linearly averaged value is adopted in the experiment. The temperature limit for the furnace is about 1200 ^{o}C.

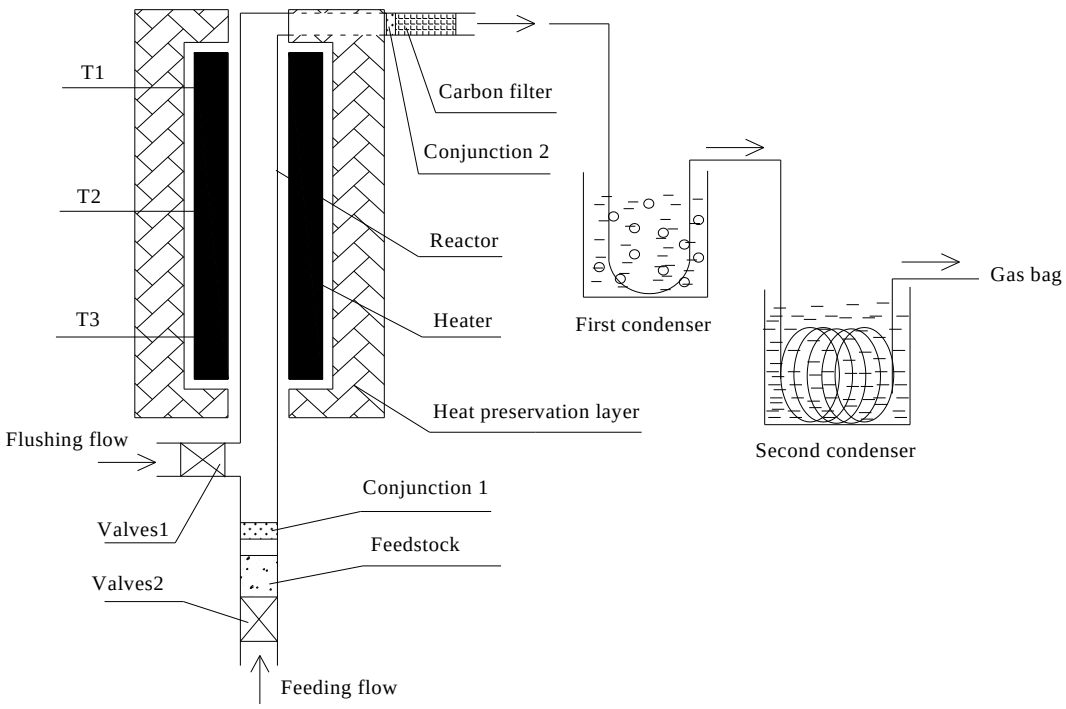

Fig. 3-6: the apparatus schematics for the biomass pyrolysis and volatiles condensation system

It should be noted that the mass-balance can be easily performed with the testing unit. The feeding system and carbon filter can be disassembled from the quartz tube reactor at the junction 1 and 2 in Fig. 3-6. The weight of feedstock can be determined precisely without pre-heating reactions before the feeding system is connected to the reactor. The carbon filter is disassembled after the experiment to obtain the weight of char residue by checking the weight difference of the carbon filter.

The bio-oil is collected by the two-step condensing system. The first condenser employs the mixture of water and ice to cool the volatile stream while most of the high molecular weight compounds (heavy tars) are condensed and collected in the U tube. The hot stream is cooled down to 50 ^{o}C after the first condenser, and then passes through the second condenser where the light tars are coagulated by the mixture of dry ice and acetone (about -30 ^{o}C), and finally is collected in a spiral circle tube.

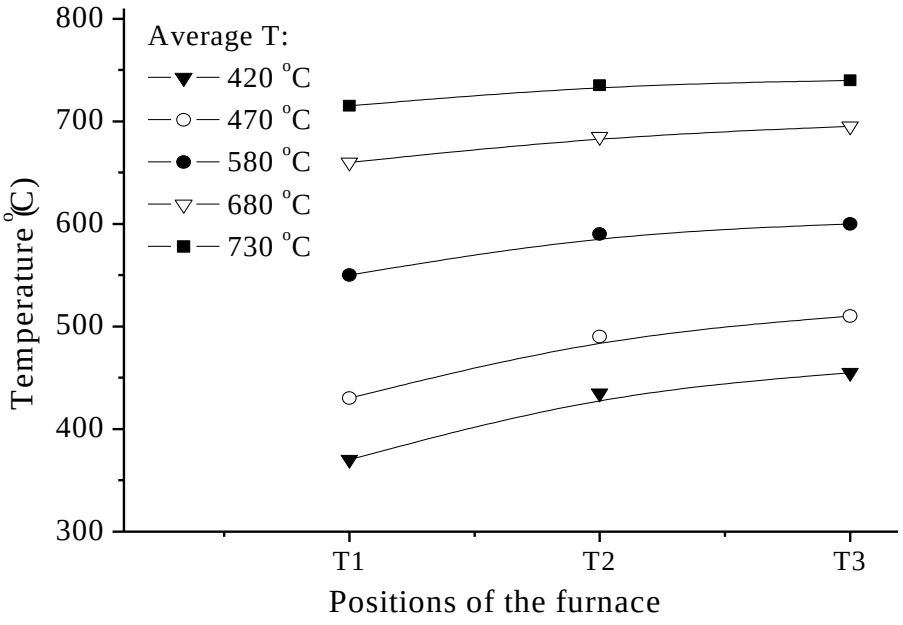

Fig. 3-7: the temperature distribution along the reactor

3.4.2 The procedure

While the experimental temperature (average value) reaches the fixed value, the feeding system is connected to the reactor via the closed valve 2 in Fig. 3-6. The flushing flow initially runs for about 1 minute to purge all oxygen out of the system to ensure the inert

atmosphere in the reactor tube. Then, the valve 1 is closed and the valve 2 is opened to carry feedstock up to the heated reactor by the feeding flow. The sample is pyrolyzed rapidly inside the reactor, and the stream mixed of produced volatiles and char residues move upward passing through a carbon filter where the char residue is separated. The purified volatile stream then flows through the two-step condensing system where tars are condensed and collected, the non-condensable volatiles together with the carrier gas (nitrogen) are collected by gas sample bags. Solid sample is pyrolyzed in this system to investigate the effect of temperature and residence on the process, through adjusting the average temperature of the furnace and the feeding flow rate. It needs to be noted that the residence time of the evolved vapors in the fluidized-bed reactor could be calculated from the feeding flow rate and the reactor size, where the temperature-rising effect should be taken into account.

3.4.3 The determination of product yield and gaseous compositions

The yield of char residue is estimated by the weight difference of the carbon filter before and after the experiment while the yield of the tars is determined by the weight difference of the U tube, spiral circle tube and the connecting tubes. The yield of gaseous products is calculated from the density and volume of the collected gaseous mixture. The density is found from the quantitative composition analysis of the mixture by GC (Voyager, Finnigan), while the volume is read from the integral flowmeter. The GC operating conditions are: GC capillary column: Wax-10 (length: 30 m, diameter: 0.25 mm), injector temperature: 250 ^{o}C; column temperature: 60 ^{o}C (5 minutes), 60→250 ^{o}C (heating rate of 10 K/min), 250 ^{o}C (25 minutes); carrier gas: helium, flow rate: 2 ml/min. The final yield of the gaseous products is found by excluding the carrier gas (N_2) in the mixture.

The estimated mass balance closure for the different experiments, described as (the yield of char, tar and gases) / (the mass of feedstock), is between 97.9 % and 101.2%. The experimental results are considered to be reasonable while the errors are less than 5% as an acceptable deviation. Normally, there are two runs for each experiment and the one would be repeated if the deviation exceeds the limitation (5%).

3.4.4 Characterization of the compounds in bio-oil

The oxygenated compositions in bio-oil from the chemical components of woody biomass are very complicated, and most of them are dissolved by ethanol. The two condensers are washed by analytical ethanol solvent to form the bio-oil- ethanol mixture. The GC-MS (Voyager, Finnigan) or GC-FTIR technique is employed to characterize the typical compounds in the bio-oil through analyzing the mixture. The column of the GC is applicable for the oxygenated and polar compounds containing hydroxyl, carbonyl and carboxyl groups The conditions for GC-MS for identifying the bio-oil from cellulose, lignin and "synthesized biomass" sample is given as: GC capillary column: Wax-10 (length: 30 m, diameter: 0.25 mm), injector temperature: 250 ^{o}C; column temperature: 60 ^{o}C (5 minutes), 60→250 ^{o}C (heating rate of 10 K/min), 250 ^{o}C (25 minutes); carrier gas: helium, flow rate: 2 ml/min, MS ionization mode: electronic ionization; electronic bombardment energy: 70 eV, scanning time: 0.5 s, scanning range: 30-500u. The yield and the structure of the compounds are determined by the computer software from the characterized GC-MS graphs. The conditions for GC-FTIR for identifying the bio-oil from hemicellulose is given as: GC capillary column: Wax-10 (length: 30 m, diameter: 0.25 mm), injector temperature: 250 ^{o}C; column temperature: 60 ^{o}C (5 minutes), 60→250 ^{o}C (heating rate of 10 K/min), 250 ^{o}C (25 minutes); carrier gas: helium, flow rate: 2 ml/min, FTIR spectrometer: 32 interferograms at a resolution of 4 wavenumbers with a scanning rate of 0.6329 cm/s, the spectral range: 4000-400 cm^{-1}.

Through the fast pyrolysis experiments (off-line pyrolysis), the fundamental issues in terms of the product yield, quantitative analysis of gaseous composition, identification of main compounds in bio-oil from the chemical components of woody biomass and "synthesized biomass" samples would be extensively specified, also involving the effects of experimental conditions such as temperature and residence time. The systematic chemical pathways for the pyrolytic reactions were proposed according to the macromolecule structure analysis of the components and the typical pyrolytic resultants. And the kinetic model/mechanism was modified with regard to the relationship of the

variation of the typical compounds production against temperature or residence time. Also, the interactions among the components under pyrolytic conditions (on-line or off-line pyrolysis) in terms of mass loss process, product yield and composition distribution in bio-oil and gases would be estimated by comparing the experimental result with the estimated/calculated data depending on the component fraction in the "synthesized biomass" sample.

Chapter 4: Results and discussion

4.1 Introduction

The on-line pyrolysis and off-line pyrolysis experiments employing TGA-FTIR and fast pyrolysis unit were carried out for the model compounds representing the chemical components in woody biomass and the "synthesized biomass" samples. These were used to gain more information about the pyrolytic breakdown of the three main component and their interactions, to propose systematic chemical pathways for pyrolytic reactions of the macromolecules and thus improve the current kinetic models. The detailed experimental results and the discussion are presented in the following parts: cellulose, hemicellulose, lignin and "synthesized biomass" sample.

4.2 Cellulose

In the TGA-FTIR experiment, the sample of crystalline cellulose powders is heated from 20 to 800 ^{o}C at heating rate of 5, 20 and 60 K/min under the inert atmosphere. Cellulose is pyrolyzed in the fast pyrolysis system to investigate the effect of temperature and residence time on the process. The reactor temperature is varied from 420 to 730 ^{o}C, while the feeding flow rate is changed from 200 to 600 l/h at the temperature of 530 ^{o}C corresponding to the residence time from 1.32 to 0.44 s.

4.2.1 TGA-FTIR analysis

Fig. 4-1 shows the TG and DTG curves for cellulose under nitrogen at three different heating rates. An "abrupt mass loss stage" is found within a small temperature interval, where most of the cellulose sample is decomposed by a series of chemical pathways. Characteristics of the DTG curve of cellulose are exhibited in Table 4-1. It is clear that the maximum mass loss rate decreases and moves toward high temperature with increased heating rate, confirming existing findings (Bradbury, et al. 1979; Bilbao, et al. 1997; Orfao 1999; Li, et al. 2001; Liao 2003). Table 3-1 shows that T^{a} and T^{c}, representing the beginning and the end of the "abrupt mass loss stage" respectively, move

toward high temperature as the heating rate increases, however, the temperature interval (the difference between T^a and T^c), corresponding to "the abrupt mass loss stage", seems to be sustained for different heating rates (83 ^oC for 5 K/min, 92 ^oC for 20 K/min and 95 ^oC for 60 K/min). This implies that the cellulose decomposes very quickly under the high heating rate and the products are released intensively within a short time interval.

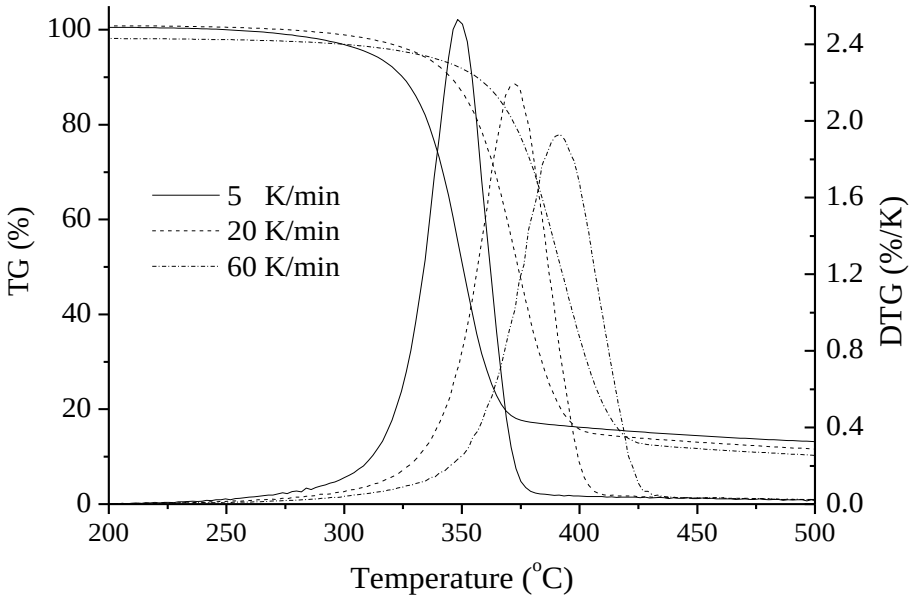

Fig. 4- 1: the TG and DTG curves of cellulose under different heating rates

Table 4-1: the characteristic points of the DTG curve under different heating rates

Heating rate (K/min)	T^a (^oC)	Y^a (%)	T^b (^oC)	$(-dY/dT)^b$ (%/K)	Y^b (%)	T^c (^oC)	Y^d (%)
5	294	96.59	348	2.53	55.54	377	10.31
20	312	96.91	373	2.19	52.79	404	8.23
60	329	95.12	392	1.93	50.38	424	7.49

a: the point where the mass loss rate begins to be more than 0.1%/K;
b: the peak point on the DTG curve;
c: the point where the mass loss rate begins to be less than 0.1%/K;
d: the point of temperature of 800 ^oC.

It is worth noting that the mass of char residue at the final temperature 800 ^{o}C increases at low heating rate (Table 4-1). This confirms the previous report that the char residue produced from the pyrolysis of cellulose increases with longer preheating at the low temperature from 250 to 300 ^{o}C (Broido and Nelson 1975). Cellulose polymer tends to be carbonized at low temperature through the dehydration and cross-linking reactions as pointed out by (Arseneau 1971). Such behaviour is explained (Maschio, et al. 1992) as the rearrangement of the cellulose structure after the preheating process at the low temperature, promoting the final production of char residue.

Table 4-2: peaks of the evolution of gaseous products detected by TG-FTIR under different heating rates

Wavenumber (cm^{-1})	Assignment (Bond)	Vibration	Products	T_{max} (^{o}C)		
				5 K/min	20 K/min	60 K/min
2972-3018	C-H	Stretching	CH_4	530	560	590
2071-2207	C-O	Stretching	CO	370	400	420
2380-2312	C=O	Stretching	CO_2	380	410	425
632-702	C=O	Dactylogram-zone				
1680-1750	C=O	Stretching	R-CHO	370	400	420
2744-2897	C-H	Bending				
1250-1339	C-C	Skeleton	R-CO-R'	370	400	420
1700-1739	C=O	Stretching				
1073-1140	C-O	Stretching	R-OH	370	400	420
3523-3648	O-H	Stretching				
1210-1320	C-O	Stretching	R-COOH	370	400	420
1717-1775	C=O	Stretching				
3523-3586	O-H	Stretching				

Through the FTIR scanning, the composition of evolved gaseous mixture under different heating rates can be determined by the characteristic wavenumber bands. The yield of the products against the time (temperature) can be found by the absorbance against minutes.

The temperature corresponding to the absorbance peak is shown as T_{max} in Table 4-2, representing the maximum evolution of the products. It is found that T_{max} moves towards high temperature as the heating rate increases, confirming the previous work (Li, et al. 2001).

It is noted that the values of T_{max} for the different gaseous products in Table 4-2 are close to T^b in Table 4-1 under the same heat rate. This implies that various gases reach the maximum production simultaneously and the cellulose decomposes intensively within the small temperature interval. The two sets of visible absorbance peaks for the characteristic bands 2071~2207 cm^{-1} and 632~702 (2312~2380) cm^{-1}, show much higher production of CO and CO_2, over other gaseous products, while more CO is generated than CO_2. Further examination of Table 4-2 shows that the formation of methane is delayed comparing to other products due to the fact that more energy is required to break the R-CH_3 bond and form CH_4 (Liao 2003), which results in the peak production of methane at higher temperature.

4.2.2 The fast pyrolysis experiment

Cellulose is pyrolyzed in the testing unit in order to investigate the effects of temperature and residence time on the product yield (gas, tar and char). The variation of residence time is achieved by changing the feeding flow rate in this experiment, i.e. higher flow rate represents low residence time.

The formation of the gaseous products (such as CO, CO_2 and CH_4) and the typical compounds in bio-oil presented in Fig. 4-2 as LG: levoglucosan, HAA: hydroxyacetaldehyde, HA: Hydroxyactone, PA: pyruvic aldehyde, GA: glyceraldehyde, 5-HMF: 5-hydroxymethyl-furfural and FF: furfural, are intensively discussed, according to the proposed chemical pathways for cellulose primary reactions and the secondary decomposition of intermediates.

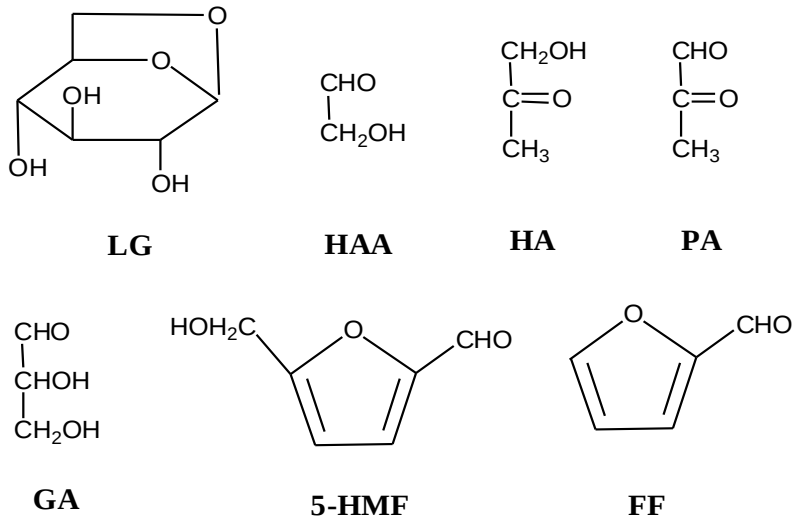

Fig. 4-2: the chemical structures of the typical compositions in bio-oil from cellulose

Product distributions

Table 4-3 shows the yields of the main products (gas, tar and char) under different temperatures (from 430 to 730 ^{o}C) and residence time (from 0.44 to 1.32 s) or feeding flow rate (from 600 to 200 l/h). It is found that the elevated temperature improves the yield of gas, decreases the yield of char, and increases the yield of bio-oil till about 570 ^{o}C followed by gradual decline. This is in line with the report that temperature for the maximum production of bio-oil (60% without moisture) is about 620 ^{o}C using the electrical-heating reactor with a temperature range of 200 to 1000 ^{o}C (Mohammed, et al. 1982). It needs to be noted that the yield of char is small (less than 5 % wt) and remains stable at temperature over 550 ^{o}C (Table 4-3). Therefore the increased yield of gas at higher temperature is attributed to direct competition over the tar formation (Piskorz, et al. 1986; Rath and Staudinger 2001; Liao 2003; Hosoya, et al. 2007; Hosoya, et al. 2007).

Considering the effect of the residence time (feeding flow rate) at the temperature of 530 ^{o}C, the production of char is not changed noticeably (all less than 5%) while the yields of gas and tar behave differently. It shows that more gas is produced within longer residence time at the expense of the tar through the secondary decomposition. It is still not clear in the literature that which mechanism (such as competitive mechanism (Capart, et al. 2004),

consecutive mechanism (Kilzer and Broido 1965; Bradbury, et al. 1979) and hybrid mechanism of both competitive and consecutive (Mamleev, et al. 2007)) decides the formation of gas and tar. Considering the complication of different pathways for the formations of gas and tar, extensive discussion on the mechanisms is given in the following sections by means of the results from the long residence time experiment.

Table 4-3: the yield of tar, gas and char from the gasification of cellulose under the different temperatures and residence times

Product	Residence time:							Temperature:	
(wt %)	0.44 s							530 °C	
	420 °C	470 °C	530 °C	580 °C	630 °C	680 °C	730 °C	0.88 s	1.32 s
Gas	20.1	24.8	26.4	27.3	29.8	34.0	42.5	29.6.	32.5
Bio-oil	30.6	60.9	68.9	72.2	67.6	63.7	56.6	63.1	60.1
Char	47.44	13.51	7.34	2.55	1.55	1.54	1.03	7.41	7.22

Bio-oil compositions

The composition of bio-oil from the thermal decomposition of biomass is very complicated and difficult to be fully characterized by a single analytical technique (Piskorz, et al. 1986; Hosoya, et al. 2007; Hosoya, et al. 2007). A large number of polar organic compounds in the bio-oil are detected by GC-MS analysis in this work. The yields of some typical products in the bio-oil, influenced by the temperature and feeding flow rate are shown in Table 4-4. The formation of the main products (levoglucosan, 5-hydromethylfurfural, furfural, hydroxylacetone, pyruvaldehyde, and some C_{1-2} compounds) in the bio-oil is extensively examined, while the evolution of the gases is investigated. The chemical pathways for primary cellulose pyrolysis and secondary decomposition of the tars are systematically proposed in Figs. 4-3 and 4-4.

Table 4-4: the yield of the typical organic compounds in bio-oil determined by GC-MS analysis

Compounds		Molar fraction (%) (530^{o}C, 600 l/h)	Molar fraction (%) (630 ^{o}C, 600 l/h)	Molar fraction (%) (530 ^{o}C, 200 l/h)
Name (Abbreviation)	Formula			
Hexane	C_6H_{14}	0.16	1.58	0.33
Acetaldehyde	C_2H_4O	0.12	0.57	0.37
Acetone	C_3H_6O	2.13	3.94	2.97
Pyruvaldehyde (PA)	C_3H_4O	0.17	0.35	1.16
Hydroxyacetone (HA)	$C_3H_6O_2$	2.22	4.69	3.43
Hydroxyacetaldehyde (HAA)	$C_2H_4O_2$	4.72	7.53	8.71
Furfural (FF)	$C_5H_4O_2$	0.75	0.97	0.92
2-Furan methanol	$C_5H_6O_2$	0.22	0.34	0.36
2-Hydroxy-2-cyclopenten-1-one	$C_5H_6O_2$	0.55	0.88	0.92
1,3-Butadiene-1-carboxylic acid	$C_5H_6O_2$	0.18	0.36	0.30
2,2-Diethoxypropionate-ethyl-ester	$C_9H_{18}O_4$	0.57	1.04	0.76
2,3-Anhydro-d-mannose (2,3-AM)	$C_6H_8O_4$	0.44	0.92	1.09
Anhydro-d-mannose （AM）	$C_6H_{10}O_5$	2.32	1.61	3.01
5-Hydroxymethl-furfural (5-HMF)	$C_6H_6O_3$	1.62	3.54	1.64
1,6-Anhydro-β-glucofuranose (1,6-AGF)	$C_6H_{10}O_5$	0.41	0.69	0.22
Levoglucosan	$C_6H_{10}O_5$	62.22	51.07	53.11

- ***Anhydro-sugars and the secondary cracking***

Table 4-4 shows that levoglucosan (1,6 anhydro-β-D-glucopyranose) is the main component in the bio-oil (50+%), confirming the results (Piskorz, et al. 1986) that the initial thermal decomposition of cellulose is the depolymerization of the cellulose polymer to form various anhydrosugar derivatives, among which levoglucosan is the most prevalent. The yield of levoglucosan is affected by the source of the cellulose and the experimental conditions (Shafizadeh, et al. 1979). Table 4-4 shows that levoglucosan is reduced at higher temperature, in contrast other products (such as HAA, HA, 5-HMF and so on), which implies a competitive mechanism between the levoglucosan and other products.

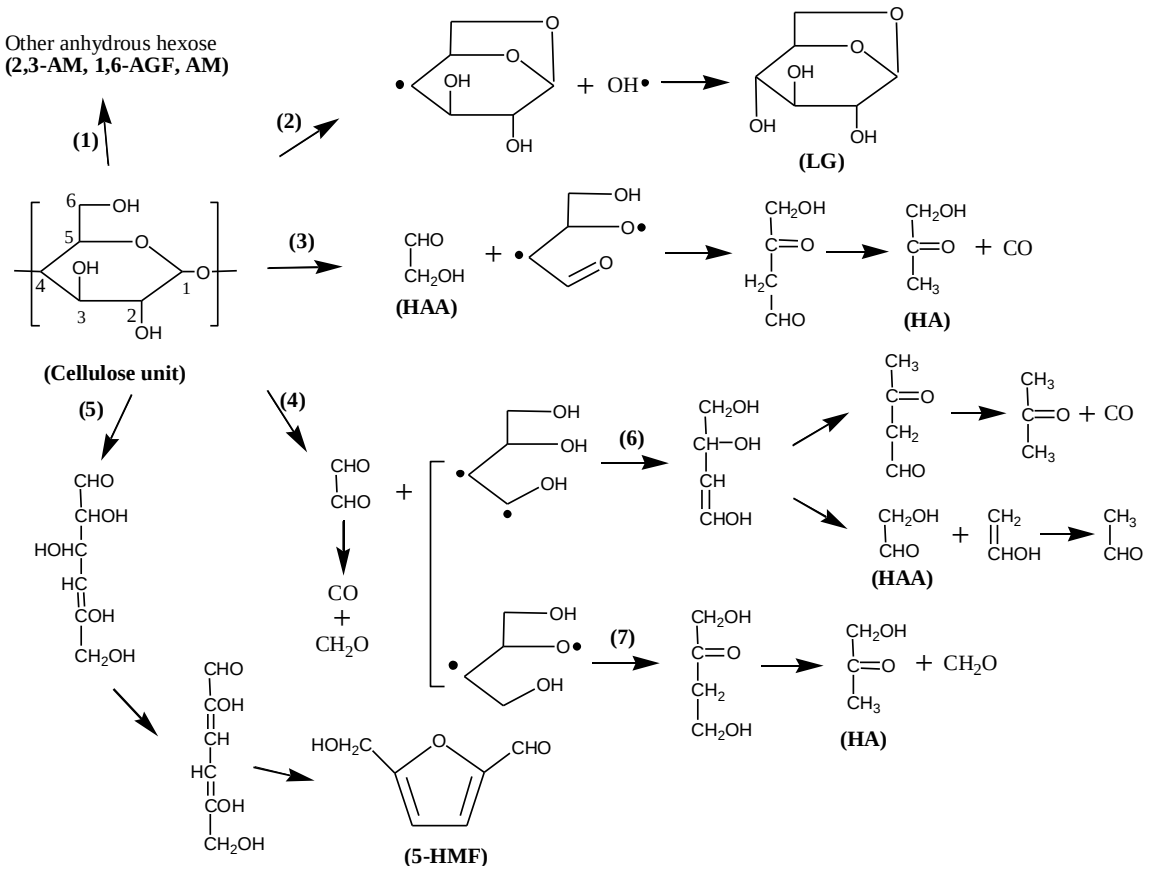

Fig. 4- 3: the speculative chemical pathways for the direct cracking of the cellulose molecules

Similar results have been reported (Richards 1987), claiming that the fragments from the ring opening reactions are enhanced under the high temperature by competing for active cellulose monomer with the levoglucosan (Fig. 4-3). Such phenomenon is also observed for the long residence time at reduced feeding flow rate, which can be interpreted as the sequential mechanism between the levoglucosan and other products, according to the research (Piskorz, et al. 1986; Richards 1987; Li, et al. 2001; Liao 2003; Kawamoto, et al. 2008). Therefore it could be claimed that levoglucosan also acts as an intermediate for the formation of the other products in the cellulose pyrolysis.

The formation of levoglucosan from cellulose pyrolysis has been proposed as the cleavage of the 1,4 glycosidic linkage in the cellulose polymer followed by intramolecular rearrangement of the monomer units (Li, et al. 2001) . A similar pathway **(2)** in Fig. 4-3 is developed to express the formation of levoglucosan (LG). The 1,4-glucosidic bond is presumably cleaved by the acetal reaction between C-1 and C-6, evolving the hydroxyl radical from C-6, then the free hydroxyl radical coalesces with the disrupted glucosidic bond on C-4 to form levoglucosan (1,6 anhydro-β-D-glucopyranose). It is thought that the evolution of the hydroxyl group (free radical) from the C-6 position might be the initiator for the formation of levoglucosan.

Other anhydrous hexoses, such as anhydro-d-mannose and 1,6-anhydro-glucofuranose, are the isomers of levoglucosan, whose formation is similarly initiated from the free hydroxyl radicals and followed by the chemical structure rearrangement (pathway **(1)** in Fig. 4-3). However the reactions of such rearrangement require more energy while competing with the secondary cracking (Piskorz, et al. 1986; Richards 1987; Liao 2003), therefore these anhydrous sugars only occupy a small portion of the bio-oil comparing to levoglucosan (Table 4-4). Noticeably, the yield of 2,3-anhydro-d-mannose are enhanced by the elevated temperature at the expense of anhydro-d-mannose. Both of them are increased with the longer residence time, since the formation reactions are predominant over their secondary cracking reactions. The yields of the 1,6-anhydro-glucofuranose is improved at higher temperature when more energy is

available for the rearrangement reactions, on the other hand, longer residence time reduces its yield overwhelmed by the secondary reactions.

The secondary decomposition of anhydrous sugars (especially levoglucosan) is shown in Fig. 4-4, while the pathways are developed based on the progress in (Shafizadeh and Lai 1972; Piskorz, et al. 1986; Liao 2003; Hosoya, et al. 2008; Kawamoto, et al. 2008). It demonstrates that thermal decomposition of levoglucosan proceeds through the ring-opening of the glucosidic 1,6-acetal bond and the rehydration to form glucopyranose monomer, followed by the prompt secondary reactions. Three main sets of chemical pathways are proposed to describe the possible fission of the glucopyranose: Pathway **(8)** suggests a ring-opening by breaking the ring glucosidic bond and the bond between C-2 and C-3 to form HAA (hydroxyacetaldehyde) and a tetrose (four carbon atoms) fragment; Pathway **(9)** breaks the ring to formaldehyde and a pentose fragment; Pathway **(10)** forms a hexose chain by the fission of hemiacetal bond on C-1 position. The plausible routes of the secondary decomposition of the ($C_{4\text{-}6}$) fragments in Fig. 4-4 explain the formation of the various products under the high temperatures, through the possible dehydration, hydration, fission, decarbonylation and decarboxylation reactions.

- ***5-HMF and FF (the $C_{5\text{-}6}$ furan-ring products)***

It is evident in Table 4-4 that the yields of 5-HMF (5-hydroxymethylfurfural) and FF (furfural) are all enhanced at the elevated temperature. It seems that the 5-HMF is mainly produced by the competitive reactions with the formation of levoglucosan. It is determined that the furfural is mainly produced by the decomposition of 5-HMF and 1-HMF (Shafizadeh and Lai 1972; Liao 2003). The yield of 5-HMF under the long residence time is slightly changed but the yield of FF is visibly increased (Table 4-4), demonstrating that a part of 5-HMF is generated from the levoglucosan degradation to balance its secondary reaction to form furfural. The formation pathways for 5-HMF and FF have not been studied thoroughly in the literature, while two of the chemical pathways are developed in this work: one is the direct ring-opening and rearrangement reactions of cellulose unit molecules (pathway **(5)** in Fig. 4-3); the other is the secondary reactions of levoglucosan (pathway **(10)** → **(16)** in Fig. 4-4).

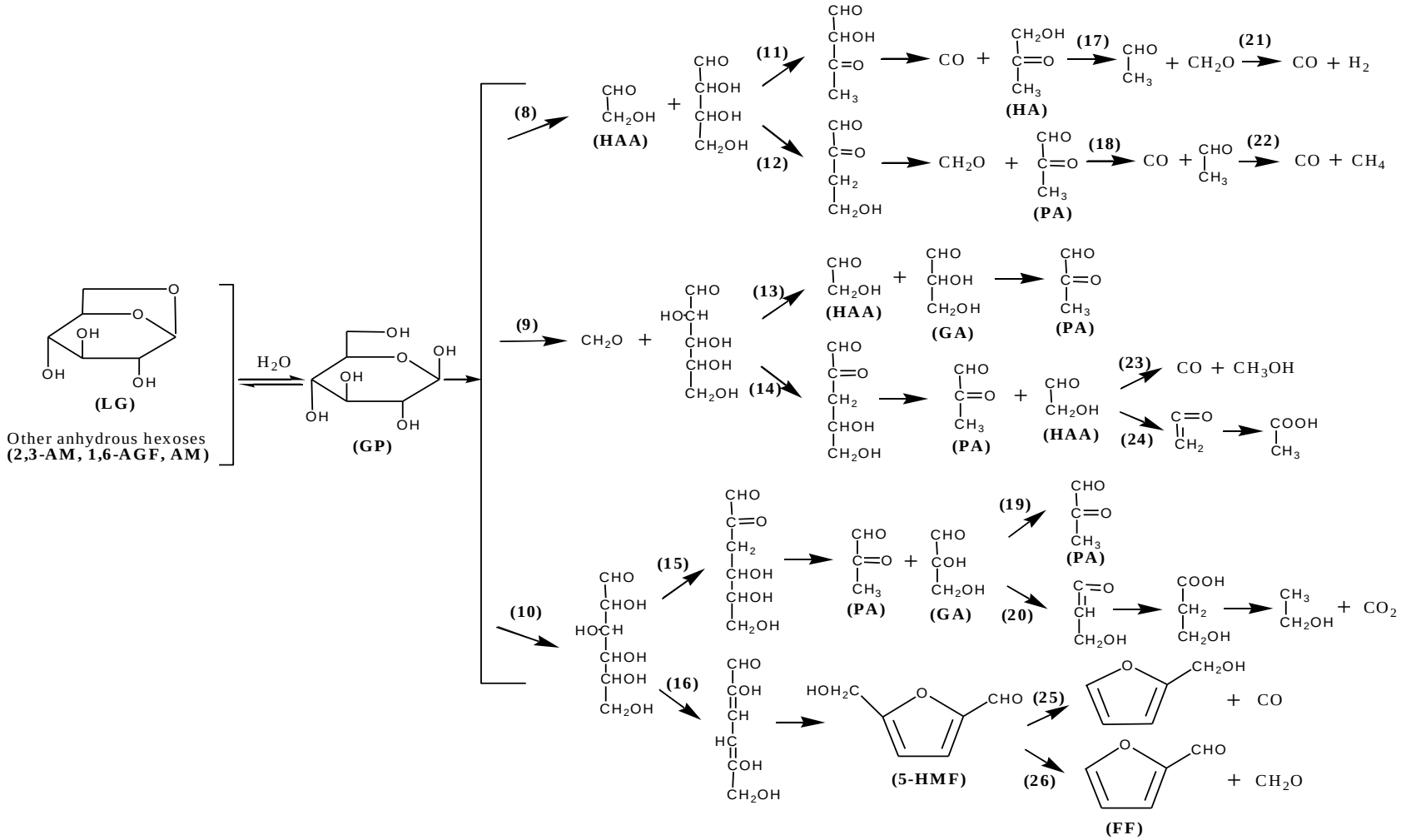

Fig. 4-4: the speculative chemical pathways for the secondary decomposition of the anhydrosugars (especially levoglucosan)

The pathway **(5)** is initiated by the cleavage of the ring glucosidic bond on cellulose unit to form an aldehyde-structure on C-1, followed by the formation of double-bond on C-4 and C-5 through the chain structure rearrangement. Another double-bond on C-2 and C-3 is formed through the dehydration of the corresponding hydroxyl groups. Then, the acetal reaction of the hydroxyl groups on C-2 and C-5 is taken as the essential step to form 5-HFM.

The secondary reactions of levoglucosan to produce 5-HMF (pathway **(10)** → **(16)** in Fig. 4-4) has been proposed before (Shafizadeh and Lai 1972), where the pyran-ring is initially cleaved to the hexose chain structure, followed by dehydration of the hydroxyl groups and sequential acetal reaction on C-2 and C-5. Regardless of the origin of the 5-HFM, the furfural (FF) is approved to be produced from the secondary reaction of 5-HFM (pathway **(26)** in Fig. 4-4), along with the formation of formaldehyde through the dehydroxymethylation reaction of the side chain of the furan-ring. Another pathway has been proposed for the secondary reaction of 5-HMF (Shafizadeh and Lai 1972), suggesting the rearrangement reaction to form aryl compounds, such as benzene and phenol, which are detectable in the bio-oil but not presented in Table 4-4.

- ***Typical C_{2-4} products***

Hydroxyacetaldehyde (HAA) is a major component of a group of the C_{2-4} oxygenated products in the bio-oil from the cellulose pyrolysis, along with hydroxyacetone (HA), glyceraldehyde (GA) and pyruvaldehyde (PA) (Piskorz, et al. 1986; Banyasz, et al. 2001; Li, et al. 2001; Liao 2003; Hosoya, et al. 2008). The typical C_{2-4} compounds with substantial proportion in bio-oil are listed in Table 4-4. It is evident that almost all of the product yields are enhanced at the elevated temperature and residence time. The corresponding formation of the products and their decomposition are discussed below based on the chemical pathways in Figs. 4-3 and 4-4.

The well-established chemical pathway for the formation of HAA is presented as the pathway **(3)** in Fig. 4-3 and **(8)** in Fig. 4-4. The ring hemiacetal bond is very active under the thermal conditions and the bond between C-2 and C-3 is longer than other

positions of the ring (Piskorz, et al. 1986). Hence, the HAA is easily produced on the C-1 and C-2 by the ring-opening through the cleavage of the above two active bonds, along with a four-carbon fragment. It is also suggested that almost all of the carbons on the ring could contribute to the formation of HAA (Liao 2003). The pathway **(4)** → **(6)** in Fig. 4-3 forms the HAA on the C-5 and C-6 through the cleavage of the rearranged four-carbon fragment. Another pathway **(9)** → **(13)** in Fig. 4-4 presents the formation of HAA on the C-2 and C-3 from the scission of the five-carbon fragment, while HAA is formed on the C-5 and C-6 through the pathway **(9)** → **(14)** in Fig. 4-4. It is concluded that the HAA is preferably formed from the C-1 and C-2, and C-5 and C-6. The decomposition of HAA under the high temperature is proposed to comply with the two chemical pathways **(23)** and **(24)** in Fig. 4-4. One (pathway **(23)**) is to produce CO and methanol through the decarbonylation reaction, while the other one (pathway **(24)**) undergoes the dehydration to be ketene structure and the sequential rehydration to the acetic acid.

The pathways **(3)** and **(4)** → **(7)** in Fig. 4-3 present the possible routes to produce HA (hydroxyacetone) through the cleavage of the four-carbon fragments from the direct conversion of the cellulose molecules. The HA produced from the decomposition of levoglucosan is speculated to proceed in only one pathway **(8)** → **(11)**, where the tetrose fragment is initially dehydrated on C-5 and C-6 and then cleaved to CO and HA by the decarbonylation on C-3 (Piskorz, et al. 1986). It is assumed that the HA is mainly produced from the direct conversion of cellulose molecules and partly from the secondary decomposition of levoglucosan, since higher temperature improves the HA yield more substantially than longer residence time (Table 4-4). The decomposition of HA is proposed to undergo the pathway **(17)** in Fig. 4-4 to produce acetaldehyde and formaldehyde, which are the precursors for the formation of CO and methane (Shafizadeh and Lai 1972).

The GA (glyceraldehyde) is an important intermediate for the formation of PA (pyruvaldehyde) through the dehydration reaction, such as the pathway **(9)** → **(13)** and **(10)** → **(15)** → **(19)** in Fig. 4-4. Other pathways for the formation of PA are proposed as

(8) → (12) and **(9) → (14)**, indicating that PA could be produced from the secondary reactions of the C_{3-6} fragments in Fig. 4-4. Comparatively, the PA is hardly produced from the direct fission of cellulose molecules while there is no reasonable pathway for the formation of PA in Fig. 4-3. This indicates that the PA is mainly from the secondary decomposition of levoglucosan, explaining that the yield of PA improves more with longer residence time than under higher temperature. The decomposition of PA is believed to produce CO and acetaldehyde by the decarbonylation reaction (Liao 2003)

The GA (C_3 fragment) undergoes the pathway **(10) → (15) → (20)** to produce propionic acid, followed by the decarboxylation reaction for CO_2 along with the formation of alcohol. The acidic compounds in bio-oil from cellulose pyrolysis are produced by the dehydration of the aldehyde-alcohol structure to a ketene structure, and then rehydration to the acidic products (such as the pathway **(9) → (14) → (24)**), according to (Piskorz, et al. 1986; Banyasz, et al. 2001; Li, et al. 2001; Liao 2003). It is believed that the C_{2-6} fragments with the structure of aldehyde-alcohol could potentially produce the acidic compounds through the dehydration, rearrangement and rehydration reactions.

Table 4-5: The yield of the main gaseous products from the gasification of cellulose under the different temperatures and residence times

Product (wt % by feedstock)	Residence time: 0.44 s						Temperature: 530 °C	
	420 °C	470 °C	530 °C	580 °C	630 °C	730 °C	0.88 s	1.32 s
CO	11.1	13.8	14.5	15.2	16.4	20.2	16.4	18.8
CO_2	8.6	9.8	10.1	9.6	9.6	9.5	9.6	10.2
CH_4	1.2	1.6	1.9	2.3	3.0	3.2	2.4	3.1
H_2	0.2	0.3	0.3	0.4	0.5	0.7	0.3	0.4

Gaseous products

The yields of the main gaseous products (CO, CO_2, CH_4 and H_2), under the influence of the elevated temperature and residence time (feeding flow rate) are shown in Table 4-5. It is apparent that the yields of CO and CO_2 are much greater than H_2 and CH_4. Furthermore, more CO is produced at the elevated temperature and residence time while the yield of CO_2 only changes slightly. This confirms the report (Li, et al. 2001) that the formation of CO is highly affected by the secondary reactions of the low molecular weight products (especially the aldehyde-type compounds) and the CO_2 is presumably produced in primary reactions or early stage of cellulose pyrolysis. Such mechanism is reflected in the corresponding formation chemical pathways in Figs. 4-3 and Fig. 4-4.

A large number of chemical pathways, both the direct fission of cellulose molecules (Fig. 4-3) and the secondary decomposition of the tars (Fig. 4-4), could account for the formation of CO, such as the pathways **(3)**, **(4) → (6), (8) → (11)**, **(9) → (14) → (23)** and **(10) → (16) → (25)**. Almost all of the C_{1-6} fragments containing aldehyde-structure, such as tetrose, HAA, HA, aldehyde and formaldehyde, can produce CO by the decarbonylation reactions. Although the carbon position of the produced CO cannot be specified, the production of CO is generally enhanced with the elevated temperature and residence time due to the intensive secondary reactions. Comparatively, CO_2 is produced primarily by the decarboxylation reactions and specified from C-1 and C-2 positions (Shafizadeh and Lai 1972). The ketene structure, as the precursor for the formation of carboxyl group (acidic structure), is mostly produced during the relative low temperature stage of the cellulose pyrolysis (Banyasz, et al. 2001; Li, et al. 2001). The formation of ketene is overshadowed by other secondary reactions producing the aldehyde-type compounds at high temperature. For instance, the pathway **(10) → (15) → (19)** (Fig. 4-4) would be more favourable than the pathway **(10) → (15) → (20)** (to produce the acidic product) at the high temperature. Therefore the yield of CO_2 changes slightly as the temperature and residence time increase.

4.2.3 The kinetic mechanism for cellulose pyrolysis

With the extensive discussion on the chemical pathway for the main products under different temperature and residence time, an improved kinetic scheme is proposed to describe the pyrolysis process of cellulose in Fig. 4-5. The levoglucosan obtained from the depolymerization of cellulose molecules is estimated to be competitive with the formation of the Tar1 (such as HAA, HA, GA and so on) and Tar2 (such as furfural and 5-HMF) through the direct ring-open reactions, and char formation through carbonization reaction together with CO_2 evolution. Meanwhile, levoglucosan also acts as a precursor for the formation of Tar1 and Tar2 through secondary decomposition and char through polymerization and cross-linking reaction.

The main formation of CO is determined from the secondary reaction of the fragments (tars), while the CO_2 is produced in the initial low-temperature stage through the decarboxylation of the ketene structure during the carbonization process. The kinetic scheme would help to improve the current kinetic model of cellulose pyrolysis involving the information of detailed pyrolytic reactions, providing the possibility to predict the formation of the specified product.

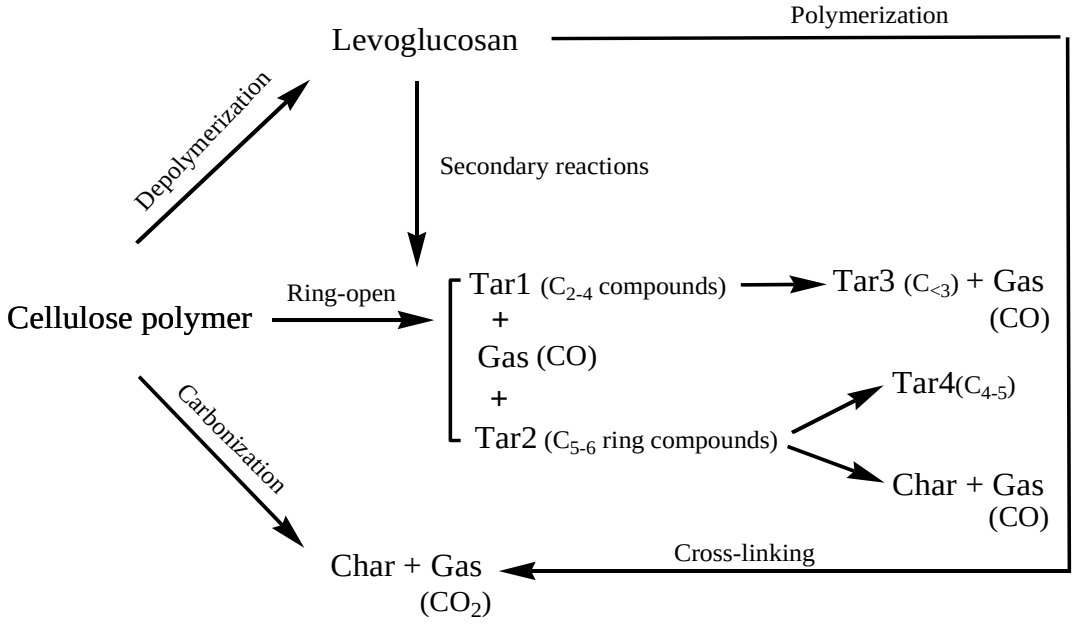

Fig. 4-5: the proposed kinetic scheme for the cellulose pyrolysis

4.2.4 Summaries

Extensive experiments using TG-FTIR and Py-GC-MS were performed to investigate the mechanism of the cellulose pyrolysis and the formation of its main products. The "abrupt mass loss" stage corresponding to the intensive evolution of the volatiles is characterized by the FTIR spectrogram. Effects of temperature and residence time on the product yield (gas, tar and char) are well discussed in the Py-GC-MS experiments. Furthermore, the formation mechanisms of specified tars and gases are extensively investigated, presenting that LG (Levoglucosan) acts as a competitor with other fragments in the primary reactions and also a main precursor for the secondary decomposition stage.

4.3 Hemicellulose

In the TGA-FTIR experiment, the sample of xylan-based hemicellulose powders is heated from 20 to 800 ^{o}C at heating rate of 3, 10, 20 and 80 K/min under the inert atmosphere. For the fast pyrolysis experiment, the reactor temperature is ranged from 400 ^{o}C to 690 ^{o}C, while the feeding flow rate is fixed at 600 l/h, in order to investigate the effect of temperature on the pyrolytic performance of hemicellulose.

4.3.1 The TGA-FTIR analysis

Figs. 4-6a and 4-6b show the TG and DTG curves for hemicellulose under nitrogen at different heating rates. A "sharp mass loss stage" is observed within a narrow range of temperature (from 200 ^{o}C to 350 ^{o}C), where most of the hemicellulose sample is decomposed by a set of chemical reactions. Most of the mass loss curves (TG curves) are found to decay smoothly from about 400 ^{o}C to the final temperature 800 ^{o}C.

T^{a} and T^{d} in Table 4-6, representing the beginning and the end of the "sharp mass loss stage" respectively, move toward high temperature as the heating rate increases. However, the temperature interval (the difference between T^{a} and T^{c}) seems to be sustained for different heating rates (around 70 ^{o}C). Two mass loss rate peaks for the "sharp mass loss stage" could be observed in Fig. 4-6b, shifting toward the high temperature with the increased heating rate, while the temperature gap between the two

peaks at different heating rates is similar as about 32 ^{o}C (Table 4-6), consistent with the reported results (Blasi and Lanzetta 1997; Colomba 1998).

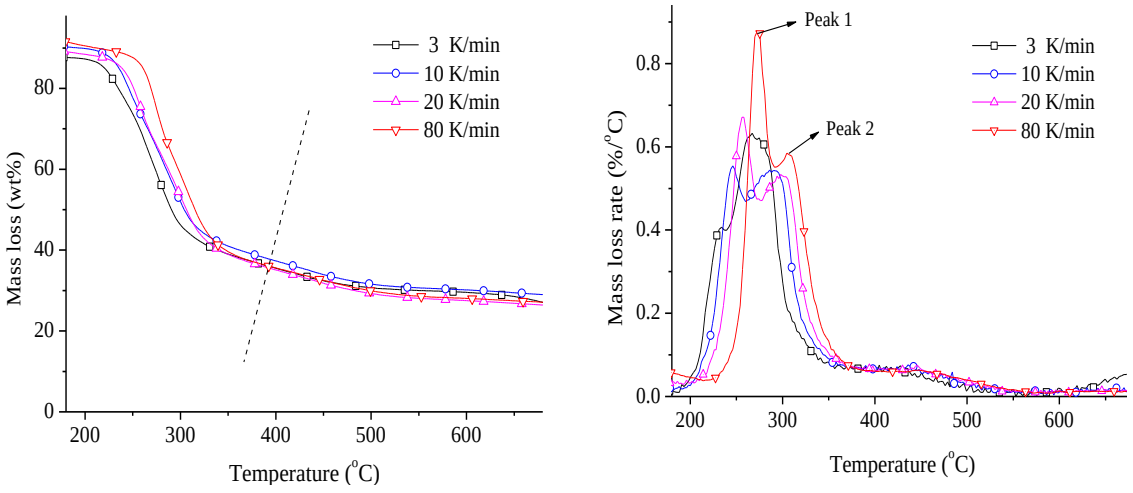

a: TG curves **b: DTG curves**

Fig. 4- 6: The TG and DTG curves of hemicellulose at the different heating rates

Table 4-6: the characteristic points of the TG and DTG curves of hemicellulose at different heating rates

Heating rate (K/min)	T^a (^{o}C)	T^b (^{o}C)	$(-dY/dT)^b$ (%/^{o}C)	T^c (^{o}C)	$(-dY/dT)^c$ (%/^{o}C)	T^d (^{o}C)
3	185	234	0.4070	267	0.6324	354
10	190	246	0.5541	290	0.5431	360
20	192	256	0.6709	298	0.5337	366
80	214	273	0.8782	304	0.5845	369

a: the minimum mass loss rate (-dY/dT) before the maximum value;
b: the first peak of DTG curve;
c: the second peak of DTG curve;
d: the point when the mass loss rate is less than 0.08 %/^{o}C after the peaks of DTG curve.

Compared to the case at the lower heating rate, the first peak at the high heating rate is much higher and more visible, while the second peak shows no obvious trend. The first

peak is mainly ascribed to the cleavage of the glycosidic bonds and the decomposition of side-chain structure (such as the 4-O-methyglucuronic acid unit), and the second one should be attributed to fragmentation of other depolymerized units (xylan units) (Shafizadeh, et al. 1972). It is difficult to separate the chemical reactions in the two peaks. The decomposition of xylan units would move forward with the elevated heating rate, enhancing the mass loss in the first peak (Ponder and Richards 1991). Thus it is sensible that the first peak is much lower than the second one at the low heating rate (3 K/min). At the high heating rate, only one peak would appear, when the decomposition of xylan units is overlapped with that of side-chain structure.

From the FTIR 3-D spectrogram (absorbance-wavenumber-minutes), the variation of evolved volatiles can be determined by the characteristic wavenumber bands, while the yield history of the products can be found by the absorbance against minutes. The temperature corresponding to the absorbance peak is shown as T_{max} in Table 4-7, representing the maximum evolution of the products. It is noted that the values of T_{max} for the different volatile products (except for CH_4) in Table 4-7 are close to T^b in Table 4-6 under the same heat rate (20 K/min). This implies that various volatiles might reach the maximum production simultaneously and the hemicellulose decomposes intensively within the narrow temperature range. The two sets of visible absorbance peaks show much higher production of CO_2 over other gaseous products. It is due to the height of absorbance qualitatively reflects the concentration of the product in the volatile mixture (Liu, et al. 2008).

The detailed evolution of the typical products from the hemicellulose pyrolysis can be explained using the 2-D FTIR spectrogram in Fig. 4-7 together with the corresponding DTG curve. It is observed that only one visible peak on the evolution curve of CO and methanol emerges during the "sharp mass loss stage", while two visible peaks are found for the production of CO_2, furfural and acetic acid. This indicates that the CO and methanol are mainly volatilized around the first peak of the sharp mass loss stage, while the second peak is essentially ascribed to the evolution of CO_2, aldehyde-type and acetic products.

Table 4-7: the main products of hemicellulose characterized by FTIR at the heating rate of 20 K/min and the temperature corresponding to their maximum evolution

Wavenumber (cm^{-1})	Assignment (Bond)	Vibration	Compounds	T_{max} (^oC)
3059-3131	C-H	Stretching	mainly CH_4	474
2920-3088	C-H	Stretching		
2150-2212	C-O	Stretching	CO	254
2058-2131	C-O	Stretching		
2313-2361	C=O	Stretching	CO_2	254
669	C=O	Dactyl-zone		
1684-1745	C=O	Stretching	R-CHO	254
2822-2915	C-H	Bending		
1145-1211	C-C	Skeleton	R-CO-R'	254
1700-1740	C=O	Stretching		
1077-1131	C-O	Stretching	R-OH	254
3585-3650	O-H	Stretching		
1210-1260	C-O	Stretching	R-COOH	254
1690-1800	C=O	Stretching		
3503-3569	O-H	Stretching		

The formation of methanol should be assigned to the O-methyl group lined to the C_4 position of the glucuronic acid unit, while the evolution of CO is attributed to the decarbonylation reactions (Ponder and Richards 1991). The CO_2 and acetic acid are evolved through the whole "sharp mass loss stage", mainly due to the cleavage of the acetyl groups from the xylan chain. The furfural is attributed to the ring-open and rearrangement reactions of the xylan unit (Shafizadeh, et al. 1972). This confirms that the ending groups and the side-chain structure are more active, contributing to the first peak in the "sharp mass loss stage", followed by the intensive decomposition of xylan unit for the second peak.

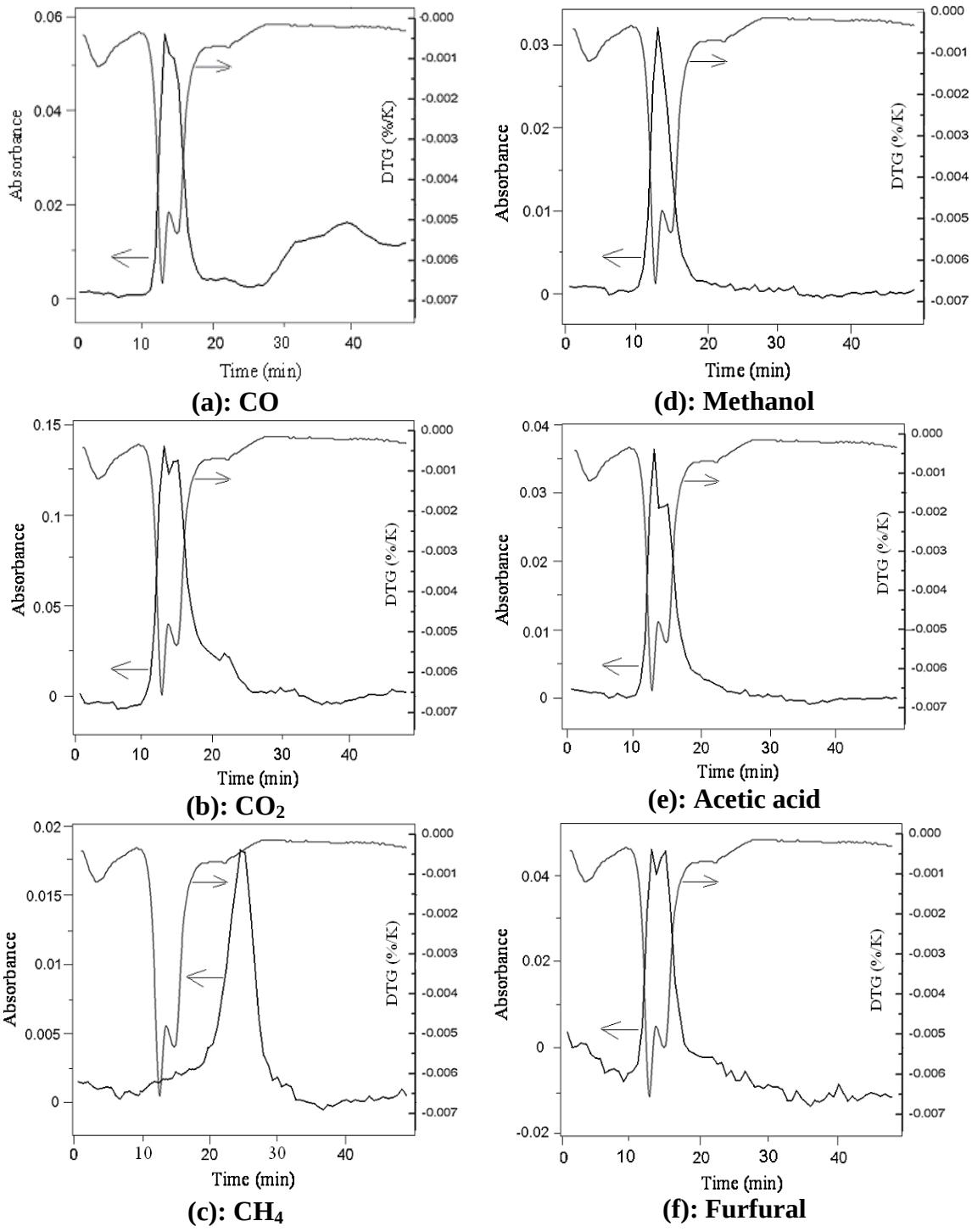

Fig. 4-7: the evolution of the main volatile products from hemicellulose pyrolysis under 20 K/min characterized by FTIR corresponding to its DTG curve

Compared to other products, the evolution of CH_4 is delayed and reaches its maximum production at the higher temperature, due to the fact that more energy is required to break the R-CH_3 bond and form CH_4 (Liao 2003).

4.3.2 The fast pyrolysis experiment

Hemicellulose samples are tested in the fast pyrolysis testing unit in order to investigate the effects of temperature on the product yield (gas, bio-oil and char). The detailed chemical pathways for the formation of the gaseous and condensible products are proposed and extensively discussed in this section.

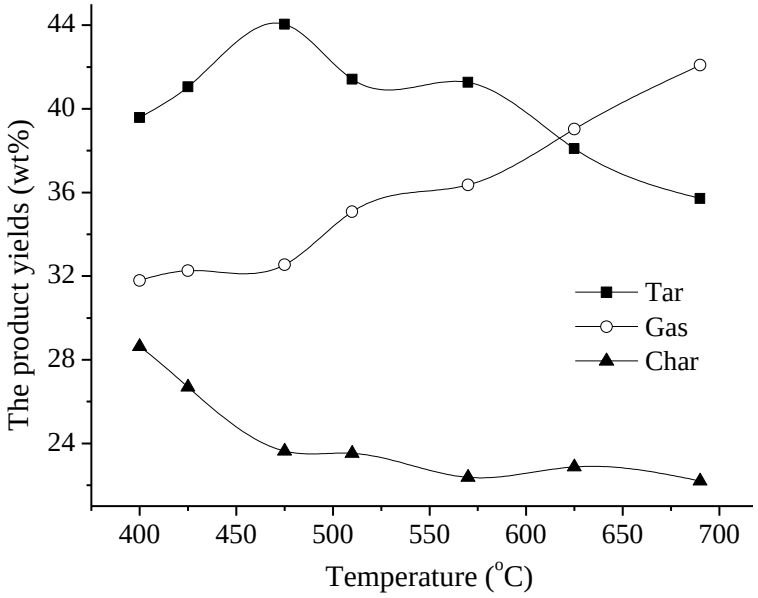

Fig. 4-8: the yields of bio-oil, gas and char from hemicellulose pyrolysis under different temperatures (feeding flow: 600 l/h)

Products (gas, tar and char) distribution

Fig. 4-8 shows the yields of the main products (gas, bio-oil and char) under different temperatures (from 400 to 690 °C) with feeding flow rate of 600 l/h. It is found that the elevated temperature improves the yield of gas (especially over 475 °C) and increases the yield of bio-oil till about 475 °C followed by gradual decline. It needs to be noted that the

yield of char is decreased before 475 ^{o}C and remains stable at temperature over 540 ^{o}C (about 22%).

The production of bio-oil is remarkably increased at the expense of the char before 475 ^{o}C, while the yield of the gaseous products is not visibly changed, owing to the fact that more energy is required to propel the secondary reactions (decomposition of the fragments from the primary reactions) to enhance the evolution of the gases. In contrast, the yield of gas at higher temperature is found to increase in proportion to the reduction of bio-oil. These findings indicate that the hybrid mechanism (the combination of competitive and consecutive mechanism) exists for the formation of gas and bio-oil.

The formation of main condensable products

The composition of bio-oil from the thermal decomposition of biomass is very complicated and difficult to be fully characterized by a single analytical technique (Piskorz, et al. 1986). A number of polar organic compounds in the bio-oil are detected by GC-FTIR analysis in this work. The yields of some typical products in the bio-oil (molar fraction), influenced by the temperature are shown in Table 4-8. Since the novelty of the paper is to reveal the detailed mechanism on the reaction mechanism of hemicellulose pyrolysis, the chemical pathways for the cracking of the hemicellulose monomeric units (including the xlyan unit, O-acetyl-xylan unit and 4-O-methylglucuronic acid unit) and secondary decomposition of the fragments are systematically proposed in Figs. 4-9 and 4-10.

Table 4-8 shows that the **1, 4-anhydro-D-xylopyranose** is one of the main condensable products from the hemicellulose pyrolysis, and the production is decreased at elevated temperature. This indicates that the high temperature inhibit the evolution of this product. The pathway **(1)** in Fig. 4-9 suggests that the formation of 1,4-anhydro-D-xylopyranose is mainly attributed to the cleavage of the glycosidic linkage of the xylan chain, followed by the rearrangement of the depolymerized molecules. It is reported that the 1, 4 intramolecular glycosidic bond on the xylopyranose is less stable than the 1, 6 glycosidic bond on the glucopyranose (levoglucose) (Ponder and Richards 1991). This implies that

most of the produced 1, 4-anhydro-D-xylopyranose would be instantly consumed to produce the two-carbon, three-carbon fragments and gases through the pathways **(2)**, **(3)**, **(4), (5)** and **(6)** in Fig. 4-9, acting as an intermediate product from the hemicellulose pyrolysis.

Table 4-8: the molar fraction of the main compounds in the bio-oil from hemicellulose pyrolysis under different temperature (feeding flow rate: 600 l/h)

Compounds	425 ^{o}C	475 ^{o}C	510 ^{o}C	570 ^{o}C	690 ^{o}C
Methanol	2.26%	2.59%	2.96%	3.12%	3.61%
Acetic acid	12.31%	11.28%	10.22%	8.82%	7.71%
Acetone	1.92%	2.23%	2.24%	2.76%	3.03%
Furfural	5.37%	5.9%	6.42%	7.89%	9.98%
1,4-anhydro-D-xylopyranose	10.66%	8.78%	7.61%	5.54%	2.18%

The **furfural (FF)** is regarded as a typical ring-containing product in the bio-oil (Shafizadeh, et al. 1972; Ponder and Richards 1991). It is found that the yield of furfural is increased as temperature rises, i.e. the high temperature favours the formation of furfural (Table 4-8). It was reported that the addition of zinc chloride also facilitates the formation of furfural from the hemicellulose pyrolysis, through the concerted cleavage of the bond between oxygen and C-5 position and ring-forming between C-2 and C-5 position on the xylan-unit along with evolving a free radical of H (Shafizadeh, et al. 1972). Compared to that, two other chemical pathways are proposed here for the production of furfural here. One is ring-opening reaction of the depolymerised xylan unit through the cleavage of the hemi-acetal bond (between oxygen and C-1 on the pyran-ring), followed by the dehydration between the hydroxyl groups on C_2 and C_5 position (pathway **(4)** → **(8)** in Fig. 4-9). The other is the cleavage of the 1, 2 glycosidic bond between the xylan unit and 4-O-methylglucuronic acid unit, followed by the ring-opening reaction and rearrangement of the 4-O-methylglucuronic acid after the elimination of CO_2 and methanol (pathway **(14)** → **(15)** → **(8)** in Fig. 4-10).

Accordingly it is found that the O-acetyl-xylan unit has no contribution to the formation of furfural (in Fig. 4-10).

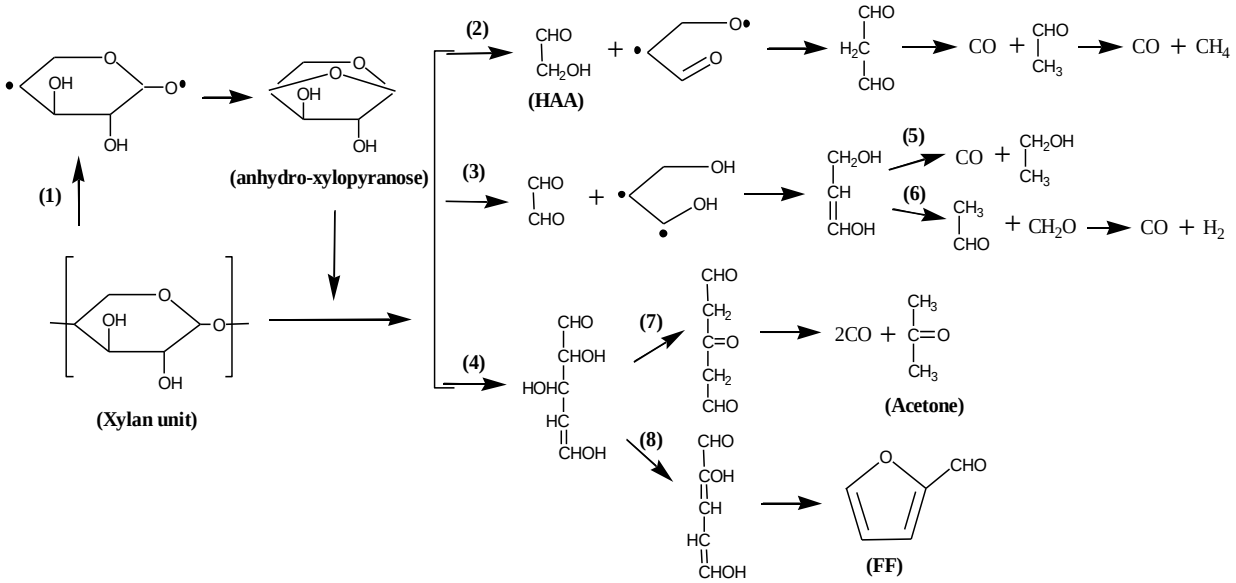

Fig. 4-9: the speculative chemical pathways for thermal decomposition of the main chain of O-acetyl-4-O-methylglucurono-xylan

Acidic products, especially acetic acid and formic acid, are commonly detected in the bio-oil from the pyrolysis of hemicellulose. The yield of acetic acid is found to decline at elevated temperature, shown in Table 4-8. It is translated that the formation reactions for acetic acid is less competitive under the high temperature. The prevalent mechanism of the formation of acetic acid is involved with the primary elimination reaction of the active O-acetyl groups linked to the main xylan chain on C_2 position (Shafizadeh, et al. 1972; Ponder and Richards 1991), described as the pathway **(11)** in Fig. 4-10. Another chemical pathway for the acetic acid production is attributed to the ketene structure of the fragment from the 4-O-methylglucuronic acid unit after the elimination of the carbonyl and O-methyl groups (secondary reaction pathway **(14)** → **(16)**). The pathway **(11)** for the formation of acetic acid is comparatively predominant over the other pathway, since the acetyl groups are in larger proportion than the 4-O-methylglucuronic acid units in the source material.

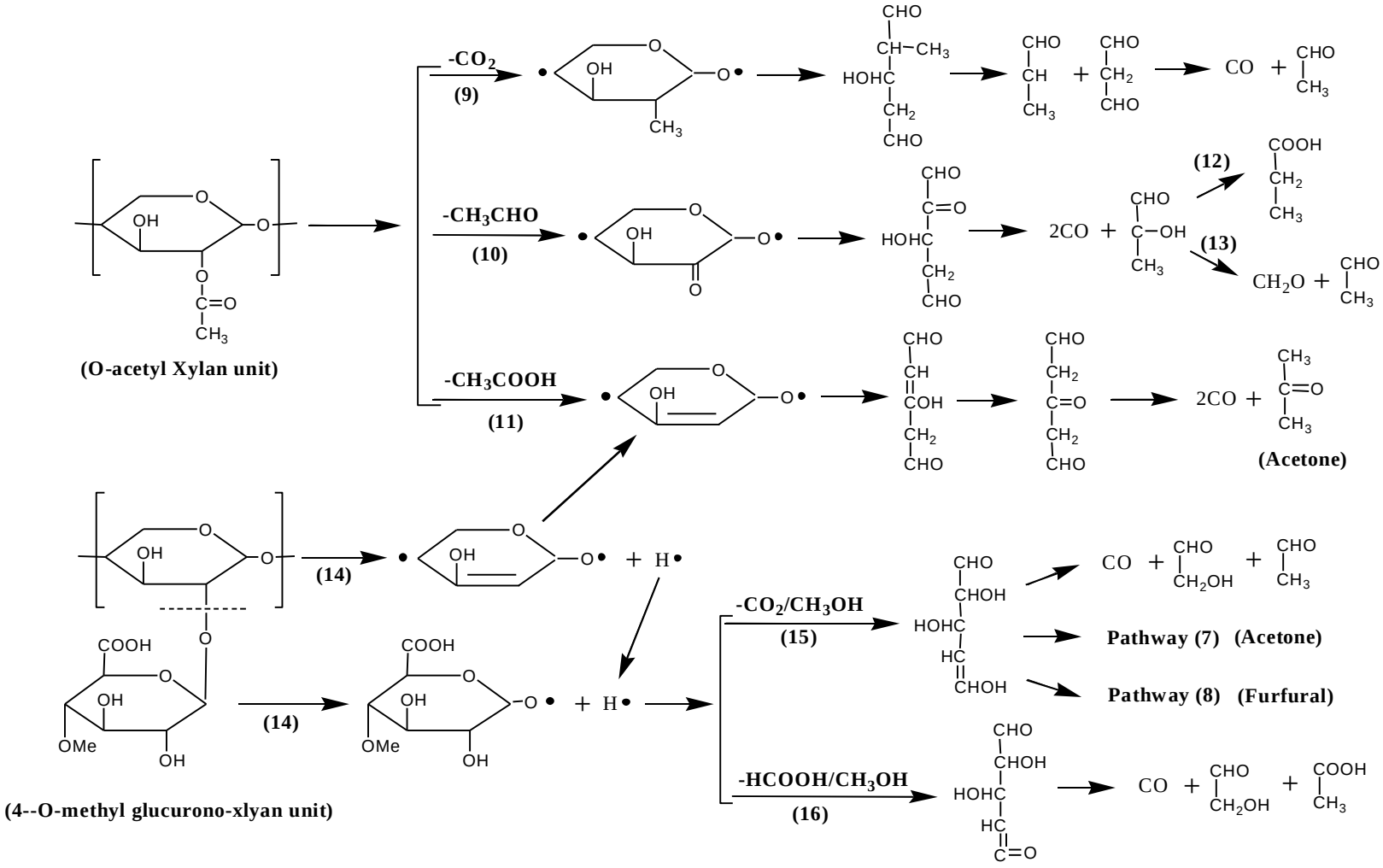

Fig. 4-10: the speculative chemical pathways for thermal decomposition of O-acetyl-xylan and 4-O-methylglucuronic acid unit

It could be approved that the chemical pathway **(11)** is less competitive than the other two pathways **(9)** and **(11)**, since the yield of acetic acid is decreased with the increased temperature. The formation mechanisms for **formic acid** and **propionic acid** are also speculated in Fig. 4-10. It could be found that the formic acid is mainly produced from the elimination reaction of the carboxyl group on 4-O-methylglucuronic acid unit, accompanying the formation of CO, hydroxylacetaldehyde and acetic acid through pathway **(14)** → **(16)**. The formation of propionic acid is attributed to the chemical pathway **(10)** → **(12)**, showing a competitive mechanism with the evolution of acetic acid from the O-acetyl-xylan unit through pathway **(11)**.

Table 4-8 also shows the effect of temperature on the yield of **methanol** and **acetone**, presenting a slightly upward trend with the increased temperature for the two products. The formation of methanol is mainly attributed to the O-methyl group on C_4 position of 4-O-methylglucuronic acid unit, primarily evolved through the pathways **(14)** → **(15)** and **(14)** → **(16)**. The yield of methanol changes slightly with the elevated temperature, due to the fact that no competitive reaction commences to consume the O-methyl groups. The formation of acetone should be complicated, as almost each unit could decompose to produce acetone (pathway **(4)** → **(7)** for xylan unit, **(11)** for O-acetyl-xylan unit and **(14)** → **(15)** → **(7)** for 4-O-methylglucurono-xylan unit). Since the acetic acid formed through pathway **(11)**, together with the formation of acetone is decreased at elevated temperature, the acetone produced from the decomposition of xylan unit should be more competitive and the main contributor for the final yield of acetone.

The evolution of gaseous products

The influence of the elevated temperature on the yields of the main gaseous products (CO, CO_2, CH_4 and H_2) is exhibited in Table 4-9. It is noticeable that the yields of CO and CO_2 are much greater than H_2 and CH_4. The overwhelming evolution of CO_2 is ascribed to the decarboxylation reaction of the large content of O-acetyl groups linked

to the xylan chain normally on C_2 position (Shafizadeh, et al. 1972; Ponder and Richards 1991). More CO is produced at the elevated temperature while the yield of CO_2 only changes slightly. It could be explained as: the formation of CO is highly affected by the decomposition of the ring-opened intermediate, the secondary reactions of the low molecular weight products (especially decarbonylation of the aldehyde-type compounds) (Hosoya, et al. 2007), CO_2 is presumably produced in the primary reactions. Such a mechanism is revealed in the corresponding formation chemical pathways in Figs. 4-9 and 4-10.

Table 4-9: the yield of the gaseous products from hemicellulose pyrolysis under different temperatures (feeding flow rate: 600 l/h)

Compounds (wt % by feedstock)	425 ^oC	475 ^oC	510 ^oC	570 ^oC	625 ^oC	690 ^oC
CO	5.35	5.23	6.02	6.93	9.24	13.33
CO_2	25.01	24.54	25.61	25.78	24.79	22.87
H_2	1.08	1.60	2.35	2.49	3.29	3.34
CH_4	0.81	0.96	1.09	1.15	1.70	2.56

The evolution of CO_2 is mainly attributed to the primary decomposition of O-acetyl-xylan unit through the decarboxylation reaction corresponding to the pathway **(9)**, and partially caused by the primary reaction of the 4-O-methylglucuronic acid through the pathway **(14)** → **(15)** in Fig. 4-10. Comparatively a large number chemical pathways could account for the formation of CO, such as the pathway **(2)**, **(3)**, **(4)** → **(7)**, **(9)**, **(10)**, **(11)** and **(14)** → **(16)**, including the decomposition of (O-acetyl) xylan units and side-chain structure (4-O-methylglucuronic acid). Almost all of the fragments containing aldehyde-structure, such as hydroxylacetaldehyde, aldehyde and formaldehyde, can

produce CO by the decarbonylation reactions. It should be noted that the yield of CO is increased at higher temperature, while the yield of CO_2 and acetic acid is simultaneously decreased as shown in Table 4-8 and Table 4-9. It is presumable that the pathway **(10)** is more competitive to consume O-acetyl-xylan units to promote the formation of CO, compared to the other two pathways **(9)** and **(11)**. Thus, it is understood that the evolution of CO is enhanced at elevated temperature where the secondary reactions are improved.

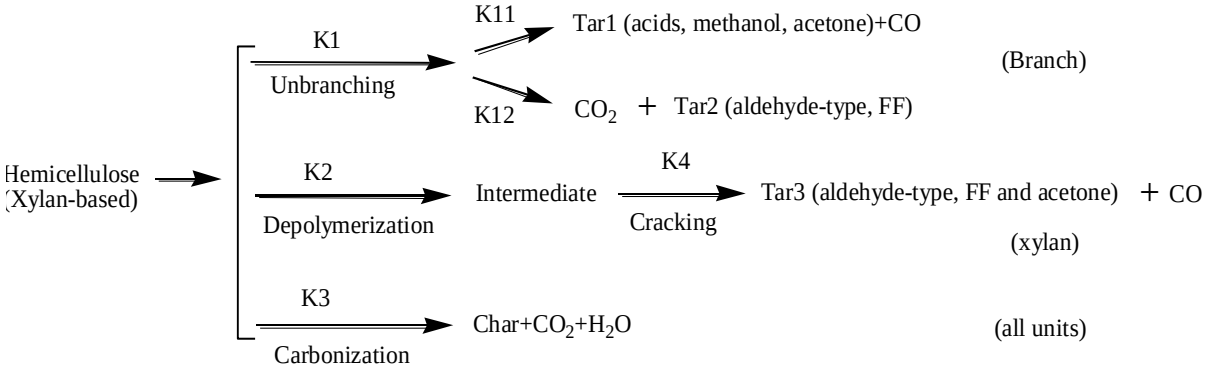

Fig. 4-11: the kinetic scheme for xylan-based hemicellulose pyrolysis

4.3.3 The kinetic mechanism for hemicellulose pyrolysis

The kinetic scheme for xylan-based hemicellulose pyrolysis is proposed as presented in Fig. 4-11. The above extensive discussion on the evolution of volatiles against temperature presents the possible chemical pathways (Fig. 4-9 and Fig. 4-10) for the decomposition of xylan-based hemicellulose and the secondary cracking of its primary products. All the units in the xylan-based hemicellulose are proposed to be pyrolyzed separately. The branch units (both O-acetyl-xylan unit and O-methylglucurono-xylan unit) are consumed by two competitive decomposition ways: one is to produce Tar1 (K11) such as acidic compounds, methanol, acetone and CO; the other is to produce Tar 2 (K12) including aldehyde-type compounds, furfural and CO_2. Comparatively, the main xlyan unit is proposed to be depolymerised to intermediate (anhydrosugars) (K2), followed by further cracking to produce Tar 3 (K4)

containing aldehyde-type products, furfural, acetone and CO. Another thermal decomposition line of all the units (K4) is to be carbonized to produce char residue together with the evolution of CO_2 and H_2O.

4.3.4 Summaries

The mechanisms of the hemicellulose pyrolysis and chemical pathways for the formation of its main products are extensively investigated using the TG-FTIR and Py-GC-MS. Two visible peaks in the "sharp mass loss stage" corresponding to the intensive evolution of the volatiles are characterized by the FTIR spectra. It is speculated that two peaks would overlap at the high heating rate due to the enhancement of the decomposition of different xylan units.

Effects of temperature on the product yield (gas, bio-oil and char) are discussed in the Py-GC-MS experiments. Furthermore, the formation mechanisms of bio-oil and gases are extensively investigated. The furfural and 1,4-anhydro-D-xylopyranose are mainly produced from the xylan units, while the formation of acetic acid and CO_2 is attributed to the primary decomposition of O-acetyl-xylan unit. The xylan unit is also the main precursor for the formation of the two-carbon, three-carbon fragments and gases (CO, H_2 and CH_4). The evolution of methanol is mainly ascribed to the primary reactions of 4-O-methyglucuronic acid unit, which could be further decomposed to almost all of the products generated from the other two units. It is worth noting that the formation of acetone and CO could be attributed to the decomposition of the ring-opened intermediate products or secondary reactions of the fragments, obtained from all three kinds of the units in the original material.

4.4 Lignin

In the TGA experiment, the sample of lignin powders is heated from 20 to 900 ^{o}C at heating rate of 20 and 40 K/min under the inert atmosphere. For fast pyrolysis

experiments, the operation temperature is ranged from 475 ^{o}C to 825 ^{o}C, while the feeding flow rate is 600 l/h.

4.4.1 The TGA-FTIR analysis

The TG and DTG curves for kraft lignin under nitrogen at two heating rates are shown in Fig. 4-12a and 4-12b, and the characteristic points are summarized in Table 4-10. A notable mass loss peak, appearing at 376 ^{o}C for 20 K/min and 390 ^{o}C for 40 K/min, are found at the second major stage of lignin pyrolysis, while the "shoulder peak" appears ~270 ^{o}C at the first pyrolysis stage. It is reported that the first major pyrolysis stage of ball-milled wood lignin is ~230 ^{o}C, corresponding to the evolution of the phenolic compounds (Liu, et al. 2008). Comparatively, the initial stage of kraft lignin pyrolysis is relatively inert and overlapped by the second pyrolysis stage, exhibiting the "shoulder peak" on the DTG curve. This is mainly due to its chemical structural changes during the preparation process causing the block of the reactive groups (Froass and Ragauskas 1996). Moreover, the two steps of the decomposition of kraft lignin are not so obvious as presented by Fenner and Lephardt (Fenner and Lephardt 1981) who indicate the first stage between 120 and 300 ^{o}C and the second between 300 and 480 ^{o}C. The difference could be attributed to the wood species as the source for kraft lignin preparation. However, the mass loss during the two major stages, presenting 50% of kraft lignin, is consistent with the result from Fenner and Lephardt (Fenner and Lephardt 1981).

It needs to be noted that char residue is one of the main products from kraft lignin pyrolysis, accounting for about 40 wt% of the feedstock. The condensation reactions contributing to the formation mechanism of char during the pyrolysis of lignin, are enhanced at the low temperature or the low heating rates (Nakamura, et al. 2007), which is confirmed by the results showing that the char yield of kraft lignin at the heating rate of 20 K/min is higher than that at 40 K/min (Y^{d} in Table 4-10). However, the reactivity of the char residue seems not to be affected by the heating rate, while

the mass loss rate of the solid residue at 600 ^{o}C ($(-dY/dT)^{c}$ in Table 4-10) and its mass loss between 600 and 900 ^{o}C are almost identical at both heating rates.

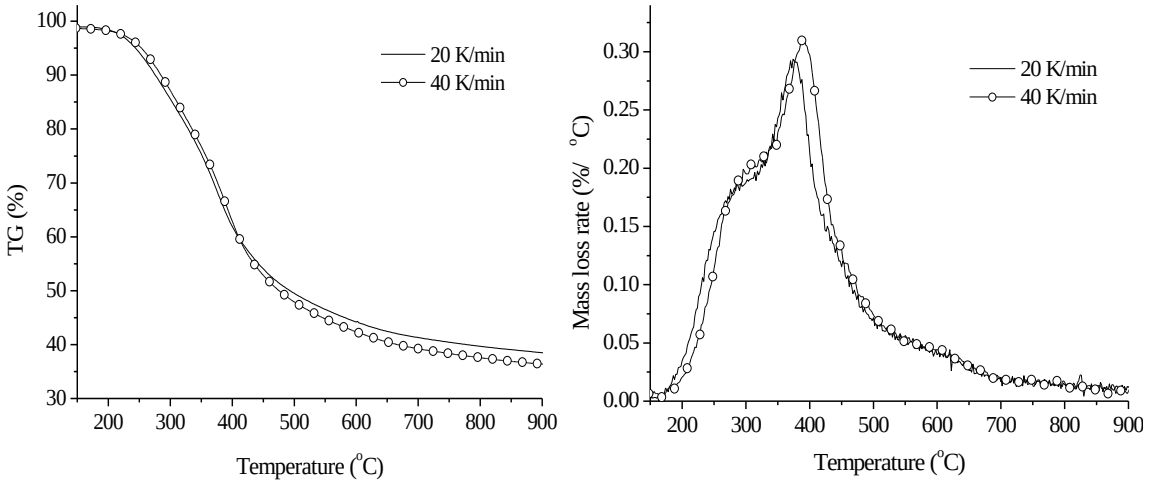

a: TG curves **b: DTG curves**

Fig. 4-12: the TG and DTG curves of the lignin at different heat rates

Table 4-10: the characteristic points of the TG and DTG curve of lignin at the two heating rates

Heating rate (K/min)	T^{a} (^{o}C)	$(-dY/dT)^{a}$ (%/^{o}C)	Y^{b} (%)	Y^{c} (%)	$(-dY/dT)^{c}$ (%/^{o}C)	Y^{d} (%)
20	376	0.2936	52.32	44.20	0.041	38.49
40	390	0.3101	48.92	42.35	0.040	36.39

a: the peak of DTG curve;
b: the point after the major mass loss stage (about 500 ^{o}C);
c: the point when the temperature is 600 ^{o}C;
d: the final temperature 900 ^{o}C;

The evolution of the volatiles is estimated according to the absorption bands from the 3-D FTIR spectra for thermal decomposition of kraft lignin. The time/temperature corresponding to the maximum yield of the volatile at the heating rate of 20 K/min is determined and shown in Table 4-11. The weight loss of kraft lignin before 150 ^{o}C is

mainly ascribed to the evaporation of water (both free water and bound water). The vapour, corresponding to the absorption bands at 1645-1750 and 3823-3870 cm^{-1}, achieves the maxima at around 110 ^{o}C. The most notable band, being predominant around the first pyrolysis stage of kraft lignin, is 1300-1400 cm^{-1}, ascribed to the bending vibration of the alcoholic and phenolic hydroxyl (-OH) groups. Other characteristic bands 1613, 1513 and 1300-1000 cm^{-1}, corresponding to the relevant bonds on the aromatic ring, reach their maximum absorbance at 270 ^{o}C (the shoulder peak of the DTG curve of kraft lignin). Meanwhile, the alkyl groups characterized by the bands at 1310-1365, 1093-1088 and 2750-2990 cm-^{1} are vigorously released during the first pyrolysis stage of kraft lignin. This indicates that the phenolic compounds containing the aromatic ring, hydroxyl group and alkyl groups (such as guaiacol, syringol and (2-methoxy-) 4-alkyl substituted phenol) are predominantly released in the first pyrolysis stage, reflecting the characteristics of the lignin structure. The evolution of methanol, identified by the other two absorption bands at 974-1058 and 2904-2979 cm^{-1}, is relatively weak in this stage compared to phenolic compounds.

Another releasing peak for methanol in the second pyrolysis stage of kraft lignin is found at ~380 ^{o}C, due to the hydrogenation of the methoxy groups (-OCH_3) on the aromatic ring, while the previous evolution maxima is attributed to the cleavage of γ-carbon ending with hydroxyl group (Evans, et al. 1986). It is reported that the methoxy groups (-OCH_3) also act as an important source for the formation of methane corresponding to the characteristic bands at 2990-3010 and 3020-3190 cm^{-1} (Liu, et al. 2008). The releasing of methane starts at ~340 ^{o}C and reaches the first maxima at 430 ^{o}C, while the evolution of methanol gradually decays after ~390 ^{o}C. This indicates that the formation of methane from the methoxy groups at the high temperatures is more competitive than that of methanol. The second evolution maxima for methane, possibly generated from the secondary cracking of the primary compounds, is found at ~535 ^{o}C due to the demand of higher energies to break the bonds.

CO_2, another major volatile released in the second pyrolysis stage, is identified by the absorption bands at 645-690 and 2210-2390 cm^{-1}. It is found that the evolution of CO_2 initiates at ~220 ^oC, reaches the maxima at 380 ^oC and ends at ~570 ^oC. The CO_2, possibly produced from the secondary cracking of the phenolic compounds, is not well clarified in the literature. The evolution of CO corresponding to the characteristic band at 2020-2220 cm^{-1} is detected over a quite broad temperature range from ~220 to 790 ^oC, showing the maxima at ~480 ^oC. The initial stage of the CO release is attributed to the decarbonylation reaction of the alkyl side-chain ending with carbonyl group (-CHO), while the evolution of CO at the high temperatures is ascribed to the secondary reactions of formaldehyde and organic compounds or other free radical coupling reactions (Fenner and Lephardt 1981; Evans, et al. 1986).

4.4.2 The fast pyrolysis experiment

The kraft lignin samples are tested in the fast pyrolysis unit in order to investigate the effect of temperature on product yield, formation of the typical organic compounds and the distribution of gaseous products. The possible chemical pathways, presented as a set of free-radical chain reactions, are proposed to describe the formation of the typical gaseous and condensable products in this section.

The yields of gas, bio-oil and char

The yield of the products (gas, tar/bio-oil and char) under different temperatures (from 475 to 825 ^oC) is shown in Fig. 4-13. It is found that the elevated temperature facilitates the formation of the gaseous products (especially over 650 ^oC), while the yield of tar reaches maxima (43 wt%) at ~630 ^oC followed by a gradual decline. The yield of char notably decreases before 650 ^oC and remains stable at the temperature over 700 ^oC. It needs to be noted that the char yield at the high temperature (825 ^oC) is ~36% of kraft lignin feedstock, similar as the results from Pakdel (38% of steam-exploded lignin at 465 ^oC in a vaccum pyrolysis unit) (Pakdel, et al. 1992) and Hosoya (40.6% of ball-milled wood lignin at 800 ^oC in a fixed bed unit) (Hosoya, et

al. 2007). Therefore lignin also performs a higher yield of char residue in this fluidized bed pyrolysis unit, compared to that from cellulose (Shen and Gu 2009) and hemicellulose (Shen, et al. 2010)

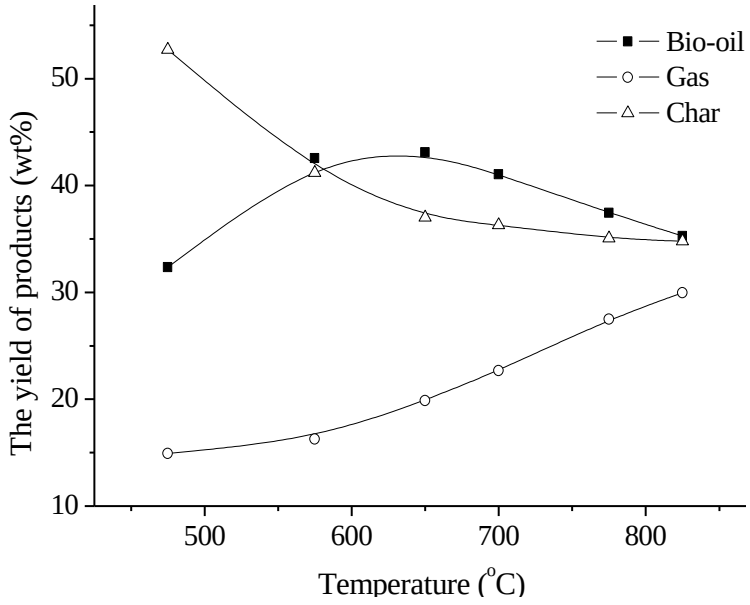

Fig. 4-13: the yield of gas, bio-oil and char from the pyrolysis of lignin under different temperatures

The yield of tar visibly increases at the consumption of char residue before 650 ^{o}C, while the evolution of gaseous products changes slightly. After then, the yield of gas increases remarkabley not only by competing with the formation of tar in the primary pyrolysis stage, but also due to the secondary cracking of the primary tarry compounds. The reduction of the tar yield between 650 and 825 ^{o}C, mainly due to the vigorous secondary reactions, is less than 10 % of the kraft lignin feedstock. This indicates that the reactivity of the tar produced by lignin pyrolysis is not significantly affected by temperature, compared to that of cellulose (Hosoya, et al. 2008).

The compounds in bio-oil

The tar/bio-oil from the lignin pyrolysis is the mixture containing various phenolic compounds (both monomers and oligomers) (Evans, et al. 1986; Pakdel, et al. 1992;

Amen-Chen 2001; Hosoya, et al. 2008). A number of monomeric (single-ring contained) compounds, predominantly distributed in the bio-oil, are identified by GC-MS in this work.

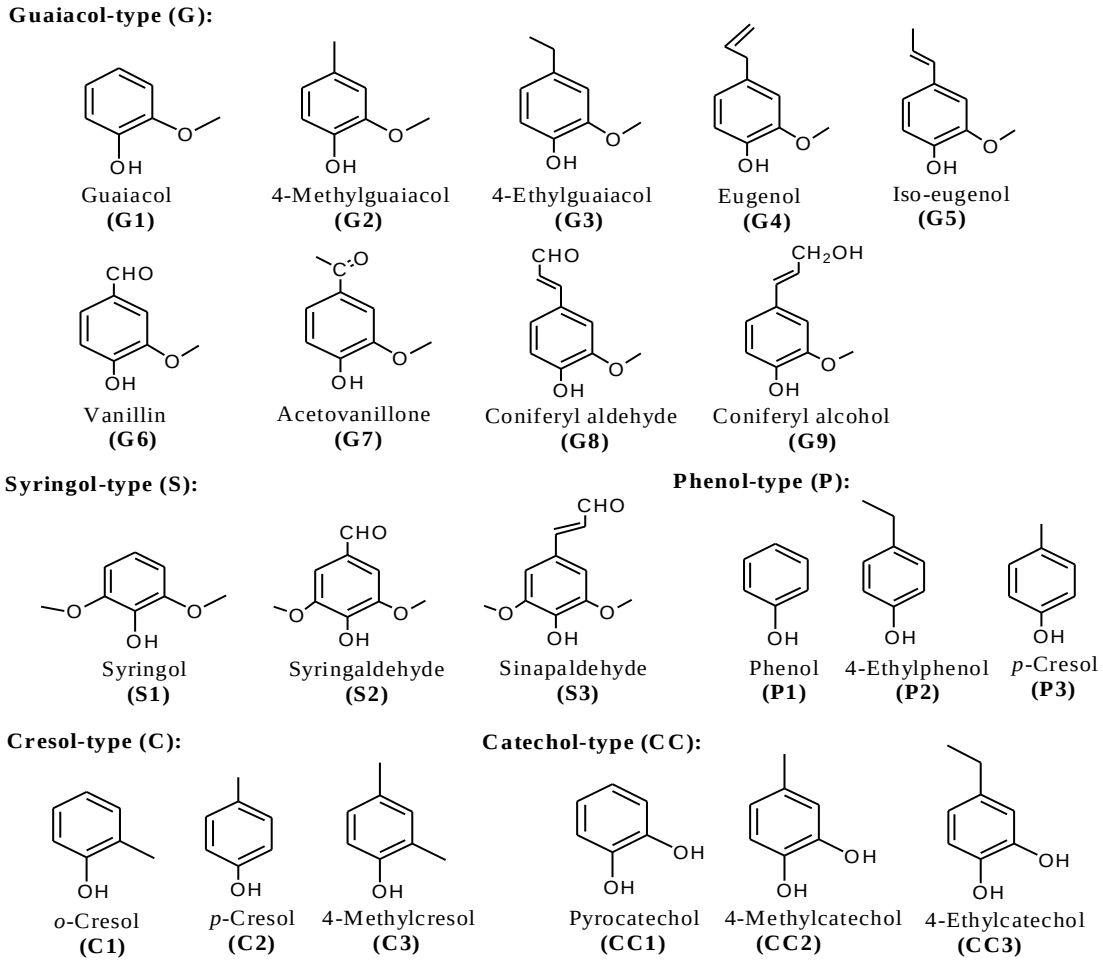

Fig. 4-14: the structure of the typical compounds in the bio-oil from the lignin pyrolysis identified by GC/MS

The chemical structures exhibited in Fig. 4-14 are classified as guaiacol-type (**G1-G9**), syringol-type (**S1-S3**), phenol-type (**P1-P3**), cresol-type (**C1-C3**) and catechol-type (**CC1-CC3**). The yields (the molar fractions) of the typical compounds in the bio-oil, influenced by the temperature, are shown in Table 4-11. The chemical pathways for the primary pyrolysis of lignin and secondary cracking of the typical products are proposed as the following free radical **chain-reactions (1)-(5)** in Figs. 4-15-19, to

improve the understanding of the relationship between the lignin structure and its pyrolytic degradation mechanism.

Guaiacol-type and syringol-type compounds

Compared to the syringol-type compounds, the guaiacol-type compounds are the predominant products from the primary pyrolysis of lignin (Table 4-11). One possible route for the formation of guaiacol (**G1**) and syringol (**S1**) is the cleavage of aryl-alkyl-aryl linkage (**B4** in Fig. 3-4), in parallel to the H-abstraction for phenoxy group to form the corresponding phenolic hydroxyl (Amen-Chen 2001). Other formation pathways would complement their high yield in the bio-oil, due to the low distribution of **B4** linkage in the lignin structure. Another part of the guaiacol and syringol might be produced by the elimination of the side-chain (**R2**) from the lignin monomers, as described by the **chain-reaction (1)** in Fig. 4-15.

(1) Guaiacol and syringol:

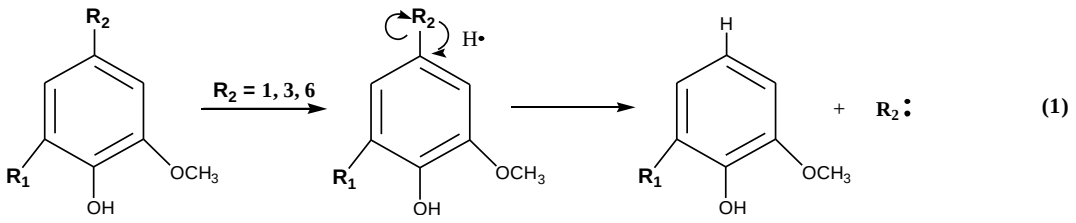

(1)

Fig. 4-15: the speculative free-radical (chain) reaction (1) for the thermolysis of the lignin monomeric (C9) units in woody biomass

The guaiacol-derivatives with the saturated alkyl side-chain structure, such as 4-methylguaiacol (**G2**) and 4-ethylguaiacol (**G3**), are possibly formed by the cleavage of the C-C linkage on the side-chain. It should be noted that almost all C_3 side-chain, except **R2=2** in Fig. 3-4, is the potential contributor for the formation of methyl and ethyl groups (**chain-reaction (5)** in Fig. 4-19). This indicates that the carbonyl groups on α-position are less reactive than those on γ-position as terminal groups for the side-chain (Hosoya, et al. 2008)

Table 4-11: the molar fraction of the main compounds in the tar/bio-oil from the pyrolysis of lignin under different temperatures

Compounds	The abbreviation in Fig. 4-13	Molar fraction （%）		
		575 ^{o}C	650 ^{o}C	700 ^{o}C
Guaiacol	**G1**	9.41	6.15	3.60
4-Methylguaiacol	**G2**	3.58	2.12	1.24
4-Ethylguaiacol	**G3**	0.72	0.44	0.31
Eugenol and isoeugenol	**G4** & **G5**	4.89	3.05	1.72
Vanillin	**G6**	1.89	1.04	0.66
Acetovanillone	**G7**	0.54	0.42	0.37
Coniferyl aldehyde	**G8**	-	-	-
Coniferyl alcohol	**G9**	-	-	-
Syringol	**S1**	7.25	4.41	2.24
Syrigaldehyde	**S2**	-	-	-
Sinapaldehyde	**S3**	-	-	-
Phenol	**P1**	6.35	8.33	12.36
4-Ethylphenol	**P2**	1.01	1.49	1.88
o-Cresol	**C1**	2.24	3.71	4.86
p-Cresol	**C2/P3**	1.67	2.58	3.34
4-Methylcresol	**C3**	1.30	1.76	2.42
Pyrocatechol	**CC1**	2.82	4.34	5.88
4-Methylcatechol	**CC2**	1.01	1.93	2.64
4-Ethylcatechol	**CC3**	0.87	1.04	1.16

-: not detected

.However, the α-carbonyl group is a considerable precursor for the formation of vanillin (**G6**) and acetovanillone (**G7**) through the cleavage of the C_α-C_β and C_β-C_γ, respectively. It is reported that the hydroxyl group on α-position is one of the possible sources for the formation of vanillin via the removal of the transferable hydrogen from –OH and the scission of the C_α-C_β bond (Evans, et al. 1986). The syrigaldehyde (**S2**) is not detected in the bio-oil, indicating insufficient hydroxyl groups or carbonyl groups on α-position of the syringol-type monomer units. Basically, the HO-functionality on α- or β-position of the lignin monomer units (**R2=6** in Fig. 3-4) is preferably pyrolyzed to produce allyl guaiacol (isoeugenol **G5**) through the dehydration reaction, while the ending hydroxyl groups (as **R2=3** in Fig. 3-4) yield the eugenol (**G4**) (Fenner and Lephardt 1981; Amen-Chen 2001). The other three guaiacol-type and syringol-type compounds, undetected in bio-oil, are coniferyl aldehyde (**G8**), coniferyl alcohol (**G9**) and sinapaldehyde (**S3**) (Table 4-11). The coniferyl aldehyde and alcohol, abundantly distributed in the softwood lignin structure, act as the significant precursor for the condensation reactions at the low temperature due to its vinyl structure on the side-chain (Nakamura, et al. 2007), and is thermally unstable to be cracked into other derivatives at the high temperatures.

It is notable that the yield of almost all of the guaiacol-type and syringol-type compounds is inhibited with the elevated temperature, due to its active substituent groups (especially -OCH_3) on the aromatic ring. The cracking of the guaiacol-type compounds to produce its derivatives (phenol-type, cresol-type and catechol-tpye) is discussed below together with the evolution of the low molecular weight free radical and volatile species, while syringol-type compounds are supposed to undergo similar cracking pathways. The specific formation pathways involving the free-radical chain reaction are presented in Fig. 4-16-19 (the chain-reaction **(2)-(5)**), in terms of the cracking of the methoxy groups and different side-chain structures, without the involvement of interactions between them.

Phenol-type compounds

It is found that the yield of phenol (**P1**) increased with the elevated temperature is predominant in bio-oil over other guaiacol-type derivatives. The "demethoxylation" of the aromatic ring of the lignin monomeric (C_9) unit can explain the formation of the phenol-type compounds (Amen-Chen 2001; Hosoya, et al. 2008), but the information concerning the relevant chemical pathways have not been specified. A series of free radical chain-reaction, exhibited in Fig.4-16, are employed to explain the formation of phenol-type compounds from the guaiacol-type.

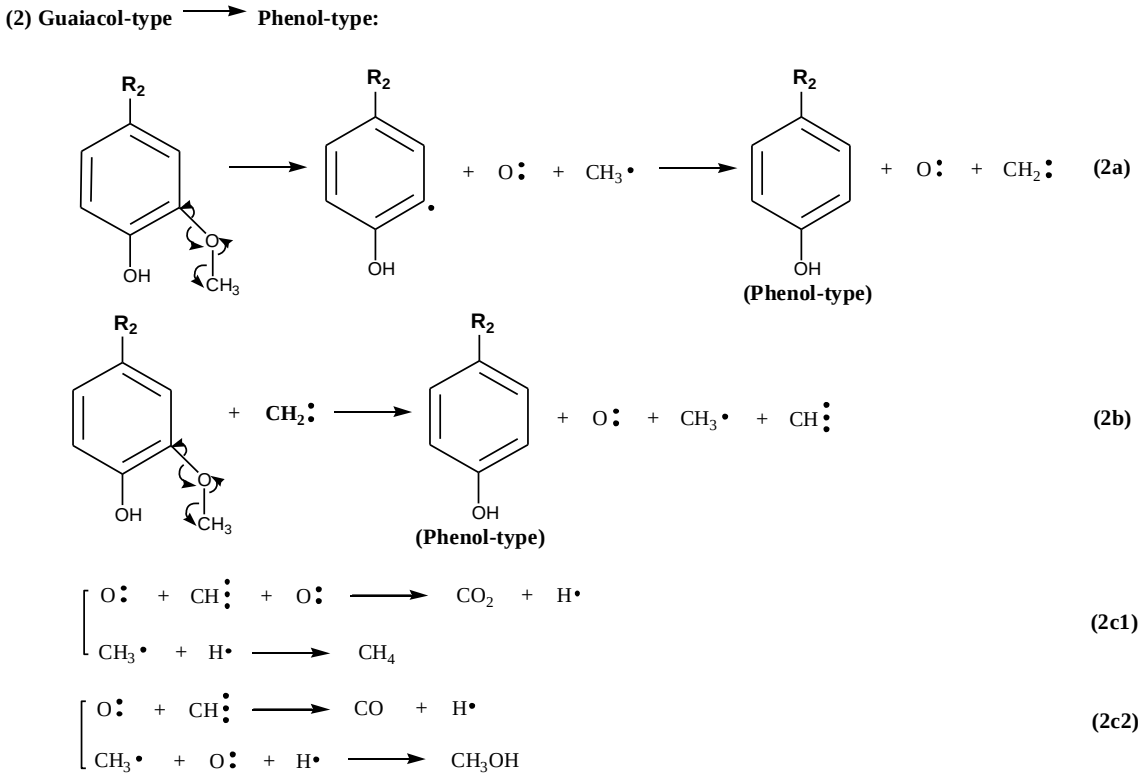

Fig. 4-16: the speculative free-radical (chain) reaction (2) for the thermolysis of the lignin monomeric (C9) units in woody biomass

The methoxy group is initially cleaved from the aromatic ring to generate the oxygen (O**:**) and methyl free radicals (step **(2a)** in **chain-reaction (2)**). The hydrogen from the methyl radical is abstracted to produce the phenol-type, along with the release of a methylene radical. Sequentially, the methylene radical acts as an H-donor for the

formation of another phenol-type and a free radical promoter to build another oxide and methyl radical from the methoxy group. For concluding the radical chain reactions, the left radicals might be coupled to produce the low molecular weight species (CO, CO_2, CH_4 and CH_3OH) though the pathway **(2c1)** and **(2c2)** in **chain-reaction (2)**.

The yield of another two phenol-type species slightly improves with the increased temperature. The 4-ethylphenol (**P2**) is probably produced from the secondary cracking of 4-ethylguaiacol (**G3**) though the pathway described in **chain-reaction (2)** (Fig.4-16). Due to the low yield of 4-ethylguaiacol at different temperatures (Table 4-11), the demethoxylation of the lignin monomer together with the cracking of its side-chain to evolve ethyl group could be another important chemical pathway for the 4-ethylphenol formation. 4-Methylphenol (**P3**), known as *p*-cresol (**C2**), is notably enhanced by temperature (Table 4-11). The formation of 4-methylphenol is possibly attributed to the secondary cracking of 4-methylguaiacol (**G2**) and the primary free radical coupling reaction as that of 4-ethylphenol.

Cresol-type compounds

The production of *o*-cresol (**C1**), the typical cresol-tpye compound in the bio-oil, is favoured at elevated temperature. The cresol-type compounds are possibly produced from the guaiacol-type though the chemical pathways in Fig. 4-17. The initial cracking stage of the guaiacol-type is step **(3a)** to evolve phenolic, oxygen and methyl radicals. Then, the cresol-type is generated via the coupling reaction of the phenolic and methyl radicals. The methyl group, cleaved from another methoxy group, is coupled with the free oxygen radical followed by cracking to formaldehyde and a hydrogen radical, along with releasing an HO-contained phenoxy radical in step **(3b)** and **(3c)**. The whole free radical chain reaction ends up with the combination of the phenoxy radical and hydrogen radical to produce a catechol-type compound (step **(3d)**). It should be clarified that the relationship between the formation of the cresol-type and catechol-type cannot be determined though the **chain-reaction (3)**,

since it is speculated to elucidate the possible pathway for the formation of the cresol-type and formaldehyde from the guaiacol-type.

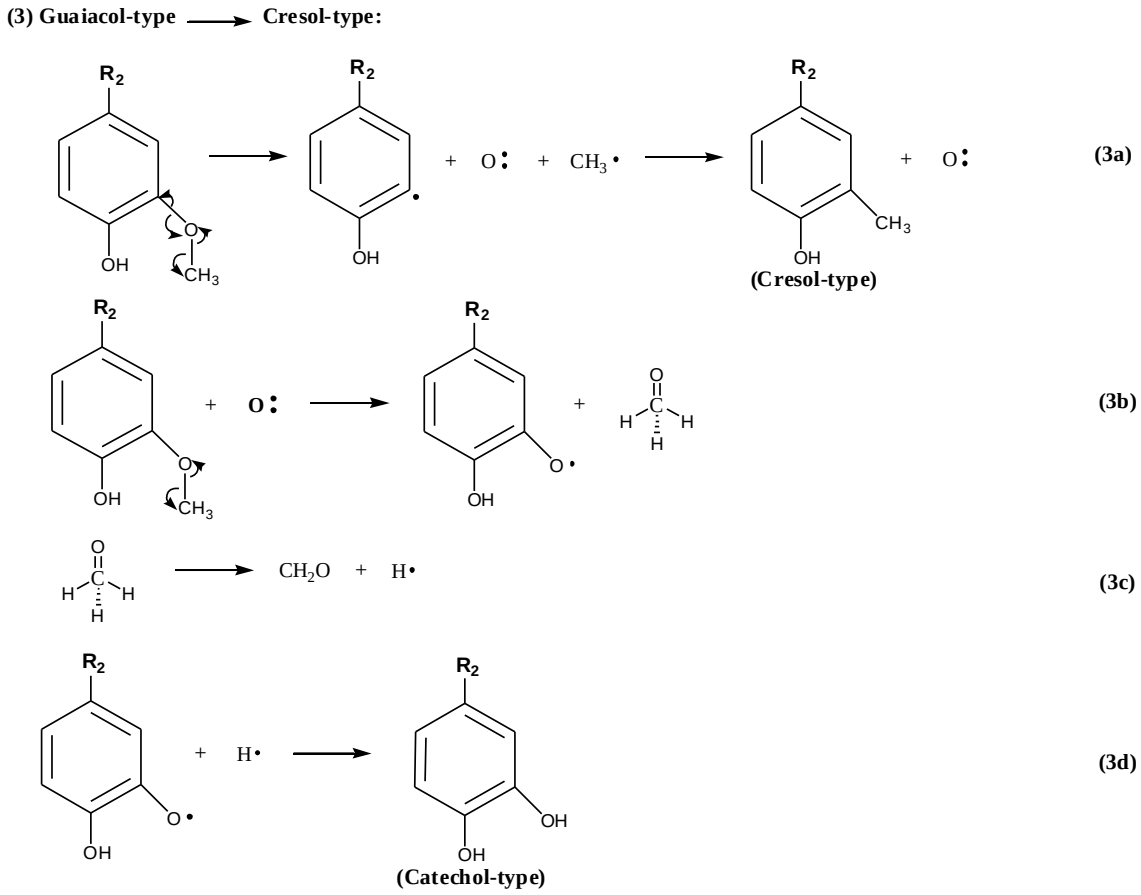

Fig. 4-17: the speculative free-radical (chain) reaction (3) for the thermolysis of the lignin monomeric (C9) units in woody biomass

Another important cresol-type compound, also promoted by increased temperature, is 4-methylcresol (**C3**). One possible pathway for producing the 4-methylcresol is the secondary cracking of the 4-methylguaiacol (**G2**) through the **chain-reaction (3)**, competing with the formation of 4-methylphenol. Another pathway is ascribed to the primary reaction of rearrangement (deoxygenation) of methoxy group on the aromatic ring of the lignin monomer in parallel to the cracking of the side-chain to generate the corresponding methyl group (**chain-reaction (5)** in Fig. 4-19).

Catechol-type compounds

The yield of pyrocatechol (**CC1**) is significantly enhanced with the increased temperature (Table 4-11), while the formation pathway of the catechol-type compounds from the guaiacol-type is described as the "demethylation process" in Fig. 4-18 (**chain-reaction (4)**). The O-CH_3 bond of the methoxy group on the aromatic ring of the guaiocol-type is initially cleaved to produce an HO-contained phenoxy radical and methyl radical in step **(4a)**. Subsequently, the phenoxy radical abstracts a transferable hydrogen from the methyl radical to form the catechol-type, releasing a methylene radical. Similar to the step **(2b)**, the methylene is an important intermediate radical as an H-donor for the formation of the phenol-type from the guaiacoal-type along with evolving a oxygen radical and a methyl radical (step **(4b)**). The remain radicals undergo the relevant coupling reactions to produce the gaseous products (CO and CH_4) (step **(4c)**).

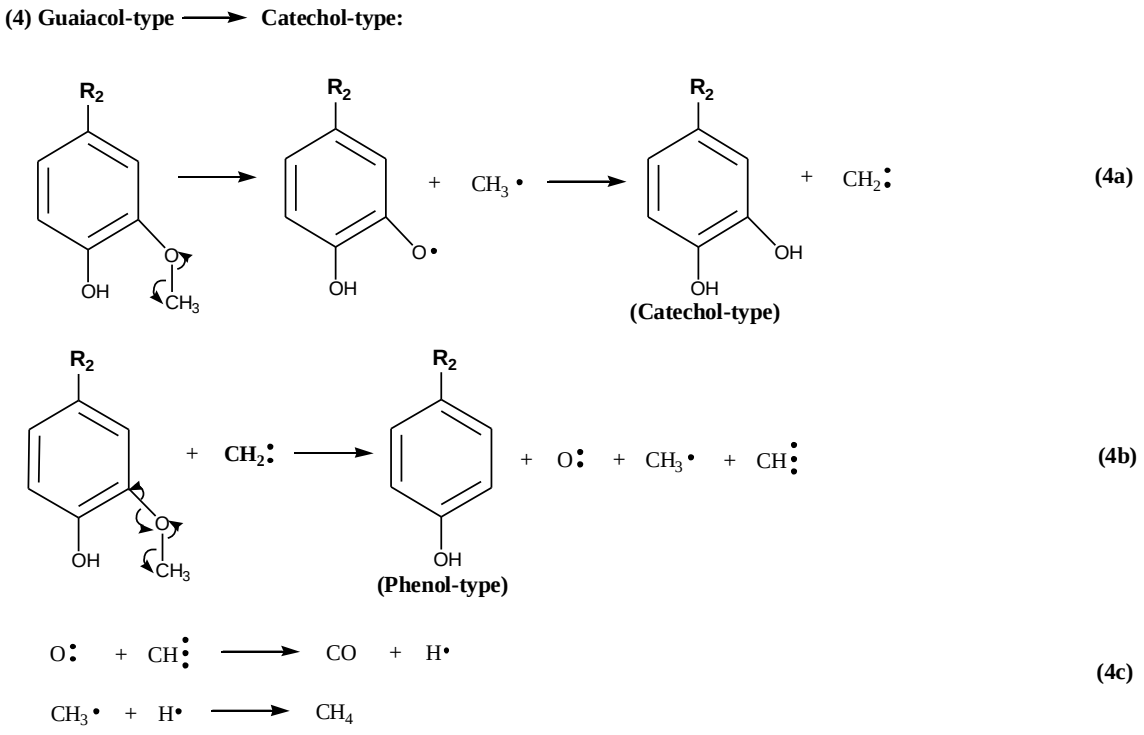

Fig. 4-18: the speculative free-radical (chain) reaction (4) for the thermolysis of the lignin monomeric (C9) units in woody biomass

Consequently, the yield of 4-methylcatechol (**CC2**) facilitated by the elevated temperature is ascribed to the vigorous secondary cracking of the relevant guaiacol-type compounds (**G2** and **G3**) at the high temperature through the **chain-reaction (4)**. The formation of 4-ethylcatechol (**CC3**) is found to be slightly enhanced with the increased temperature (Table 4-11). One possible reason is that the formation of 4-ethylphenol from the guaiacol-type is more competitive than that of 4-ethylcatechol at the high temperature. Another explanation is that the cracking of the side-chain to form methyl group is preferable over the formation of ethyl groups in parallel to the "demethylation" of the lignin monomers as the temperature is increased. This coincides with the notable increment of 4-methylcatechol at high temperatures.

The main products in gas (CO, CO_2 and CH_4)

The yield of CO_2, one of the largest gaseous products, is significantly enhanced by the elevated temperature before 700 ^oC, while the production is stabilized 700 ^oC (Table 4-12). This indicates that most of the CO_2 is produced in the primary pyrolysis reactions of lignin, while the secondary reaction of the volatiles makes marginal contribution to the yield of CO_2 at high temperature.

Table 4-12: the gas composition from the kraft lignin pyrolysis under different temperatures

Gas composition (wt% by feedstock)	475 ^oC	575 ^oC	650 ^oC	700 ^oC	775 ^oC	825 ^oC
CO	4.79	5.02	5.84	7.23	8.67	10.65
CO_2	7.37	8.55	10.34	11.08	11.53	11.74
CH_4	1.58	1.73	2.14	3.31	4.52	5.86
H_2	0.13	0.18	0.27	0.42	0.58	0.71

Some possible pathways for the formation of CO_2 are summarized as: 1) the dehydrogenation reaction on the carbonyl group as the ending group for the side-chain to be a ketene structure, followed by the hydration reaction to be a carboxyl group as the precursor for the formation of CO_2 (**chain-reaction (5)** when **R2=4** in Fig. 4-19); 2) the process along with the formation of the phenol-type from the guaiacol-type from the **chain-reaction (2)**; 3) the rearrangement and cracking of the glyceraldehyde structure cleaved from the glyceraldehyde-2-aryl ether linkage (**B7** in Fig. 3-4) (Shen and Gu 2009). Most of the above routes perform well before 700 ^{o}C and seem not to be further enhanced at higher temperatures.

(5) Side-chain (R_2) cracking:

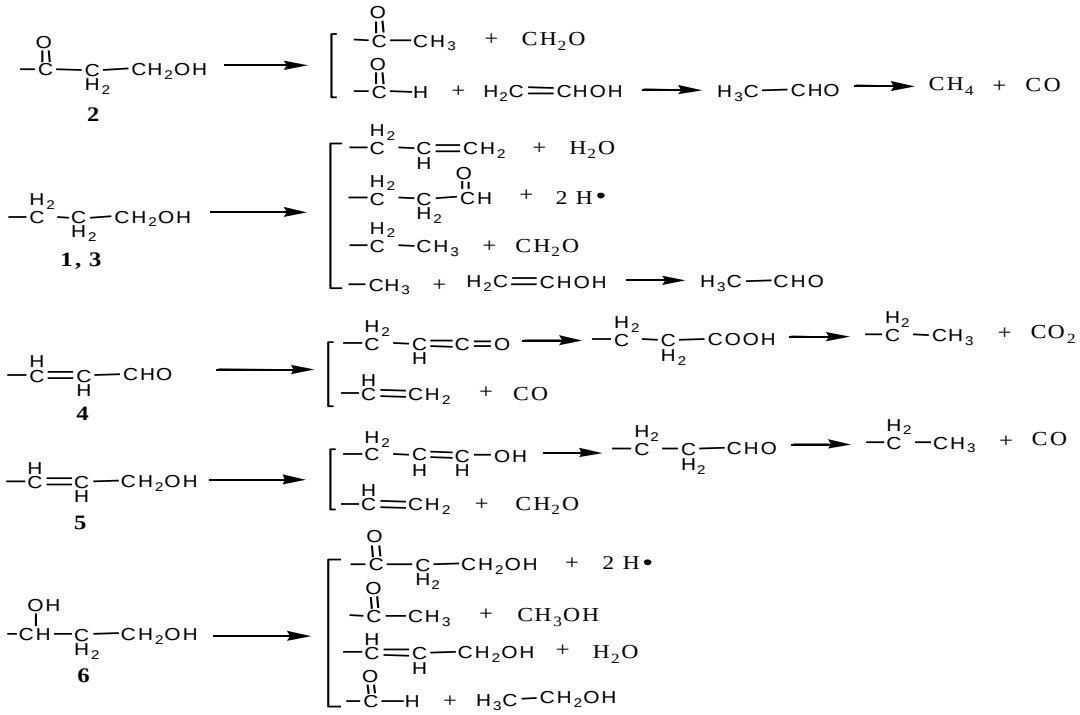

Fig. 4- 19: the speculative free-radical (chain) reaction (5) for the thermolysis of the lignin monomeric (C9) units in woody biomass

In contrast to CO_2, the formation of CO and CH_4 is steadily increased before 650 ^{o}C and remarkably enhanced above 650 ^{o}C. Most of the side-chains ending with the hydroxyl group (**R2=2, 3** and **5** in Fig. 3-4) could behave as the precursor for the

formation of CO, through the dehydrogenation of the ending group as the H-donor for the cracking of side-chain to produce the carbonyl group or aldehyde-type compounds (**chain-reaction (5)** when **R2=2, 3** and **5** in Fig. 4-19). Another well-established pathway for the CO production is the direct decarbonylation reaction of the terminal group (C_γ) of the side-chian (such as **R2=4** in **chain-reaction (5)**) (Evans, et al. 1986; Amen-Chen 2001; Hosoya, et al. 2008; Liu, et al. 2008; Shen and Gu 2009). The CO produced from the secondary reactions of the organic compounds, is well presented in **chain-reaction (2)** step **(2c2)** and **chain-reaction (4)** step **(4c)**. It could be found that the step **(2c2)** to produce CO and CH_3OH might be more competitive than step **(2c1)** to produce CO_2 and CH_4 at the higher temperatures, due the notable increment of the CO yield.

Considering the remarkable increase of the CH_4 yield after 650 ^oC, the chemical pathway in step **(4c)** to produce CH_4 would be predominant over the step **(2c1)** at the higher temperatures. Another route for the CH_4 formation, probably enhanced by the elevated temperature, is the cracking of the ethanol generated from the side-chain as described in **chain-reaction (5)** when **R2=6**. It could be found that CO and CH_4, enhanced at the higher temperatures, are the notable products from the secondary reactions, since the methoxy group is one of the predominant precursors for the CO and CH_4 formation through the relevant free-radical chain reactions.

4.4.3 The kinetic mechanism for lignin pyrolysis

The chemical pathways for the rearrangement of the lignin C_9 units and formation of the typical condensable products are extensively proposed and discussed in the above sections. It is known that the structure of natural lignin is very complex, leading to the difficulties in proposing the precise kinetic scheme involving most of the pyrolytic reactions.

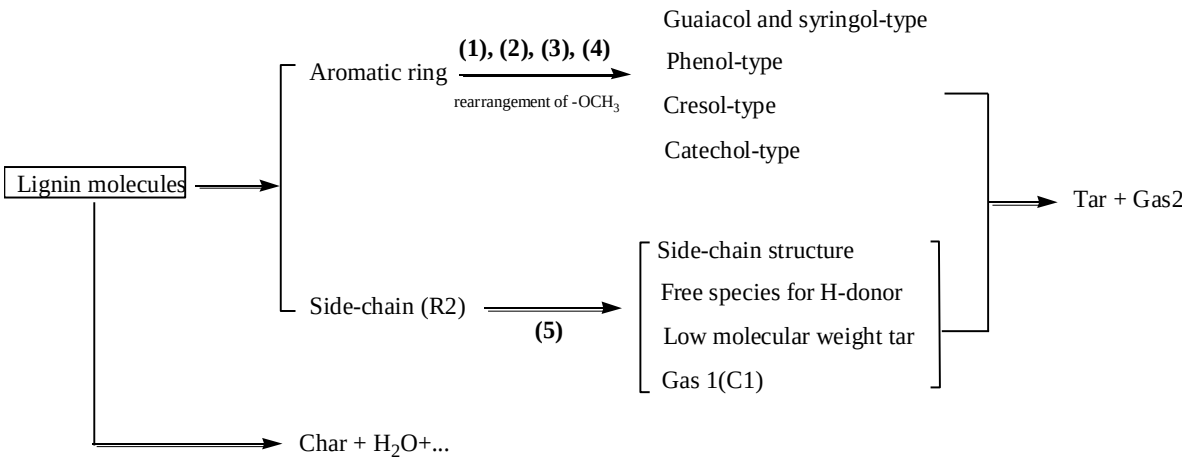

Fig. 4-20: the kinetic scheme for lignin pyrolysis

Here, the predominant chemical pathways would be involved in the proposed kinetic scheme (Fig. 4-20), representing the pyrolysis of lignin and formation of typical compounds. The rearrangement of the methoxy group (-OCH_3) on the aromatic ring of the lignin molecule give the production of guaiacol-type, syringol-type, phenol-type, cresol-type and catechol-type compounds. The cracking of the alkyl side-chains offers C1/C2 substituents or H-donor for those aromatic ring-contained compounds to produce tar through the coupling reactions presented above, together with the evolution of Gas1 and Gas 2. Another competitive decomposition route for lignin with the formation of Tar and Gas2 is to produce char along with the evolution of H_2O and other light species. However, it needs to be noted that the structure of the char residue from lignin decomposition is not identified, and the corresponding chemical pathway for carbonization process is not specified.

4.4.4 Summaries

Extensive experiments have been carried out to investigate the mechanism of lignin pyrolysis. In the TG-FTIR experiments, the initial pyrolysis stage of kraft lignin, corresponding to the vigorous evolution of the phenolic compounds, is relatively inert and overlapped by the second pyrolysis stage, exhibiting the “shoulder peak” on the DTG curve. The guaiacol-type and syringol-type compounds are mostly produced

by the cracking of the side-chain of the lignin monomeric units in parallel to the cleavage of the α- or β-4-aryl ether linkage. These act as the precursors for the formation of the relevant derivatives (phenol-type, cresol-type and catechol-type) through the corresponding cracking mode of the methoxy group (-OCH_3) on the aromatic rings. Furthermore, the methoxy group performs as an important source for the formation of CO, CO_2 and CH_4 through the relevant radical chain reactions, as well as the cracking of the side-chain structures.

4.5 Interactions among the components

The "synthesized biomass" samples with different mass fractions of the components for off-line pyrolysis study are listed in Table 4-13. It needs to be noted that the synthesized sample tested in fast pyrolysis unit contains constant cellulose mass fraction, but varied the mass fraction for lignin and hemicellulose (Table 4-13).

Table 4-13: the tested synthesized samples with different mass ratios of the components

No.	Cellulose	Hemicellulose	Lignin	Experiment
1	5	3	1	Py-GC-MS
2	5	2	2	Py-GC-MS
3	5	1	3	Py-GC-MS

For fast pyrolysis experiments (off-line pyrolysis study), the operation temperature is 550 ^{o}C, while the feeding flow rate is fixed at 600 l/h. The experimental data from fast pyrolysis studies (such as the yield of the products and the compositions in bio-oil) is compared with the calculated results governed by following mass-fraction equation, revealing the quantitative interactions among the components in the synthesized sample:

Y_{mix}=a|Y_{cell}| + b|Y_{hemi}| + c|Y_{lignin}|

where a, b and c are the mass fraction of cellulose, hemicellulose and lignin, respectively, while Y_{cell}, Y_{hemi} and Y_{lignin} are the experimental result of cellulose, hemicellulose and lignin.

4.5.1 The yields of gas, bio-oil and char residue

The yield of products from the individual component pyrolysis at 550 ^{o}C in fluidized bed reactor is shown in Table 4-15, giving 26.8% of gas, 70.2% of bio-oil and 3.0% of char for cellulose, 36%, 42% and 22% for hemicellulose and 17%, 41% and 42% for lignin. The yield of products from the synthesized sample in the fluidized bed reactor is also shown in Table 4-15, while the yield difference value for the products, defined as the ratio of (experimental yield)/(calculated yield), is shown in Fig. 4-21 for estimating deviation between experimental and calculated data. It is found that the production of gas and char is enhanced in spite of the mass fraction of components in synthesized sample, while the production of bio-oil is accordingly decreased (Table 4-15).

Table 4-14: the experimental and calculated product yields from different synthesized samples under 550 oC with the feeding flow rate of 600 l/h

Products	Components (wt%)			Synthesized samples (wt%)					
	Cellulose	Hemi-cellulose	Lignin	C/H/L: 5/3/1		C/H/L: 5/2/2		C/H/L: 5/1/3	
				exp.	cal.	exp.	cal.	exp.	cal.
Gas	26.8	36	17	33.6	28.8	32.8	26.7	34.1	24.6
Bio-oil	70.2	42	41	51.6	57.6	49.1	57.4	45.7	57.3
Char	3.0	22	42	14.8	13.6	18.1	15.9	20.3	18.1

The difference value of gas yield is greatly enhanced with the increased mass fraction of lignin in synthesized sample (Fig. 4-21). Correspondingly, the yield difference

value for bio-oil is decreased with the increased lignin fraction in synthesized sample. This might be attributed to the enhancement of the lignin-derived products on cracking of anhydrosugars from cellulose pyrolysis, resulting in the increasing yield of gaseous products (Hosoya, et al. 2007). The difference value for char yield is not significantly affected by the lignin mass fraction in the synthesized sample. This may be attributed to the mutual promotion of the char production from hemicellulose and lignin in hemicellulose-lignin pyrolysis, regardless of their relative mass fractions.

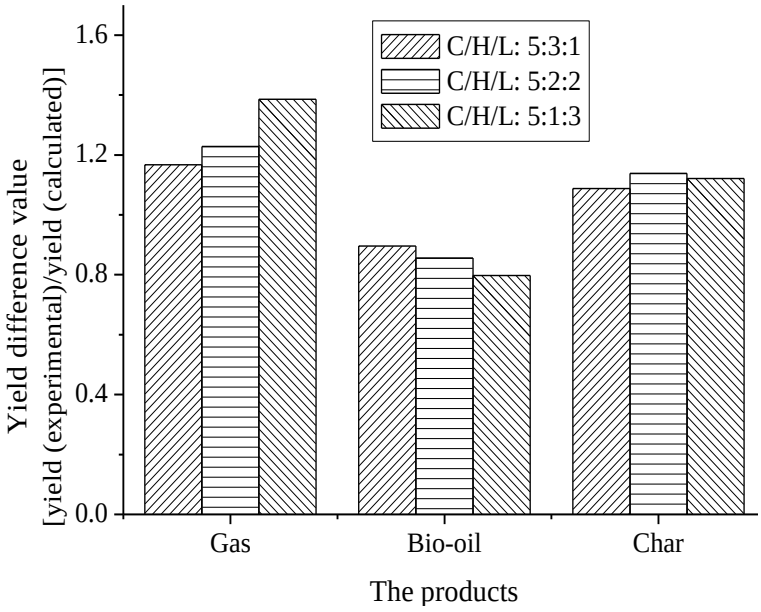

Fig. 4-21: the difference value of the experimental and calculated yield of products from different synthesized samples

4.5.2 The formation of the specific compositions in bio-oil

The specific compositions in the bio-oil of its individual components and in synthesized samples from pyrolysis in the fluidized bed reactor are characterized by GC-MS. The peak area of the characterized compositions in the bio-oil is exhibited in Table 4-16, while the peak area difference value (experimental peak area/calculated peak area) of the compositions varied with the mass fraction of components in the

synthesized sample is shown in Fig. 4-22. The peak area for hydroxyaldehyde mainly ascribed to cellulose pyrolysis in synthesized sample pyrolysis is vigorously enhanced by comparing with the calculated data, while that for levoglucosan is visibly inhibited. Hosoya et al. (Hosoya, et al. 2009) showed that the yield of low-molecular-weight products from cellulose pyrolysis are promoted at the expense of the formed anhydrosugars in cellulose-lignin pyrolysis. The peak area difference value for hydroxyaldehyde is decreased with the lignin mass fraction, while that for levoglucosan is increased. This reveals that the effect of lignin-derived volatiles on inhibiting the formation of anhydrosugars might be weakened with the increased mass fraction of lignin in the synthesized sample.

Table 4-15: the experimental and calculated peak area of typical condensable products from different synthesized samples determined by GC-MS

Condensible products	Components (area %)			Synthesized samples (area %)					
	Cellulose	Hemi-cellulose	Lignin	C/H/L: 5/3/1		C/H/L: 5/2/2		C/H/L: 5/1/3	
				exp.	cal.	exp.	cal.	exp.	cal.
Hydroxyaldehyde (HAA)	9.84	0.81	/	16.97	5.74	13.38	5.65	10.09	5.56
Levoglucosan (LG)	46.25	/	/	2.69	25.69	10.89	25.69	17.04	25.69
Furfural (FF)	0.78	11.04	/	5.28	4.11	1.48	2.89	/	1.66
Acetic acid (AA)	0.43	14.89	/	9.87	5.20	2.58	3.55	1.39	1.89
Phenol (Ph)	/	/	6.24	0.66	0.69	1.59	1.39	3.01	2.08
Guaiacol	/	/	9.53	1.20	1.06	7.29	2.12	12.77	3.18
Cresol (Cre)	/	/	3.09	0.47	0.34	1.31	0.69	1.82	1.03

Except in the caese of the synthesized sample with the mass fraction of 5/3/1 for cellulose/hemicellulose/lignin, the peak area for 2-furfural and acetic acid mainly produced from hemicellulose pyrolysis is visibly inhibited in hemicellulose-cellulose-lignin mixture pyrolysis, compared to the calculated data

(Table 4-16). The inhibition is possibly attributed to the interactions between these two volatiles and lignin-derived products, since the peak area difference value of 2-furfural and acetic acid is decreased with the increased lignin content (Fig. 4-22). This analysis is consistent with the result of TGA of hemicellulose-lignin (Fig. 4-23(b)) that pyrolysis of lignin is accelerated by the hemicellulose-derived volatiles through the vapor-phase interactions. Therefore, more 2-furfural and acetic acid would be consumed because of the increased lignin mass fraction, resulting in the decreased peak area difference value.

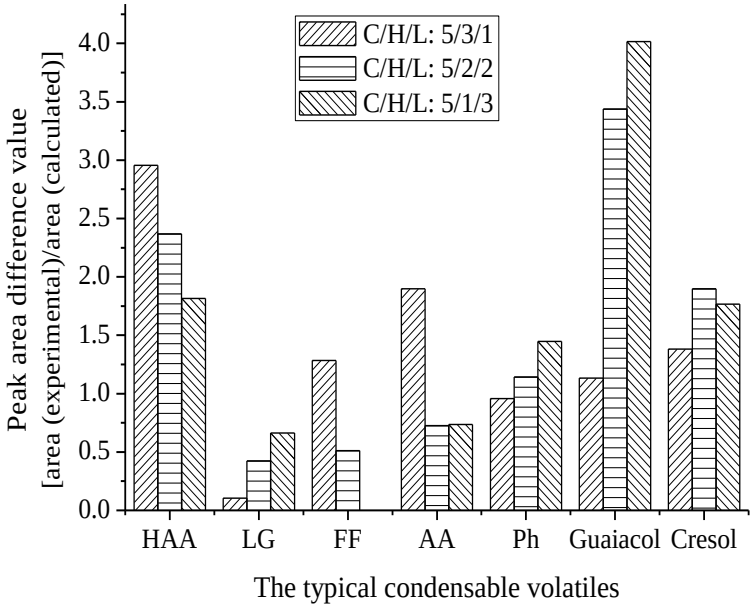

Fig. 4-22: the difference value of the experimental and calculated peak area of condensable volatiles from different synthesized samples

The peak area difference value of phenol, guaiacol and cresol, which are marked compounds from lignin pyrolysis, is significantly increased with the lignin mass fraction in synthesized sample pyrolysis, further proving the above plausible explanation. The formation of phenol, guaiacol and cresol from lignin is found to be enhanced in synthesized sample pyrolysis compared to the calculated data (Table 4-16). Another possible reason is obtained in Hosoya et al. (Hosoya, et al. 2009) in the cellulose-lignin pyrolysis, presenting that cellulose enhances the formation of

lignin-derived products, such as guaiacol and cresol but retards the secondary char formation from lignin.

4.5.3 The evolution of the gaseous products

The yield of gaseous products (mainly CO, CO_2, CH_4 and H_2) from the pyrolysis of individual components and synthesized samples is summarized in Table 4-16, while the yield difference value for the products from the synthesized sample pyrolysis is shown in Fig. 4-23. It could be found that the interaction among the components promotes the yield of CO and CH_4, but suppresses the formation of H_2.

Table 4-16: the experimental and calculated yields of gaseous products from different synthesized samples

Gaseous products	Components (wt%)			Synthesized samples (wt%)					
	Cellulose	Hemicellulose	Lignin	C/H/L: 5/3/1		C/H/L: 5/2/2		C/H/L: 5/1/3	
				exp.	cal.	exp.	cal.	exp.	cal.
CO	14.46	6.85	4.89	15.69	10.86	15.62	10.64	19.38	10.42
CO_2	9.84	25.05	8.47	13.65	14.76	12.03	12.92	10.62	11.07
H_2	0.19	1.42	0.17	0.31	0.60	0.14	0.46	0.29	0.32
CH_4	0.07	0.13	1.65	0.39	0.27	0.51	0.43	0.81	0.60

CO is possibly produced partly from the cracking of anhydrosugars, which might be promoted by the lignin-derived volatiles (Hosoya, et al. 2009). Consequently, the yield difference value for CO is significantly increased with the lignin mass fraction in the synthesized sample (Fig. 4-23). H, the original free radical for the formation of H_2, is vigorously consumed during the volatilization of lignin. Therefore, the yield of H_2 is visibly inhibited by the interaction in synthesized sample pyrolysis, since the yield difference value for H_2 is much lower than 1 (Fig. 4-23).

The yield of CO_2 from the synthesized sample pyrolysis is not visibly changed by the interaction among the components, which is consistent with the results in cellulose-lignin pyrolysis study by Hosoya et al. (Hosoya, et al. 2009). CO_2 is estimated to be the primary product from the degradation of the individual components (Li, et al. 2001; Shen and Gu 2009), thus the interaction which mainly occurred in the vapor-phase in fluidized bed reactor has no significant effect on the yield of CO_2.

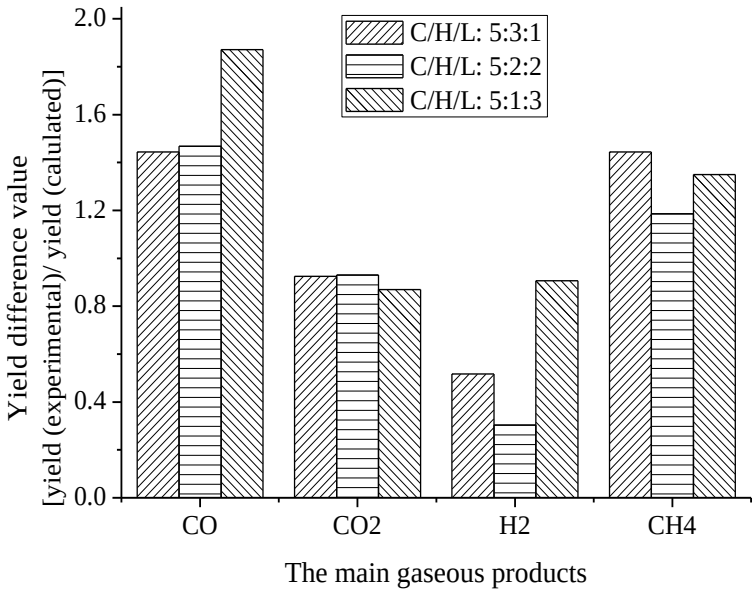

Fig. 4-23: the difference value of the experimental and calculated yield of main gaseous products from different synthesized sample

4.5.4 Summaries

According to the PY-GC-MS analysis of the synthesized sample composed of the three components, the interactions among the components are extensively discussed. The remarkable results are summarized as: 1) the yield of gas from synthesized sample pyrolysis is enhanced by the interactions among the components while the yield of bio-oil is suppressed; 2) the char yield from the synthesized sample pyrolysis is not visibly changed with the increased lignin mass fraction possibly due to the

mutual enhancement of char production from hemicellulose and lignin, according to the relatively constant yield difference value; 3) the levoglucosan ascribed to cellulose pyrolysis is inhibited by the interactions while hydroxyaldehyde is enhanced; 4) the yield of compositions ascribed to lignin pyrolysis, such as phenol and guaiacol, is significantly promoted by the interactions in synthesized sample; 5) the interaction among the components promotes the yield of CO and CH_4, but suppresses the formation of H_2. Some results for estimating the interaction among the three components might be equivocal, since the interactions between the two components are not specified in the fast pyrolysis study. Moreover, the synthesized sample pyrolyzed in the fluidized bed reactor favors the interactions in the vapour-phase among the components, but not involving the possible interactions in solid/liquid phase.

Chapter 5: Conclusions

The on-line pyrolysis and off-line pyrolysis of the main chemical components of woody biomass (xylan-based hemicellulose, cellulose and lignin) and "synthesized biomass" samples have been extensively investigated. This has involved investigating the mass loss of solid together with the on-line identification of the evolved volatiles; yield of pyrolyzed products, distribution of the typical compounds; the chemical pathways for pyrolysis reactions; and the interactions among the chemical components. The chemical pathways, indicating the possible competitive and/or consecutive relationship among the prominent compounds in bio-oil and gaseous product, give hints to improve the current kinetic scheme of the individual components. The detailed results would help understand the pyrolytic mechanism of whole woody biomass and its components, optimize the operation conditions to maximize the valuable fuels/chemicals production, and reduce the by-product yield.

Cellulose

During cellulose on-line pyrolysis, the "abrupt mass loss" and the peak of mass loss rate move towards the high temperature when the heating rate is increased; more char residue is produced under lower heating rates due to the prolonged preheating; most of the produced gases are released to their maxima simultaneously while CH_4 is delayed due to the higher formation energy.

Depending on the experiments in the pyrolysis testing system, the yield of char reaches the minimum (less than 5 % wt) and remains stable when temperature exceeds 550 ^{o}C relatively independent from the residence time; the yield of gaseous products is enhanced at higher temperature and longer residence time; the yield of bio-oil decreases when the temperature exceeds 570 ^{o}C. It is expected that the formation of gases is competing with the formation of tars and their secondary decomposition.

Levoglucosan is the major component in the bio-oil. The evolution of the hydroxyl group (free radical) from the C-6 position is proposed to be the initiator for the formation of levoglucosan. The yield of levoglucosan is inhibited with the elevated temperature and residence time, since it is preferably cleaved to the C_{4-6} fragments as the intermediates to generate the C_{1-4} products and furan-ring products through a set of secondary reactions (such as dehydration, fission, decarbonylation, rehydration and decarboxylation).

Almost all of the main products (5-HMF, FF, HAA, HA, PA and Acetone) are enhanced when the temperature or residence time is increased. Most of the 5-HMF is produced from the competitive reaction with the formation of levoglucosan, as a part of 5-HMF is formed from the levoglucosan degradation The HAA is preferably formed from the C-1 and C-2, and the C-5 and C-6 through both direct scission of cellulose molecules and secondary reactions of the fragments. Most of HA is presumably produced from the direct conversion of cellulose molecules, while the formation of PA is mainly from the secondary decomposition of levoglucosan. It is found that almost all of the C_{2-6} fragments with the structure of aldehyde-alcohol, could potentially produce the acidic compounds through the dehydration, rearrangement and rehydration reactions.

The production of CO is substantially improved with the elevated temperature and residence time in comparison to the slight change of CO_2. It could be explained that almost all of the C_{1-6} fragments containing aldehyde-strucutre, such as tetrose, HAA, HA, aldehyde and formaldehyde, can produce CO by decarbonylation reaction and CO_2 is produced primarily by the decarboxylation reactions of the acidic compounds.

An improved kinetic scheme is proposed to describe the pyrolysis process of cellulose (Fig. 4-5). The levoglucosan obtained from the depolymerization of cellulose molecules is estimated to be competitive with the formation of the Tar1 (such as HAA, HA, GA and so on) and Tar2 (such as furfural and 5-HMF) through the direct

ring-open reactions, and char formation through carbonization reaction together with CO_2 evolution. Meanwhile, levoglucosan also acts as a precursor for the formation of Tar1 and Tar2 through secondary decomposition and char through polymerization and cross-linking reaction.

Hemicellulose

A "sharp mass loss stage", containing two visible peaks is observed within a narrow range of temperature (from 200 ^{o}C to 350 ^{o}C), where most of the xylan-based hemicellulose sample is decomposed by a set of chemical reactions. Most of the mass loss curves (TG curves) are found to decay smoothly from about 400 ^{o}C to the final temperature 800 ^{o}C. The first peak is mainly ascribed to the cleavage of the glycosidic bonds and the decomposition of side-chain structure (such as the 4-O-methyglucuronic acid unit), while the second one should be attributed to fragmentation of other depolymerized units (xylan units). The decomposition of xylan units move forward with the elevated heating rate, enhancing the mass loss in the first peak. Thus it is sensible that the first peak is much lower than the second one at the low heating rate (3 K/min). At the high heating rate, only one peak would appear, when the decomposition of xylan units is overlapped with that of side-chain structure. It is speculated that two peaks would be highly overlapped at the high heating rate, due to the enhancement of the decomposition of different xylan units.

Two visible peaks in the "sharp mass loss stage" together with the intensive evolution of the volatiles are characterized by the FTIR spectra. It is found that various volatiles might reach the maximum production simultaneously and the hemicellulose decomposes intensively within the narrow temperature range. The two sets of visible absorbance peaks show much higher production of CO_2 over other gaseous products. It is due to the height of absorbance qualitatively reflects the concentration of the product in the volatile mixture.

Effects of temperature (from 400 to 690 ^{o}C) on the product yield (gas, tar and char) are discussed in the fast pyrolysis experiments. It was found that the elevated temperature improves the yield of gas (especially over 475 ^{o}C) and increases the yield of bio-oil till about 475 ^{o}C followed by gradual decline. It needs to be noted that the yield of char is decreased before 475 ^{o}C and remains stable at temperature over 540 ^{o}C (about 22%). the yield of gas at higher temperature is found to increase in proportion to the reduction of bio-oil. These findings indicate that the hybrid mechanism (the combination of competitive and consecutive mechanism) exists for the formation of gas and bio-oil.

The formation mechanisms of specified tars and gases are extensively investigated, and indicate that the furfural and 1,4-anhydro-D-xylopyranose are mainly produced from the xylan units, while the formation of acetic acid and CO_2 is attributed to the primary decomposition of O-acetylxylan unit. The xylan unit is also the main precursor for the formation of the two-carbon, three-carbon fragments and gases (CO, H_2 and CH_4). The evolution of methanol is mainly ascribed to the primary reactions of 4-O-methyglucuronic acid unit, which could be further decomposed to almost all of the products produced from the other two units. It is worth noting that the formation of acetone and CO could be attributed to the decomposition of the ring-opened intermediate products or secondary reactions of the fragments, obtained from all three kinds of the units in the original material.

The kinetic scheme for xylan-based hemicellulose pyrolysis is proposed (Fig. 4-10) through the above extensive discussion on the evolution of volatiles against temperature and the possible chemical pathways. All the units in the xylan-based hemicellulose are proposed to be pyrolyzed separately. The branch units (both O-acetyl-xylan unit and O-methylglucurono-xylan unit) are consumed by two competitive decomposition ways: one is to produce Tar1 such as acidic compounds, methanol, acetone and CO; the other is to produce Tar 2 including aldehyde-type compounds, furfural and CO_2. Comparatively, the main xlyan unit is proposed to be

depolymerised to intermediate (anhydrosugars), followed by further cracking to produce Tar 3 containing aldehyde-type products, furfural, acetone and CO. Another thermal decomposition line of all the units is to be carbonized to produce char residue together with the evolution of CO_2 and H_2O.

Lignin

The kraft lignin as a residue from the pulping industries, which exists in a large amounts and at low cost, is a promising feedstock for the thermal conversion of biomass, in terms of producing the high-value chemicals and polymers. Therefore, the information on promoting the formation of the specific products during the process is highlighted in both current and future work. Here, the kraft lignin is selected to represent one of the main components of the woody biomass. A speculative polymeric structure is proposed to express the complexity of woody lignin, with regard to the linkage distribution and the diversity of the side-chain structure from different aromatic types (guaiacol and syringol).

In the TG-FTIR experiments, A notable mass loss peak, appearing at 376 ^{o}C for 20 K/min and 390 ^{o}C for 40 K/min, are found at the second major stage of lignin pyrolysis, while the "shoulder peak" appears ~270 ^{o}C at the first pyrolysis stage. The initial stage of kraft lignin pyrolysis is relatively inert and overlapped by the second pyrolysis stage, exhibiting the "shoulder peak" on the DTG curve, due to its chemical structural changes during the preparing process causing the block of the reactive groups.

The char residue is one of the main products from kraft lignin pyrolysis, accounting for about 40 wt% of the feedstock. The condensation reactions contributing the formation mechanism of char during the pyrolysis of lignin are enhanced at the low temperature or the low heating rates. However, the reactivity of the char residue seems not to be affected by the heating rate, while the mass loss rate of the solid

residue at 600 ^{o}C and its mass loss between 600 and 900 ^{o}C are almost identical at both heating rates.

In the fast pyrolysis tests, the elevated temperature facilitates the formation of the gaseous products (especially over 650 ^{o}C), while the yield of tar reaches maxima (43 wt%) at 630 ^{o}C followed by a gradual decline. The yield of char notably decreases before 650 ^{o}C and remains stable at the temperature over 700 ^{o}C. It needs to be noted that the char yield at the high temperature (825 ^{o}C) is ~36% of kraft lignin feedstock. Lignin gives a higher yield of char residue in this fluidized bed pyrolysis unit, compared to that from cellulose and hemicellulose. Meanwhile the reactivity of the tar/bio-oil produced by the lignin in the pyrolysis unit is not significantly affected by temperature.

The yield of tar visibly increases as a result of the consumption of char residue before 650 ^{o}C, while the evolution of gaseous products changes slightly. After then, the yield of gas increases remarkabley not only by competing with the formation of tar in the primary pyrolysis stage, but also due to the secondary cracking of the primary tarry compounds. The reduction of the tar yield between 650 and 825 ^{o}C, mainly due to the vigorous secondary reactions, is less than 10 % of the kraft lignin feedstock. This indicates that the reactivity of the tar produced by lignin pyrolysis is not significantly affected by temperature, compared to that of cellulose.

The formation of the prominent compounds in bio-oil from lignin off-line pyrolysis is extensively discussed. the yield of almost all of the guaiacol-type and syringol-type compounds is inhibited with the elevated temperature, due to its active substituent groups (especially -OCH_3) on the aromatic ring. The guaiacol-type products are mostly produced by the cracking of the side-chain of the lignin monomeric units in parallel to the cleavage of the α- or β-4-aryl ether linkage, acting as the precursors for the formation of the relevant derivatives (phenol-type, cresol-type and catechol-type) through the corresponding cracking mode of the methoxy group (-OCH_3) on the

aromatic rings together with the formation of CO, CO_2 and CH_4 as well as the cracking of the side-chain structures.

The yield of CO_2, one of the major gaseous products, is significantly enhanced by the elevated temperature before 700 ^oC, while the production is stabilized 700 ^oC. This indicates that most of the CO_2 is produced in the primary pyrolysis reactions of lignin, while the secondary reaction of the volatiles makes only a marginal contribution to the yield of CO_2 at high temperature. Some possible pathways for the formation of CO_2 are summarized as: 1) the dehydrogenation reaction on the carbonyl group as the ending group for the side-chain to be a ketene structure, followed by the hydration reaction to be a carboxyl group as the precursor for the formation of CO_2; 2) the process along with the formation of the phenol-type from the guaiacol-type; 3) the rearrangement and cracking of the glyceraldehyde structure cleaved from the glyceraldehyde-2-aryl ether linkage. Most of the above routes perform well before 700 ^oC and seem not to be further enhanced at higher temperatures.

The formation of CO and CH_4 is steadily increased before 650 ^oC and remarkably enhanced above 650 ^oC. Most of the side-chains ending with the hydroxyl group could behave as the precursor for the formation of CO, through the dehydrogenation of the ending group as the H-donor for the cracking of the side-chain to produce the carbonyl group or aldehyde-type compounds. Another well-established pathway for the CO production is the direct decarbonylation reaction of the terminal group (C_γ) of the side-chian. Considering the remarkable increase of the CH_4 yield after 650 ^oC, the chemical pathway to produce CH_4 would be predominantat the higher temperatures. Another route for the CH_4 formation, probably enhance by the elevated temperature, is the cracking of the ethanol generated from the side-chain. It could be found that CO and CH_4, enhanced at the higher temperatures, are the notable products from the secondary reactions, since the methoxy group is one of the predominant precursors for the CO and CH_4 formation through the relevant free-radical chain reactions.

The structure of the nature lignin is very complex, leading to the difficulties in proposing the precise kinetic scheme involving most of the pyrolytic reactions. The kinetic scheme for lignin pyrolysis is proposed involving most prominent chemical pathways for the pyrolytic reactions. The rearrangement of the methyoxy group ($-OCH_3$) on the aromatic ring of the lignin molecule give the production of guaiacol-type, syringol-type, phenol-type, cresol-type and catechol-type compounds. The cracking of the alkyl side-chains offers C1/C2 substituents or H-donor for those aromatic ring-contained compounds to produce tar through the coupling reactions presented above, together with the evolution of Gas1 and Gas 2. Another competitive decomposition way of lignin with the formation of Tar and Gas2 is to produce char along with the evolution of H_2O and other light species. However, it needs to be noted that the structure of the char residue from lignin decomposition is not identified, and the corresponding chemical pathway for carbonization process is not specified.

The interactions among the components

The tested synthesized sample for fast pyrolysis study is composed of three components with the fixed cellulose mass fraction. Compared to the calculated result, the yield of gas from the pyrolysis of "synthesized biomass" samples is enhanced by the interactions among the components while the yield of bio-oil is suppressed. The char yield from the synthesized sample pyrolysis is not visibly changed with the increased lignin mass fraction possibly due to the mutual enhancement of char production from hemicellulose and lignin, according to the relatively constant yield difference value.

The levoglucosan ascribed to cellulose pyrolysis is inhibited by the interactions while hydroxyaldehyde is enhanced. 2-furfural and acetic acid mainly produced from hemicellulose pyrolysis is visibly inhibited in hemicellulose-cellulose-lignin mixture pyrolysis, compared to the calculated data. The yield of compositions ascribed to lignin pyrolysis, such as phenol and guaiacol, is significantly promoted by the

interactions in the synthesized sample. The interaction among the components promotes the yield of CO and CH_4, but suppresses the formation of H_2. CO is possibly produced partly from the cracking of anhydrosugars, which might be promoted by the lignin-derived volatiles. Comparatively, the yield of H_2 is visibly inhibited by the interaction in synthesized sample pyrolysis, because of the existence of lignin as the H abstractor. CO_2 is estimated to be the primary product from the degradation of the individual components, thus the interaction mainly occurred in the vapor-phase in a fluidized bed reactor has no significant effect on the yield of CO_2.

Chapter 6: Future work

Though the on-line pyrolysis (TGA-FTIR) and off-line pyrolysis (fast pyrolysis unit) study of the model compounds of hemicellulose, cellulose and lignin and their "synthesized biomass" samples, the pyrolytic mechanism of the individual components in woody biomass and their interactions under pyrolytic conditions were extensively investigated in terms of the mass loss process of solid and evolution of the volatiles against temperature, yield of the products, distribution of the prominent compounds in bio-oil and gaseous product. The chemical pathways for the structural changes of the macromolecules and the secondary cracking of the fragments under the pyrolytic conditions were successfully proposed, leading to the improvement of the current kinetic scheme of the individual components. However, some limitations of this work and the challenges for future work should be specified, in order to gain the further understanding of the pyrolytic mechanism of woody biomass from the view of the pyrolysis of the individual component.

1) As far as the chemical components of wood are concerned, a distinction should be made between the main macromolecular cell-wall components: cellulose, hemicellulose (polyoses) and lignin, which are dispersed in all woods, and the minor low-molecular-weight components (extractives and mineral), which are generally more related to the specific wood species in kind and amount. The proportion of the high-polymeric compounds (cellulose, hemicellulose and lignin) building up the cell walls account for 97-99% of the wood material in temperate zone. For tropical woods this value may decrease to an average value of 90%, while 65-75% of the wood consists of polysaccharides (cellulose and hemicellulose). Comparatively, the low-molecular-weight substances contribute only a few percent to the wood mass, however, the further study on the pyrolytic behavior of the extractives and catalytic effect of the minerals would help to improve the understanding of the pyrolytic mechanism of woody biomass system.

2) It is known that cellulose is a uniform component in all woods (linearly polymerized glucopyranose through the β-(1-4) glycosidic linkages), but the proportions and chemical structures of hemicellulose and lignin differ in softwood and hardwood. The sugar units (anhydro-sugars) consisting of hemicelluloses could be categorized into groups as pentoses, hexoses, hexuronic acids and deoxy-hexoses. It was estimated that hardwoods contain more hemicellulose than softwoods and softwood hemicelluloses consist of glucomannan, galactoglucomannan, arabinan and a small amount of arabino-(4-O-methylglucurono)-xylan. Compared to softwoods, the hardwood hemicelluloses are represented by xylans and a small portion of glucomannanose. Therefore, the extensive investigation on the pyrolysis of the hemicelluloses extracted from softwood (such as mannan and arobinan) would help understand the pyrolytic behavior of the woody biomass containing the similar hemicellulose-sugar(s) as softwood.

The chemical structure of lignin is very complex, altered from not only the wood species but also the isolation methods (such as Klason lignin, Bjorkman's method, milled wood lignin, Kraft lignin and so on). The milled wood lignins (MWL) are estimated to be the best lignin preparation now available, however they are still not identical with the native lignin in biomass, due to the fragmentation of the lignin macromolecules during the vibratory ball milling process. Therefore, the isolation method needs to be further improved to extract the lignin which could represent the original lignin to the most extent. This would help reveal the chemical structure of lignin in woody biomass and understand their pyrolytic mechanisms precisely.

3) The cell-wall structure of woody biomass is mainly composed of cellulose microfibrils formed the framework of cell wall, which is deposited by hemicellulose and lignin. The interactions among the components in woody biomass under the pyrolytic conditions should be considered in terms of the vapor-phase interactions, mass transfer in solid-phase, interlinkages in morphological-level. The vapor-phase interaction among the components is favored and investigated in the fluidized bed

reactor in terms of the yield of the products and variation of the prominent compounds in bio-oil and gaseous product, but the interactions in liquid/solid phase are not involved. The challenge for evidencing the interactions among the components in the real biomass under pyrolytic conditions is the preparation of the synthesized sample, which should contains the **characterized** information of interlinkages and the morphological relationship among the components. Consequently, the pyrolytic behavior of different woody biomass systems could be well predicted from the pyrolytic mechanism of individual components and the identified interactions among them with the help of the constituent analysis.

List of references

Adler, E., (1977). The lignin chemisty-past, present, future. Wood Science and Technology, 11: 169-218.

Agrawal, R. K., (1988). Kinetics of reactions involved in pyrolysis of cellulose, II. the modified Kilzer-Broido Model. Canadian Journal of Chemical Engineering, 66: 413-418.

Aho, A., Kumar, N., Eranen, K., Holmbom, B., Hupa, M., Salmi, T., Murzin, D. Y., (2008). Pyrolysis of softwood carbohydrates in a fluidized bed reactor. International Journal of Molecular Sciences, 9: 1665-1675.

Alen, R., Kuoppala, E., Oesch, P., (1996). Journal of Analytical and Applied Pyrolysis, 36: 137.

Alen, R., Kuoppala, E., Oesch, P., (1996). Formation of the main degradation compound groups from wood and its components during pyrolysis. Journal of Analytical and Applied Pyrolysis, 36: 137-148.

Amen-Chen, C., (2001). Production of monomeric phenols by thermochemical conversion of biomass: a review. Bioresource Technology, 79: 277-299.

Antal, M. J., (1985). Advance in solar energy. New York, ASES Publication.

Antal, M. J., Friedman, H. L., Rogers, F. E., (1980). Kinetics of Cellulose Pyrolysis in Nitrogen and Steam Combustion Science and Technology, 21: 141-152.

Antal, M. J., Leesomboon, T., Mok, W. S., Richards, G. N., (1991). Mechanism of formation of 2-furaldehyde from D-xylose. Carbohydrate Research, 217: 71-85.

Antal, M. J., Varhegyi, G., (1995). Cellulose pyrolysis kinetics: the current state of knowledge. Industrial and Engineering Chemistry Research, 34: 703-717.

Arias, M. E., Polvillo, O., Rodriguez, J., Hernandez, M., Gonzalez-Perez, J. A., Gonzalez-Villa, F. J., (2006). Thermal transformations of pine wood components under pyrolysis/gas chromatography/mass spectrometry conditions. Journal of Analytical and Applied Pyrolysis, 77: 63-67.

Arseneau, D. F., (1971). Competitive reaction in the thermal decomposition of cellulose. Canadian Journal of Chemistry, 49: 632-638.

Avni, E., Coughlin, R. W., (1983). Preprints-American Chemical Society, Division of Fuel Chemistry, 28: 307.

Avni, E., Coughlin, R. W., (1985). Kinetic analysis of lignin pyrolysis using non-isothermal TGA data. Thermochimica Acta, 90: 157-167.

Avni, E., Devoudzadeh, F., Coughlin, R. W., (1985). Fundamentals of thermochemical biomass conversion. Barking, Elsevier Applied Science Publishers.

Banyasz, J. L., Li, S., Lyons-Hart, J. L., Shafer, K. H., (2001). Cellulose pyrolysis: the kinetics of hydroxyacetaldehyde evolution. Journal of Analytical and Applied Pyrolysis, 57: 223-248.

Bar-Gadda, R., (1980). The kinetics of xylan pyrolysis. Thermochimica Acta, 42: 153-163.

Basch, A., Lewin, M., (1973). The influence of fine structure on the pyrolysis of cellulose. Journal of Polymer Sciences, 11: 3071.

Beenackers, A. A. C. M., (1999). Biomass gasification in moving bed, a review of european technologies. Renewable Energy, 16: 1180-1186.

Benson, S. W., (1976). Thermochemical kinetics. New York, Wiley, 2nd ed.

Benson, S. W., (1978). Thermochemical kinetics. New York, Wiley.

Bilbao, R., Mastral, J. F., Aldea, M. E., Ceamanos, J., (1997). Kinetic study for the thermal decomposition of cellulose and pine sawdust in an air atmosphere. Journal of Analytical and Applied Pyrolysis, 39: 53-64.

Bilbao, R., Millera, A., Arauzo, J., (1989). Kinetics of weight loss by thermal decompostition of xylan and lignin, influence of experimetnal conditions. Thermochimica Acta, 143: 137-148.

Blasi, C. D., (1993). Analysis of convection and secondary reaction effects within porous solid fuels undergoing pyrolysis. Combustion Science and Technology, 90: 1121-1132.

Blasi, C. D., Branca, C., Santoro, A., Hernandez, E. G., (2001). Pyrolytic behavior and products of some wood varieties. Combustion and Flame, 124: 165-177.

Blasi, C. D., Lanzetta, M., (1997). Intrinsic kinetics of isothermal xylan degradation in inert atmosphere. Journal of Analytical and Applied Pyrolysis, 40-41: 287-303.

Boutin, O., Ferrer, M., Lede, J., (1998). Radiant flash pyrolysis of cellulose-evidence for the formation of short life time intermediate liquid species. Journal of Analytical and Applied Pyrolysis, 47: 13-31.

Bradbury, A. G. W., Sakai, Y., Shafizadeh, F., (1979). Journal of Applied Polymer Science, 23: 3271-3280.

Bradbury, A. G. W., Sakai, Y., Shafizadeh, F., (1979). A kinetic model for pyrolysis of cellulose. Journal of Applied Polymer Science, 23: 3271-3280.

Branca, C., Blasi, C. D., (2003). Kinetics of the isothermal degradation of wood in the temperature range 528-708 K. Journal of Analytical and Applied Pyrolysis, 67: 207-219.

Brezny, R., Mihalov, V., Kovacik, V., (1983). Low temperature thermolysis of lignins I. reactions of β-O-4 model compounds. Holzforschung, 37: 99-204.

Bridgwater, A. V., (1999). Principles and practice of biomass fast pyrolysis processes for liquids. Journal of Analytical and Applied Pyrolysis, 51: 3-22.

Bridgwater, T., (2008). Fast pyrolysis of biomass. UK, CPL.

Briodo, A., Javier-Son, A. C., Ouano, A. C., Barrall, E. M., (1973). Molecular weight decrease in the early pyrolysis of crystalline and amorphous cellulose. Journal of Applied Polymer Science, 17(12): 3627.

Broido, A., (1976). Kinetics of solid-phase cellulose pyrolysis. In Thermal Uses and Properties of Carbohydrates and Lignins, Academic Press: New York.

Broido, A., Kilzer, F. J., (1963). A critique of the present state of knowledge of the mechanism of cellulose pyrolysis. Fire Research Abstract and Reviews, 5: 157.

Broido, A., Nelson, M. A., (1975). Char yield on pyrolysis of cellulose. Combustion and Fame, 24: 263-268.

Broido, A., Weinstein, M., (1971). Kinetics of solid-phase cellulose pyrolysis. The 3rd International Conference on Thermal Analysis, Wiedemann (Ed.), Birkhauser Verlag: Basel.

Byrne, G. A., Gardner, D., Holmes, F. H., (1966). Journal of Applied Chemistry, 16: 81.

Caballero, J. A., FOnt, R., Marcilla, A., (1996). Study of primary pyrolysis of Kraft lignin at hihg heating rates: yields and kinetics. Journal of Analytical and Applied Pyrolysis, 36: 159-178.

Caballero, J. A., Font, R., Marcilla, A., Conesa, J. A., (1995). New kinetic model for thermal decomposition of heterogeneous materials. Industrial and Engineering Chemistry Research, 34: 806-812.

Caballero, J. A., Font, R., Marcilla, A., Conesa, J. A., (1995). New kinetic model for thermal decompostion of heterogeneous materials. Industrial and Engineering Chemistry Research, 34: 806-812.

Capart, R., Khezami, L., Burnham, A. K., (2004). Assessment of various kinetic models for the pyrolysis of a microgranular cellulose. Thermochimica Acta, 417: 79-89.

Charlton, W., Haworth, W. N., Peat, S., (1926). A revision of the structural formula of glucose. Journal of Chemical Society, 13: 89-101.

Chu, S. S. C., Jeffrey, G. A., (1968). The refinement of the crystal structures of β-D-glucose and cellobiose. Acta Crystallography, 24: 830-838.

Colomba, D. B., (1998). Comparison of semi-global mechanisms for primary pyrolysis of lignocellulosic fuels. Journal of Analytical and Applied Pyrolysis, 47: 43-64.

Conesa, J. A., Cabollero, J. A., Marcillar, A., Font, R., (1995). Analysis of different kinetic model in the dynamic pyrolysis of cellulose. Thermochimica Acta, 254: 175-192.

Couhert, C., Commandre, J. M., Salvador, S., (2009). Is it possible to predict gas yields of any biomass after rapid pyrolysis at high temperature from its composition in cellulose, hemicellulose and lignin? Fuel, 88: 408-417.

Czenik, S., Bridgwater, A. V., (2004). Overview of applicatin of biomass fast pyrolysis oil. Energy and Fuels, 18: 590-598.

Dammstrom, S., Salmen, L., Gatenholm, P., (2009). On the interactions between cellulose and xylan, a biomimetic simulation of the hardwood cell wall. BioResources, 4(1): 3-14.

Demirbas, A., (2008). Biodiesel. London, Springer.

Diebold, J. P., (1994). A unified, global model for the pyrolysis of cellulose. Biomass and Bioenergy, 7(1-6): 75-85.

Dobele, G., Rossinskaja, G., Dizhbite, T., Telysheva, G., Meier, D., Faix, O., (2005). Application of catalysts for obtaining 1,6-anhydrosaccharides from cellulose and wood by fast pyrolysis. Journal of Analytical and Applied Pyrolysis, 74: 401-405.

Domburg, G. E., Rossinskaya, G., Sergeeva, V. N., (1974). Study of thermal stability of β-ether bonds in lignins and its models, Birkhauser, Basel.

Domburg, G. E., Sergeeva, V. N., Kalninsh, A. I., (1972). Thermal analysis of lignin Birkhayser, Basel.

Dominguez, J. C., Oliet, M., Alonso, M. V., Gilarranz, M. A., Rodriguez, F., (2008). Thermal stability and pyrolysis kinetics of organosolv lignins obtained from *Eucalyptus globulus*. Industrial Crops and Products, 27: 150-156.

Dumitriu, S., (2005). Polysaccharides: structures diversity and functional versatility, 2nd edition. New york, Marcel Dekker.

El-kalyoubi, S. F., El-shinnawy, N. A., (1985). Thermal behaviour of lignins extracted from different raw materials. Thermochimica Acta, 94: 231-238.

Essig, M. G., Richard, G. N., Schenck, E. M., (1989). Mechanisms of formation of the major volatile products from the pyrolysis cellulose. In Cellulose and Wood Chemistry and Technology. New York, J. Wiley & Sons.

Essig, M. G., Richards, G. N., (1988). 1,5-anhydro-beta-L-arabinofuranose from pyrolysis of plant cell wall materials (biomass). Carbohydrate Research, 181: 189-196.

EU, (1999). Biomass conversion technoogies, EUR 18029 EN ISBN 92-828-5368-3.

Evans, R. J., Milne, T. A., Soltys, M. N., (1984). 16th Biomass Thermochemical Conversion Contractors Meeting, Battelle Pacific Northwest Lab., PNL-SA-12403.

Evans, R. J., Milne, T. A., Soltys, M. N., (1986). Direct mass spectrometric studies of the pyrolysis of carbonaceous fuels III. primary pyrolysis of lignin. Journal of Analytical and Applied Pyrolysis, 9: 207-236.

Faix, O., Jakab, E., Till, F., Szekely, T., (1988). Study on low mass thermal degradation products of milled wood lignins by thermogravimetry-mass spectrometry. Wood Science and Technology, 22: 323-334.

Faix, O., Meier, D., Fortmann, I., (1988). Pyrolysis-gas chromatography-mass spectrometry of two trimeric lignin model compounds with alky-aryl ether structure. Journal of Analytical and Applied Pyrolysis, 14: 135-148.

Faix, O., Meier, D., Grobe, I., (1987). Studies on isolated lignins and lignins in woody materials by pyrolysis-gas chromatography-mass spectrometry and off-line pyrolysis-gas chromatography with flame ionization detector. Journal of Analytical and Applied Pyrolysis, 11: 403-416.

Fang, M. X., Shen, D. K., Li, Y. X., Yu, C. J., Luo, Z. Y., Cen, K. F., (2006). Kinetic study on pyrolysis and combustion of wood under different oxygen concentrations by using TG-FTIR analysis. Journal of Analytical and Applied Pyrolysis, 77: 22–27.

Fengel, D., (1969). The ultrastructure of cellulose from wood Wood Science and Technology, 3: 203-217.

Fengel, D., Wegener, G., (1984). Wood: Chemistry, Ultrastructure, Reactions. Berlin, Walter de Gruyter.

Fenner, R. A., Lephardt, J. O., (1981). Examination of the thermal decomposition of kraft pine lignin by Fourier transform infrared evolved gas analysis. Journal of Agricultural and Food Chemistry, 29: 846-849.

Ferdous, D., Dalai, A. K., Bej, S. K., Thring, R. W., (2002). Pyrolysis of lignins: experimental and kinetics studies. Energy and Fuels, 16: 1405-142.

Frankiewicz, T. C. (1980). Proc. Specialists workshop on fast pyrolysis biomass. Golden, CO, Solar Energy Research Institute**:** 123-136.

Freudenberg, K., Neish, A. C., (1968). Constituents and biosynthesis. New York, Springer.

Froass, P. M., Ragauskas, A. J., (1996). Chemical struture of residual lignin from kraft pulp. Journal of Wood Chemistry and Technology, 16(4): 347-365.

Funazukuri, T. (1983). Fast pyrolysis of cellulose in a micro fluidized bed. Department of Chemcial Engineering Waterloo, University of Waterloo. **PhD**.

Fushimi, C., Katayama, S., Tsutsumi, A., (2009). Elucidation of interaction among cellulose, lignin and xylan during tar and gas evolution in steam gasification Journal of Analytical and Applied Pyrolysis, 86: 82-89.

Garcia-bacaicoa, P., Mastral, J. F., Ceamanos, J., Berrueco, C., Serrano, S., (2008). Gasification of biomass/high density polyethylene mixtures in a downdraft gasifier. Bioresource Technology, 99: 5485-5491.

Garcia, A. N., Font, R., Marcilla, A., (1995). Kinetic study of the flash pyrolysis of municipal solid waste in a fluidized bed reactor at high temperature. Journal of Analytical and Applied Pyrolysis, 31.

Gardner, D. J., Schultz, T. P., McGinns, G. D., (1985). The pyrolytic behavior of selected lignin preparations. Journal of Wood Chemistry and Technology, 5(1): 85.

Gilbert, K. E., Gajewski, J. J., (1982). Coal liquefaction model studies: free radial chain decomposition of diphenylpropane, dibenzyl ether and phenyl ether via β-scission reactions. Journal of Organic Chemistry, 47: 4899-4902.

Golova, O. P., (1975). Chemical effects of heat on cellulose. Russian Chemistry Review, 44: 687.

Goodwin, A. K., Rorrer, G. L., (2009). Conversion of xylose and xylose-phenol mixtures to hydrogen-rich gas by supercritical water in an isothermal microtube flow reactor. Energy and Fuels, 23: 3818-3825.

Goodwin, T. W., Mercer, E. I., (1983). Introduction to plant biochemistry: The plant cell wall, New York: Pergamon Press.

Graham, R. G., Mok, L. K., Bergougnou, M. A., Lasa, H. I. D., Freel, B. A., (1984). Fast pyrolysis (ultrapyrolysis) of cellulose. Journal of Analytical and Applied Pyrolysis, 6: 363-374.

Grioui, N., Halouani, K., Zoulalian, A., Halouani, F., (2007). Thermal chemical modeling of isothermal carbonization of thick wood particle - effect of reactor temperature and wood particle size. Energy Conversion and Management, 48: 927-936.

Hajaligol, M. R., Howard, J. B., Longwell, J. P., Peters, W. A., (1982). Product compositions and kinetics for rapid pyrolysis of cellulose Industrial and Engineering Chemistry, 21(3): 457-465.

Hakka, K., Jumppanen, J. (2009). Rare sugars from wood hemicellulose. The 2nd Nordic Wood-Biorefinery Conference. Helsinki, Finland.

Hao, X. H., Guo, L. J., Zhang, X. M., Guan, Y., (2005). Hydrogen production from catalytic gasification of cellulose in supercritical water. Chemical Engineering Journal, 110: 56-65.

Hon, D. N. S., Shiraishi, N., (2001). Wood and cellulosic chemistry, 2nd ed., rev. and expanded, Marcel Dekker, Inc.

Hosoya, T., Kawamoto, H., Saka, S., (2007). Cellulos-hemicellulose and cellulose-lignin interactions in wood pyrolysis at gasifcation temperature. Journal of Analytical and Applied Pyrolysis, 80: 118-125.

Hosoya, T., Kawamoto, H., Saka, S., (2007). Pyrolysis behaviors of wood and its constituent polymers as gasification temperature. Journal of Analytical and Applied Pyrolysis, 78: 328-336.

Hosoya, T., Kawamoto, H., Saka, S., (2008). Different pyrolytic pathways of levoglucosan in vapor- and liquid/solid - phases. Journal of Analytical and Applied Pyrolysis, 83: 64-70.

Hosoya, T., Kawamoto, H., Saka, S., (2008). Pyrolysis gasification reactivities of primary tar an char fractions from cellulose and lignin as studied with a closed ampoule reactor. Journal of Analytical and Applied Pyrolysis, 83: 71-77.

Hosoya, T., Kawamoto, H., Saka, S., (2008). Secondary reactions of lignin-derived primary tar components. Journal of Analytical and Applied Pyrolysis, 83: 78-87.

Hosoya, T., Kawamoto, H., Saka, S., (2009). Solid/liquid- and vapor-phase interactions between cellulose- and lignin-derived pyrolysis products. Journal of Analytical and Applied Pyrolysis, 85(1－2): 237－246.

Islam, M. N., Zailani, R., Ani, F. N., (1999). Pyrolytic oil from fluidized bed pyrolysis of oil palm shell and its characterisation. Renewable Energy, 17: 73-84.

Jakab, E., Faix, O., Hill, F., Szekely, T., (1991). Thermogravimetry-mass spectrometry of various lignosulfonates as well as of a kraft and acetosolv lignin. Holzforschung, 45: 355-360.

Jakab, E., Faix, O., Till, F., (1997). Thermal decompositin of milled wood lignins studied by thermogravimetry/mass spectrometry. Journal of Analytical and Applied Pyrolysis, 40-41: 171-186.

Jakab, E., Faix, O., Till, F., Szekely, T., (1993). The effect of cations on the thermal decomposition of lignins. Journal of Analytical and Applied Pyrolysis, 25: 185-194.

Jakab, E., Faix, O., Till, F., Szekely, T., (1995). Thermogravimetry/mass spectrometry study of six lignins within the scope of an international round robin test. Journal of Analytical and Applied Pyrolysis, 35: 167-179.

Jiang, T. D., (2001). Lignin. Beijing, Chemical Industry Press.

Kaaden, A. V. d., Haverkamp, J., Boon, J. J., Leeuw, J. W. D., (1983). Ananlytical pyrolysis of carbohydrates. Journal of Analytical and Applied Pyrolysis, 5: 199.

Kang, J. C., Chen, P. H., Johnson, W. R., (1976). Thermal uses and properties of carbohydrates and lignins. New York, Academic Press.

Kawamoto, K., Morisaki, H., Saka, S., (2008). Secondary decompositionof levoglucosan in pyrolytic production from cellulosic biomass. Journal of Analytical and Applied Pyrolysis: doi: 10.1016/j.jaap.2008.08.009.

Keegstra, K., Talmadge, K. W., Bauer, W. D., Albersheim, P., (1973). The structure of plant cell walls: I. The hemicelluloses of the walls of suspension-cultured sycamore cells. Plant Physiol, 51: 174-185.

Kilzer, F. J., Broido, A., (1965). Speculation on the nature of cellulose pyrolysis. Pyrodynamics, 2: 151-163.

King, H. H., Solomon, P. R., (1983). Preprints-American Chemical Society, Division of Fuel Chemistry, 28: 319.

Klein, M. T. (1981). lignin thermolysis pathways, Department of Chemical Engineering, Massachussetts Institute of Technology. **PhD**.

Korobkov, V. Y., Grigorieva, E. N., Bykov, V. I., Senko, O. V., Kalechitz, V. I., (1988). Effect of the structure of coal-related model ether on the rate and mechanism of their thermolysis. 1. effect of the number of methylene groups in the R-$(CH_2)_n$-O-$(CH_2)_m$-R structure. Fuel, 67: 657-662.

Koufopanos, C. A., Maschio, G., Lucchesi, a., (1989). Kinetic modeling of the pyrolysis of biomass and biomass components. Canadian Journal of Chemical Engineering, 67: 75-84.

Kumar, A., Eskridge, K., Jones, D. D., Hanna, M. A., (2009). Steam-air fluidized bed gasification of distillers grains: Effects of steam to biomass ratio, equivalence ratio and gasification temperture. Bioresource Technology, 100: 2062-2068.

Kuroda, K., (1994). Pyrolysis of arylglycol-β-propylphenyl ether lignin model in the presence of borolilicate glass fibres I. pyrolysis of β-ether compounds. Journal of Analytical and Applied Pyrolysis, 30: 173-182.

Lede, J., Blanchard, F., Boutin, O., (2002). Raidant flash pyrolysis of cellulose pellets: products and mechanisms involved in transient and steady state conditions. Fuel, 81: 1269-1279.

Lee, T. V., Beck, S. R., (1984). New integral approximation formula for kinetics analysis of nonisothermal TGA data. AIChEJ, 30: 517-519.

Li, S., Lyons-Hart, J., Banyasz, J., Shafer, K., (2001). Real-time evolved gas analysis by FTIR method: an experimental study of cellulose pyrolysis. Fuel, 80: 1809-1817.

Liao, Y. F. (2003). Mechanism study of cellulose pyrolysis, PhD Thesis, ZheJiang University, HangZhou, China.

Lipska, A. E., Wodley, F. A., (1969). Isothermal pyrolysis of cellulose: kinetics and gas chromatographic mass spectrometric analysis of the dgradation products. Journal of Applied Polymer Science, 13: 851.

Liu, L., Yao, Y., Yoshioka, M., Shiraishi, N., (1997). Liquefaction mechanism of lignin in the presence of phenol at elevated temperature without catalysts. Holzforschung, 51: 316-324.

Liu, N. A., (2002). Kinetic modeling of thermal decomposition of natural cellulosic materials in air atmosphere. Journal of Analytical and Applied Pyrolysis, 63: 303-325.

Liu, Q., Wang, S. R., Zhen, Y., Luo, Z. Y., Cen, K. F., (2008). Mechanism study of wood lignin pyrolysis by using TG-FTIR analysis. Journal of Analytical and Applied Pyrolysis, 82: 170-177.

Madorsky, S. L., Hart, V. E., Straus, S., (1958). Journal of Research of the National Bureau of Standards, 60: 343.

Mamleev, V., Bourbigot, S., Yvon, J., (2007). Kinetic analysis of the thermal decomposition of cellulose: the change of the rate limitation. Journal of Analytical and Applied Pyrolysis, 80: 141-150.

Manya, J. J., E.Velo, Puigjanaer, L., (2004). Industrial and Engineering Chemistry Research, 42: 434.

Maschio, G., Koufopanos, C., Lucchesi, A., (1992). Pyrolysis, a promising route for biomass utilization. Bioresource Technology, 42: 219-231.

Masuku, C. P., (1991). Thermal reactions of the bonds in lignin IV. thermolysis of di-methoxyphenols. Holzforschung, 45: 181-190.

Masuku, C. P., Vuori, A., Bredenberg, J. P., (1988). Thermal reactions of the bonds in lignin I. thermolysis of 4-propylguaiacol. Holzforschung, 42: 361-368.

McDermott, J. B., Klein, M. T., Obst, J. R., (1986). Chemical modeling in the deduction of process concepts: a proposed novel process for lignin

liquefaction. Industrial and Engineering Chemistry Process Design and Development, 25: 885-889.

McKendry, P., (2002). Energy production from biomass (part 1): overview of biomass. Bioresource Technology, 83: 37-46.

McKendry, P., (2002). Energy production from biomass (part 2): conversion technologies. Bioresource Technology, 83: 47-54.

Miller, R. S., Bellan, J. A., (1997). Combustion Science and Technology, 126: 97.

Milosavljevic, I., Suuberg, E. M., (1995). Cellulose thermal decomposition kinetics: Global mass loss kinetics. Industrial and Engineering Chemistry Research, 34: 1081-1091.

Min, k., (1977). Vapor-phase thermal analysis of pyrolysis products from cellulosic materials. Combustion and Fame, 30: 285.

Miyazaki, K., (1975). Mokuzai Gakkaish., 21: 120-121.

Mohammed, R. H., Howard, J. B., Longwell, J. P., (1982). Product compositions and kinetics for rapid pyrolysis of cellulose. Journal of Industrial and Engineering Chemistry, 21: 457-465.

Mohan, D., Pittman, C. U., Steele, P. H., (2006). Pyrolysis of wood/biomass for bio-oil: a critical review. Energy and Fuels, 20(3): 848-889.

Mok, W. S.-L., Antal, M. J., Szabo, P., Varhegyi, G., Zelei, B., (1992). Fromation of charcoal from biomass in a sealed reactor. Industrial and Engineering Chemistry Research, 31: 1162-1166.

Mok, W. S. L., Antal, M. J., (1983). Effects of pressure on biomass pyrolysis. I. Cellulose pyrolysis products. Thermochimica Acta, 68: 155-164.

Muller-Hagedorn, M., Bockhorn, H., Krebs, L., Muller, U., (2003). A comparative kinetic study on the pyrolysis of three different wood species. Journal of Analytical and Applied Pyrolysis, 68-69: 231-249.

Nakamura, T., Kawamoto, H., Saka, S., (2007). Condensation reactions of some lignin related compounds at relatively low pyrolysis temperature. Journal of Wood Chemistry and Technology, 27: 121-133.

Nguyen, T., Zavarin, E., Barrall, E. M., (1981). Thermal analysis of lignocellulosic materials I. unmodified materials. Journal of Macromolecular Sciences and Reviews: Macromolecular Chemistry, C20(1): 1-65.

Nowakowski, D. J., Jones, J. M., (2008). Uncatalytic and potassium-catalysed pyrolysis of the cell-wall constituents of biomass and their model compounds. Journal of Analytical and Applied Pyrolysis, 83: 12-25.

Nunn, T. R., Howard, J. B., Longwell, J. P., Peters, W. A., (1985). Industrial and Engineering Chemistry Process Design and Development, 24: 844.

Obst, J. R., (1983). Analytical pyrolysis of hardwood and softwood lignins and its use in lignin-type determination of hardwood vessel elements. Journal of Wood Chemistry and Technology, 3(4): 377-397.

Ohnishi, A., Kato, K., Takagi, E., (1977). Carbohydrate Research, 59: 387-395.

Orfao, J. J. M., (1999). Pyrolysis kinetics of lignocellulosic materials-three independent reactions model Fuel, 78: 349-358.

Osada, M., Sato, T., Watanabe, M., (2004). Low temperature catalytic gasification of lignin and cellulose with a ruthenium catalyst in supercritical water. Energy and Fuels, 8(2): 327-333.

Padkel, H., Roy, C., (1991). Hydrocarbon content of liquid products and tar from pyrolysis and gasification of wood. Energy and Fuels, 5: 427-436.

Pakdel, H., Caumia, B. D., Roy, C., (1992). Vacuum pyrolysis of lignin derived from steam-exploded wood. Biomass and Bioenergy, 3(1): 31-40.

Pan, W., Richards, G. N., (1989). Influence of metal ions on volatile products of pyrolysis of wood. Journal of Analytical and Applied Pyrolysis, 16: 117-126.

Park, H. J., Park, Y. K., Kim, J. S., (2008). Influence of reaction conditions and the char seperation system on the production of bio-oil from radiata pine sawdust by fast pyrolysis. Fuel Processing Technology, 89(8): 797-802.

Pasquali, C. E. L., herrera, H., (1997). Pyrolysis of lignin and IR analysis of residues. Thermochimica Acta, 293: 39-46.

Piskorz, J., Majerski, P., Radlein, D., Vlasars-Usas, A., Scott, D. S., (2000). Flash pyrolysis of cellulose for production of anhydro-oligomers. Journal of Analytical and Applied Pyrolysis, 56: 145-166.

Piskorz, J., Radlein, D., Scott, D. S., (1986). On the mechanism of the rapid pyrolysis of cellulose. Journal of Analytical and Applied Pyrolysis, 9: 121-137.

Piskorz, J., Radlein, D., Scott, D. S., Czernik, S., (1989). Pretreatment of wood and cellulose for production of sugars by fast pyrolysis. Journal of Analytical and Applied Pyrolysis, 16(2): 127-142.

Piskorz, J., Scott, D. S., Radlein, D., (1988). Pyrolysis oils from biomass: producing, analyzing and upgrading. Symposium Series, vol. 376, Washington, DC: American Chemical Society.

Ponder, G. R., Richards, G. N., (1990). Polysaccharides from thermal polymerization of glucosides. Carbohydrate Research, 208: 93-104.

Ponder, G. R., Richards, G. N., (1991). Thermal synthesis and pyrolysis of a xylan. Carbohydrate Research, 218: 143-155.

Pouwel, A. D., Eijkel, G. B., Boon, J. J., (1989). Curie-point pyrolysis-capillary gas chromatography-high resolution mass spectrometry of microcrystalline cellulose Journal of Analytical and Applied Pyrolysis, 14: 237.

Pouwel, A. D., Tom, A., Eijkel, G. B., Boon, J. J., (1987). Journal of Analytical and Applied Pyrolysis, 11: 417-436.

Prins, M. J., Ptasinski, K. J., Janssen, F. J. J. G., (2006). Torrefaction of wood Part1. Weight loss kinetics. Journal of Analytical and Applied Pyrolysis, 77: 28-34.

Prins, M. J., Ptasinski, K. J., Janssen, F. J. J. G., (2006). Torrefaction of wood Part 2. Analysis of products. Journal of Analytical and Applied Pyrolysis, 77: 35-40.

R.J. Evans, Milne, T. A., (1987). Molecular characterization of the pyrolysis of biomass. Energy and Fuels, 1(2): 123-137.

Radlein, D., Piskorz, J., Scott, D. S., (1991). Fast pyrolysis of natural polysaccharides as a potential industrial process. Journal of Analytical and Applied Pyrolysis, 19: 41-63.

Ramiah, M. V., (1970). Journal of Polymer Sciences, 14: 1323-1337.

Rath, J., Staudinger, G., (2001). Cracking reactions of tar from pyrolysis of spruce wood. Fuel, 80: 1379-1389.

Richards, G. N., (1987). Glycoaldehyde from pyrolysis of cellulose. Journal of Analytical and Applied Pyrolysis, 10(2): 251-255.

Richards, G. N., Shafizadeh, F., (1982). Fromation of "Glucometasaccharinollactones" in the pyrolysis of curdlan, A (1>3)-beta-d-glucan. Carbohydrate Research, 106(1): 83-91.

Richards, G. N., Zheng, G. C., (1991). Influence of metal ions and of salts on products from pyrolysis of wood: applications to thermochemical processing of newsptint and biomass. Journal of Analytical and Applied Pyrolysis, 21: 133-146.

Safi, M. J., Mishra, I. M., Prasad, B., (2004). Global degradation kinetics of pine needles in air Thermochimica Acta, 412 (1-2): 155-162.

Sandford, P. A., Baird, J., (1983). In Molecular biology. New York, Aspinall, G.O.; Ed;Acedamic Press.

Schulten, H. R., Gortz, W., (1978). Curie-point pyrolysis and field ionization mass spectrometry of polysaccharides. Analytical Chemistry, 50: 428.

Scott, D. S., Piskorz, J., (1982). The flash pyrolysis of aspen-poplar wood. Canadian Journal of Chemical Engineering, 60(5): 666.

Scott, D. S., Piskorz, J., (1984). The continuous flash pyrolysis of biomass. Canadian Journal of Chemical Engineering, 62(3): 404-412.

Severian, D., (2008). Polysaccharides: structural diversity and functional versatility. 2nd Edition, Marcel Dekker: New York.

Shafizadeh, F., (1982). Introduction to pyrolysis of biomass. Journal of Analytical and Applied Pyrolysis, 3: 283-305.

Shafizadeh, F., Bradbury, A. G. W., (1979). Thermal degradation of cellulose in air and nitrogen at low temperature. Journal of Applied Polymer Science, 23: 1431-1442.

Shafizadeh, F., Furneaux, R. H., Cochran, T. G., Scholl, J. P., Sakai, Y., (1979). Production of levoglucosan and glucose from pyrolysis of cellulosic materials. Journal of Applied Polymer Science, 23: 3525-3539.

Shafizadeh, F., Lai, Y. Z., (1972). Thermal degradation of 1,6-anhydro-.beta.-D-Glucopyranose. Journal of Organic Chemistry, 37: 278-284.

Shafizadeh, F., McGinnis, G. D., (1971). Chemical composition and thermal analysis of cottonwood. Carbohydrate Research, 16(2): 273-277.

Shafizadeh, F., Mcginnis, G. D., Philpot, C. W., (1972). Thermal degradation of xylan and related compounds. Carbohydrate Research, 25: 23-33.

Shafizadeh, F., Philpot, C. W., Ostojic, N., (1971). Thermal analysis of 1,6-anhydro-beta-D-glucopyranose. Carbohydrate Research, 16(2): 279-287.

Shafizadeh, F., Susott, R. A., McGinnis, G. D., (1972). Pyrolysis of substituted phenyl β-D-glucopyranosides and 2-deoxy-α-D-arabino-hexopyranosides. Carbohydrate Research, 22(63-73).

Shen, D. K., Gu, S., (2009). The mechanism for thermal decompostion of cellulose and its main products. Bioresource Technology, 100: 6496-6504.

Shen, D. K., Gu, S., Bridgwater, A. V., (2010). Study on the pyrolytic behaviour of xylan-based hemicellulose using TG-FTIR and Py-GC-FTIR. Journal of Analytical and Applied Pyrolysis, 87(2): 199-206.

Shen, D. K., Gu, S., Luo, K. H., Bridgwater, A. V., (2009). Analysis of wood structural changes under thermal radiation. Energy and Fuels, 23: 1081-1088.

Shen, D. K., Gu, S., Luo, K. H., Bridgwater, A. V., Fang, M. X., (2009). Kinetic study on thermal decomposition of woods in oxidative environment. Fuel, 88: 1024-1030.

Shen, D. K., Gu, S., Luo, K. H., Wang, S. R., Fang, M. X., (2010). The pyrolytic degradation of wood-derived lignin from pulping process. Bioresource Technology, 101(15): 6136-6146.

Shimizu, K., Teratani, F., (1969). Journal of Japanese Wood Reseach Society, 16: 114.

Shin, E. J., Nimlos, M. R., Evans, R. J., (2001). Kinetic analysis of hte gas-phase pyrolysis of carbohydrates. Fuel, 80: 1697-1709.

Simkovic, I., Hirsch, J., Ebringerova, A., Konigstein, J., (1987). Thermal decomposition of model compounds with blocked hemiacetal group related to (4-O-methyl-D-glucourono)-D-xylan. JOurnal of Applied Polymer Science, 33: 1473-1477.

Simkovic, I., K.Balog, Csomorova, K., (1995). Thermal degradation and thermooxidation of O-acetyl-(4-O-methyl-D-glucurono)-D-xylan and related derivatives. Holzforschung, 49: 512-516.

Simkovic, I., Varhegyi, G., Antal, M. J., (1988). Thermogravimetric/mass spectrometric characterization of thermal decompostitin of (4-O-methyl-D-glucourono)-D-xylan. JOurnal of Applied Polymer Science, 36: 721-728.

Simmons, G. M., Gentry, M., (1986). Particle size limitations due to heat transfer in determining pyrolysis kinetics of biomass. Journal of Analytical and Applied Pyrolysis, 10: 117-127.

Sjostrom, E., (1993). Wood chemistry: fundamentals and applications, 2nd edition, Academic Press.

Sondreal, E. A., Benson, S. A., Hurley, J. P., Mann, M. D., Pavlish, J. H., Swanson, M. L., Weber, G. F., Zygarlicke, C. J., (2001). Review of advances in combustion technology and biomass cofiring. Fuel Processing Technology, 71: 7-38.

Spearpoint, M. J. (1999). Predicting the ignition and burning rate of wood in the cone calorimeter using an integral model, NIST. **GCR 99-975**.

Squire, K. R., Solomon, P. R. (1983). Characterization of biomass as a source of chemicals, Final Report , N.S.F. Contract No. CPE-8107453.

Stamm, A. J., (1956). Thermal degradation of wood and cellulose. Industrial and Engineering Chemistry, 48: 418-425.

Stevenson, T. T., Stenkamp, R. E., Jensen, L. H., Cochran, T. G., F.Shafizadeh, Furneaux, R. H., (1981). The crystal structure of

1,5-anhydro-4-deoxy-D-glycero-hex-1-en-3-ulose. Carbohydrate Research, 90(1): 319-325.

Sutton, L. E., (1958). Table of interatomic distances and configuration in molecules and ions, The Chemical Society, London Spec. Pub.

Teng, J., Wei, Y. C., (1998). industrial and Engineering Chemistry Research, 37(3806).

Theander, O., (1985). In: R.P. Overand, T.A. Mile, L.K. Mudge (eds.) Fundamentals of thermochemical biomass conversion. New York, Elsevier.

Varhegyi, G., Antal, M. J., Jakab, E., Szabo, P., (1997). Kinetic modeling of biomass pyrolysis. Journal of Analytical and Applied Pyrolysis, 42: 73-87.

Varhegyi, G., Antal, M. J., Szekely, T., Szabo, P., (1989). Kinetics of the thermal decomposition of cellulose, hemicellulose, and sugar cane bagasse. Energy and Fuels, 3: 329-335.

Varhegyi, G., Jakab, E., Antal, M. J., (1994). Is the Broido-Shafizadeh model for cellulose ture? Energy and Fuels, 8: 1345-1352.

Varhegyi, G., Szabo, P., Mok, W. S. L., Antal, M. J., (1993). Kinetics of the thermal decompostion of cellulose in sealed vessels at elevated pressure. Journal of Analytical and Applied Pyrolysis, 26: 159-174.

Vuori, A., Bredenberg, J. B., (1987). Thermal chemistry pathways of substituted anisoles. Industrial and Engineering Chemistry Research, 26: 359-365.

Wang, G., Li, W., Li, B., al., e., (2008). TG study on pyrolysis of biomass and its three components under syngas. Fuel, 87(4-5): 552-558.

Ward, S. M., Braslaw, J., (1985). Experimental weight loss kinetics of wood pyrolysis under vacuum. Combustion and Fame, 61(3): 261-269.

Watanabe, M., Inomata, H., Arai, K., (2002). Catalytic hydrogen generation from biomass (glucose and cellulose) with ZrO_2 in supercritical water. Biomass and Bioenergy, 22: 405-410.

Williams, P., Besler, S., (1993). The pyrolysis of rice husks in a thermogravimetric analyser and static batch reactor. Fuel, 72(2): 151-159.

Wooten, J. B., Seeman, J. I., Hajaligol, M. R., (2004). Observation and characterization of cellulose pyrolysis intermediates by ^{13}C CPMAS NMR. A new mechanistic model. Energy and Fuels, 18(1): 1-15.

Worasuwannarak, N., Sonobe, T., Tanthapanichakoon, W., (2007). Pyrolysis behaviors of rice straw, rice husk and corncob by TG-MS technique. Journal of Analytical and Applied Pyrolysis, 78: 265-271.

Yang, H. P., Yan, R., Chen, H. P., Zheng, C. G., Lee, D. H., Liang, D. T., (2006). In-depth investigation of biomass pyrolysis based on three major components: hemicellulose, cellulose and lignin. Energy and Fuels, 20: 388-393.

Zheng, J. L., Yi, W. M., Wang, N. N., (2008). Bio-oil production from cotton stalk. Energy Conversion and Management, 49(6): 1724-1730.

Publications

The publications during the PhD study in University of Southampton are listed:

1） D.K. Shen, S. Gu, K.H. Luo, M.X. Fang and A.V. Bridgwater, Kinetic study on thermal decomposition of woods in oxidative environment, Fuel, 88(6) (2009) 1024-1030.

2) D.K. Shen, S. Gu, K.H. Luo and A.V. Bridgwater, Analysis of wood structural changes under thermal radiation, Energy and Fuels, 23(2) (2009) 1081-1088.

3) D.K. Shen, S. Gu, The mechanism for thermal decomposition of cellulose and its main products, Bioresource Technology, 100(24) (2009) 6496-6504.

4) D.K. Shen, S. Gu, A.V. Bridgwater, Study on the pyrolytic behavior of xylan-based hemicellulose using TG-FTIR and Py-GC-FTIR, Journal of Analytic and Applied Pyrolysis, 87(2) (2010) 199-206.

5) D.K. Shen, S. Gu, K.H. Luo, S.R. Wang, The pyrolytic degradation of wood-derived lignin from pulping process, Bioresource Technology, 101(15) (2010) 6136-6146.

6) D.K. Shen, S. Gu, Pyrolytic behavior of cellulose in a fluidized bed reactor, Cellulose Chemistry and Technology, 44(1-3) (2010) 79-87.

7） D.K. Shen, S. Gu, A.V. Bridgwater, The thermal performance of the polysaccharides extracted from hardwood: cellulose and hemicellulose, Carbohydrate Polymers, 82(1) (2010) 39-45.

8) D.K. Shen, S. Gu, B.S. Jin, M.X. Fang, Thermal degradation mechanisms of wood under inert and oxidative environments using DAEM methods, Bioresource Technology, 102 (2011) 2047-2052.

9) D.K. Shen, M.X. Fang, Z.Y. Luo, K.F. Cen and S. Gu, Modeling the pyrolysis and auto-ignition of wet wood by thermal radiation, In Proceedings of the 32th International Symposium on Combustion, McGill University, Montreal, Canada, August 3-8 2008

10) D.K. Shen, S. Gu, The evolution of the main products from the thermal decomposition of crystalline cellulose, in proceeding of the 2nd Nordic Wood Biorefinery Conference in Helsinki, Finland, September 2-4 2009.

11) D.K. Shen, S. Gu. N.H. Dong, A.V. Bridgwater, The thermal conversion of cellulose and hemicellulose in thermogravimetric apparatus and a fluidized-bed reactor, Bioten, Aston, UK, September 21-23 2010.